NOTICE

The quality of this microform is heavily dependent upon the quality of the original thesis submitted for microfilming. Every effort has been made to ensure the highest quality of reproduction possible.

If pages are missing, contact the university which granted the degree.

Some pages may have indistinct print especially if the original pages were typed with a poor typewriter ribbon or if the university sent us an inferior photocopy.

Reproduction in full or in part of this microform is governed by the Canadian Copyright Act, R.S.C. 1970, c. C-30, and subsequent amendments.

AVIS

La qualité de cette microforme dépend grandement de la qualité de la thèse soumise au microfilmage. Nous avons tout fait pour assurer une qualité supérieure de reproduction.

S'il manque des pages, veuillez communiquer avec l'université qui a conféré le grade.

La qualité d'impression de certaines pages peut laisser à désirer, surtout si les pages originales ont été dactylographiées à l'aide d'un ruban usé ou si l'université nous a fait parvenir une photocopie de qualité inférieure.

La reproduction, même partielle, de cette microforme est soumise à la Loi canadienne sur le droit d'auteur, SRC 1970, c. C-30, et ses amendements subséquents.

Applications of Solid State NMR to the Study of Molecular Structure

by Ronald D. Curtis

Submitted in partial fulfilment of the
requirements for the degree of
Doctor of Philosophy
at
Dalhousie University
Halifax, Nova Scotia
June, 1990

ISBN 0-315-64573-3

Dalhousie University

Faculty of Graduate Studies

The undersigned hereby certify that they have read and recommend to the Faculty of Graduate Studies for acceptance a thesis titled **"Applications of Solid State NMR to the Study of Molecular Structure"** by Ronald D. Curtis in partial fulfilment of the requirements for the degree of Doctor of Philosophy.

Dated 28th August 1990

External Examiner

Research Supervisor

Examining Committee

Dalhousie University

Date [redacted]

Author Ronald Dean Curtis

Title Applications of Solid State NMR
to the Study of Molecular Structure

Department of Chemistry

Degree : Ph.D. Convocation : October Year : 1990

Permission is herewith granted to Dalhousie University to circulate and to have copied for non-commercial purposes, at its discretion, the above title upon the request of individuals or institutions.

[redacted]
Signature of Author

To my wife, Tammy, for whom it is hoped that the intellectual fire of modern day researchers will benefit her.

"*Men love to wonder, and that is the seed of our science.*"

Ralph Waldo Emerson,
Society and Solitude,
February, 1870.

Contents

...Continued

List of Figures

...Continued

...Continued

...Continued

...Continued

List of Tables

...Continued

Abstract

This thesis illustrates several applications of dilute spin I=1/2 solid state nmr spectroscopy to the study of molecular structure in systems of chemical interest. Specifically, the compounds studied include benzylideneaniline and several related imines, the first stable iminophosphenium cation containing a N,P triple bond and several tetracyclines.

The first two applications describe the use of dipolar-chemical shift nmr of "isolated" spin-pairs to fully characterize chemical shift tensors. For example, the carbon and nitrogen shift tensors of the C=N linkage of the Schiff base benzylideneaniline have been completely specified. The most shielded principal component of both carbon and nitrogen shift tensors is approximately perpendicular to the imine fragment. For the imine carbon, the intermediate component of the shift tensor is directed approximately along the C=N bond whereas the corresponding component of the nitrogen shift tensor is oriented along the direction of the nitrogen lone pair. Examination of the nitrogen chemical shift parameters for several related imines suggests that variations in the least shielded principal component are mainly responsible for changes in the nitrogen shieldings in the imine system. For the N,P moiety of the iminophosphenium cation, the most shielded principal component of both nitrogen and phosphorus tensors is oriented along the N,P bond axis. Comparison of both shift tensors with those of related compounds suggests that the electronic environment surrounding the N,P moiety is similar to other systems containing a formal triple bond.

The final application section demonstrates the utility of high-resolution ^{13}C and ^{15}N cp/mas nmr for studying the molecular structure of solid tetracycline antibiotics. Comparison of ^{15}N chemical shifts in the solid state to those determined in $(CD_3)_2SO$ solutions indicates for the first time that the structural integrity of the A ring of the tetracyclines is maintained in solution.

List of Symbols

$\vec{B}_o$	external magnetic field vector
B_o	magnitude of the static external magnetic field in T
$\vec{B}_1$	radio-frequency field vector
B_1	amplitude of pulsed radio-frequency field in T
B_2	amplitude of a second radio frequency field in T
B_{eff}	effective local magnetic field in T
$C_{j\beta}$	$2p_\beta$ orbital coefficient of the j^{th} MO on atom A
$\hat{D}$	direct dipolar tensor
H	Hamiltonian operator in Joules
h	Planck constant (6.6262×10^{-34}) in J·s
I	magnetic quantum number (or spin number); also referred to as the abundant spins
$\vec{I}_A$	nuclear spin operator for nucleus A
$\vec{I}_{A,i}$	component of the nuclear spin operator
I_{A+}	raising operator for nucleus A
I_{A-}	lowering operator for nucleus A
I_o	intensity which corresponds to the optimum contact time
I_s	observed intensity in a cp/mas nmr spectrum
$\hat{J}$	indirect dipolar coupling tensor
$J_\parallel$	parallel component of the J tensor in Hz
$J_\perp$	perpendicular component of the J tensor in Hz
J_{iso}	isotropic J coupling in Hz; $(1/3\ Tr(\hat{J}))$
ΔJ	anisotropy in J; $(J_\parallel - J_\perp)$
k	Boltzmann constant (1.38062×10^{-23}) in $J\ K^{-1}$
M_o	equilibrium magnetization of a spin system in B_o ($J\ T^{-1}$)
$M_{2,AI}$	second moment of a nmr spectrum
m_I	magnetic component quantum number
N	total number of nuclei of a given type in a sample
R	dipolar coupling constant in s^{-1}
R'	effective dipolar coupling constant in s^{-1}
R_{AI}	cross polarization rate in s^{-1}
r_{AX}	internuclear separation between nuclei A and X in m
S	a model independent order parameter

T	absolute temperature in K
T_1	spin-lattice relaxation time in s
$T_{1\rho,I}$	rotating frame spin-lattice relaxation time of I in s
T_2	spin-spin relaxation time in s
T_{AI}	cross polarization relaxation time in s
t_{aq}	acquisition time in s
t_c	contact time in ms
$t_{c,o}$	optimum contact time in ms
t_d	"dead" time of the spectrometer after a pulse in μs
t_p	pulse length in μs
t_r	recycle time in s
$\hat{V}$	electric field gradient (efg) tensor
V_{ii}	principal components of the efg tensor in J C^{-1} m^{-2}
θ, ϕ	Polar and azimuthal angles which relate r_{AX} to the magnetic field vector, $\vec{B}_o$
α, β	Euler angles which orient r_{Ax} in the principal axis system (pas) of the chemical shift tensor
ϑ, φ	Polar and azimuthal angles which relate $\vec{B}_o$ to the pas of the chemical shift tensor
ξ, Ω	Polar and azimuthal angles which relate $\vec{B}_o$ to the pas of the efg tensor
α^D, β^D	Euler angles which relate r_{AX} to the principal axis system of the efg tensor of the X nucleus.
α^{CS}, β^{CS}, γ^{CS}	Euler angles which relate the principal axis system of the chemical shift tensor of A to the principal axis system of the electric field gradient tensor of X
Θ	"flip angle" generated by a radio-frequency pulse
ν_o	Larmor frequency in Hz
ν_r	Larmor frequency of a reference compound in Hz also used for the frequency of a spinning rotor in Hz
$\nu_{1/2}$	width of a resonance line at half height in Hz
ν_s	Larmor frequency of a sample nucleus in Hz
ω_o	Larmor frequency in rad s^{-1}

ω_r	frequency of a spinning rotor in rad s^{-1}
ω	radio-frequency carrier rad s^{-1}
ω_1	radio-frequency field in rad s^{-1}
μ_A	magnetic dipole moment of nucleus A in m^2 A
μ_o	permeability constant ($4\pi x10^{-7}$) in kg m s^{-2} A^{-2}
γ_A	gyromagnetic ratio of nucleus A in rad T^{-1} s^{-1}
μ_B	Bohr magneton in J T^{-1}
Ψ	wave function
ψ	half angle of the cone traced out by a libration in °
$\hat{\delta}$	chemical shift tensor
δ_{ii}	principal component of the chemical shift tensor in ppm
δ_{iso}	isotropic chemical shift in ppm; $(1/3(Tr\hat{\delta}))$
$\Delta\delta$	chemical shift anisotropy; $(\delta_{11}-\delta_{33})$
$\hat{\sigma}$	chemical shielding tensor
σ_{ii}	principal component of the chemical shielding tensor
σ_{iso}	isotropic chemical shielding constant; $(1/3(Tr\hat{\sigma}))$
σ_{ii}^p	paramagnetic shielding of a principal component in ppm
σ_{ii}^d	diamagnetic shielding of a principal component in ppm
$\sigma_\perp$	perpendicular component of an axially symmetric $\hat{\sigma}$
$\sigma_\parallel$	parallel component of an axially symmetric $\hat{\sigma}$
$\Delta\sigma$	chemical shielding anisotropy; $(\sigma_{33}-\sigma_{11})$
η_δ	asymmetry parameter of the chemical shift tensor
η_σ	asymmetry parameter of the shielding tensor
η_Q	asymmetry parameter of the efg tensor
χ	nuclear quadrupolar coupling constant in MHz
τ	Hahn-echo dephasing delay in μs
τ_{DD}	dipolar dephasing delay time in μs

Acknowledgements

There are a number of people who have provided both direct and indirect influences on the work presented in this thesis. Primarily, I wish to acknowledge my wife, Tammy, for her loving support of my research endeavours. I would also like to express my sincere thanks to my parents for their guidance and support. To my research supervisor, Dr. Rod Wasylishen, I extend my utmost thanks for his patience, assistance and friendship throughout my stay at Dalhousie. In addition, his enthusiasm and persistence in helping to prepare this thesis have been greatly appreciated. The helpful discussions and extra curricular "meetings" with members of the nmr research group - Dr. Jan Kwak, Dr. Glenn Penner, Dr. Zhisheng Gao, Dr. Marco Gruwel, Bill Power, Gerry Marangoni, Mark MacIntosh and Réjean Labonté - have been greatly appreciated. Mr. Bill Power deserves special thanks for adapting and perfecting the computer simulation routines which I have used throughout this report. In particular, his help with the theoretical description and interpretation of the benzylideneaniline nmr results are noted. A special thanks is extended to Mr. Mark MacIntosh for his help in the preparation of some of the figures in this thesis.

Mr. Jim Hilborn is to be acknowledged for his help preparing some of the compounds discussed in the thesis and for his friendship over the last few years. Mr. Bruce Macdonald is recognized for instilling in me the need for a detailed "time-consuming" set up of nmr experiments. In addition, his triweekly visits with me to the Dalplex and the ensuing friendship are noted. I would like to thank Dr. Don Hooper at the ARMRC for interesting conversations in the lab as well as for the acquisition of several solution nmr spectra. His help in proof reading of this thesis is also appreciated. Helpful discussions with the members of the inorganic group - Dr. Neil Burford, Dr. Mel Schriver and Dr.

Bruce Royan - has been greatly appreciated. In particular, only the keen desire of Mel to investigate the first stable solid containing a N,P triple bond, allowed me to successfully complete this project in first class form. The help of Dr. Bruce Royan who spent long hours packing and repacking... air sensitive solid samples in the glove box is appreciated. Dr. Tony Linden is acknowledged for performing a crystal structure determination of p-nitrobenzylideneaniline and for retrieving structural information on the tetracycline antibiotics. The help and friendship of Ms. Vicky Allen along the way is also recognized. I am grateful to Ms. Jennifer Walsh for her assistance in printing this thesis. I thank Mr. Ken Schmidt at the University of Calgary for sending me several PNP salts. I thank Dr. R. Kirchlechner of Merck company in Darmstadt, West Germany, for sending a sample of thiatetracycline hydrochloride. Dr. M. McKinnon is acknowledged for acquiring some cp/mas nmr spectra of the tetracyclines. Dr. S.J. Opella and Dr. N. Clayden are acknowledged for sending our research group copies of the Fortran programs for simulating magic angle spinning nmr spectra. Mr. Brian Millier at Dalhousie University and Mr. Stan Woodman at Bruker Spectrospin Canada Ltd., are both to be acknowledged for their technical assistance with the Bruker MSL-200 spectrometer.

I would like to acknowledge the Dalhousie University Department of Chemistry for giving me the privilege of being the first holder of the Walter J. Chute scholarship in chemistry. In addition, I acknowledge the I.W. Killam foundation for a postgraduate fellowship throughout my stay at Dalhousie. The financial contribution of the W.C. Sumner foundation during my second and third years at Dalhousie is also appreciated. Finally, I would like to thank the Natural Science and Engineering Research Council of Canada for financial support in the form of a postgraduate scholarship over the past four years at Dalhousie University.

I. Introduction

The utility of high-resolution nuclear magnetic resonance (nmr) spectroscopy for the study of molecular structure and dynamics in solution has become well established. The principal basis of this technique has relied on the empirical correlation of observed chemical shifts (δ's), spin-spin coupling constants (J's) and assorted nmr relaxation phenomena (e.g., T_1's, T_2's, nOe's) with experimental and theoretical results for model systems of known structure. In contrast, high-resolution solid state nmr spectroscopy is a relative newcomer as an experimental technique for the study of molecular structure. Consideration of early applications of nmr to the study of solids provides an indication of reasons for the delay in the development of this method.

The principal problem encountered when attempting to obtain a high-resolution nmr spectrum of a solid is how to overcome the larger inherent line widths observed in the nmr spectra of solids as compared to those from liquids. For example, the ^1H nmr line width of a liquid sample of water at room temperature is less than 1 Hz whereas Pake observed a ^1H nmr spectrum for the hydrated water molecules of powdered samples of gypsum, $CaSO_4 \cdot 2H_2O$, that exceeded 40 kHz in breadth [1]. The difference in behaviour between the solid and liquid samples is well understood and can be attributed to the anisotropic nature of spin interactions in solids which are effectively removed in solution by rapid random rotational

molecular motions. Pake recognized this fact and derived an expression to account for the influence of the anisotropic intramolecular homonuclear dipolar interaction between the two hydrogen nuclei of each water molecule in solid $CaSO_4 \cdot 2H_2O$. For a particular orientation (figure I.1) of the ^1H-^1H internuclear vector in the magnetic field, B_o, the effective field, B_{eff}, at one of the ^1H nuclei is :

$$B_{eff} = B_o \pm 3/4\ (\mu_o/4\pi)(h/2\pi)\ r_{HH}^{-3}\ \gamma_H\ (3\cos^2\theta - 1) \qquad [I.1]$$

Here r_{HH} is the ^1H-^1H separation, γ_H the magnetogyric ratio for hydrogen and θ is the angle between the ^1H-^1H internuclear vector and the static magnetic field, B_o. Thus, for a specific orientation of r_{HH} in the static magnetic field (e.g., an oriented single crystal), two resonance signals are observed in the ^1H nmr spectrum. Since all orientations of the ^1H-^1H internuclear vector are possible for a powdered sample, the resulting ^1H nmr spectrum represents a collective average of a large number of allowed transitions and a characteristic powder line shape is observed. An example of this type of ^1H nmr spectrum is shown in figure I.2. The orientations where the ^1H-^1H internuclear vector is parallel to the magnetic field (θ=0°) and perpendicular to the magnetic field (θ=90°) are indicated. Analysis of the orientation dependent dipolar splittings in nmr spectra such as figure I.2 allows one to calculate the ^1H-^1H internuclear separation, r_{HH}. Pake exploited this fact and determined that for each molecule of hydration in $CaSO_4 \cdot 2H_2O$, the intramolecular internuclear

Figure I.1

The angle θ defines the orientation of the ^1H-^1H internuclear vector with respect to the static magnetic field, B_o.

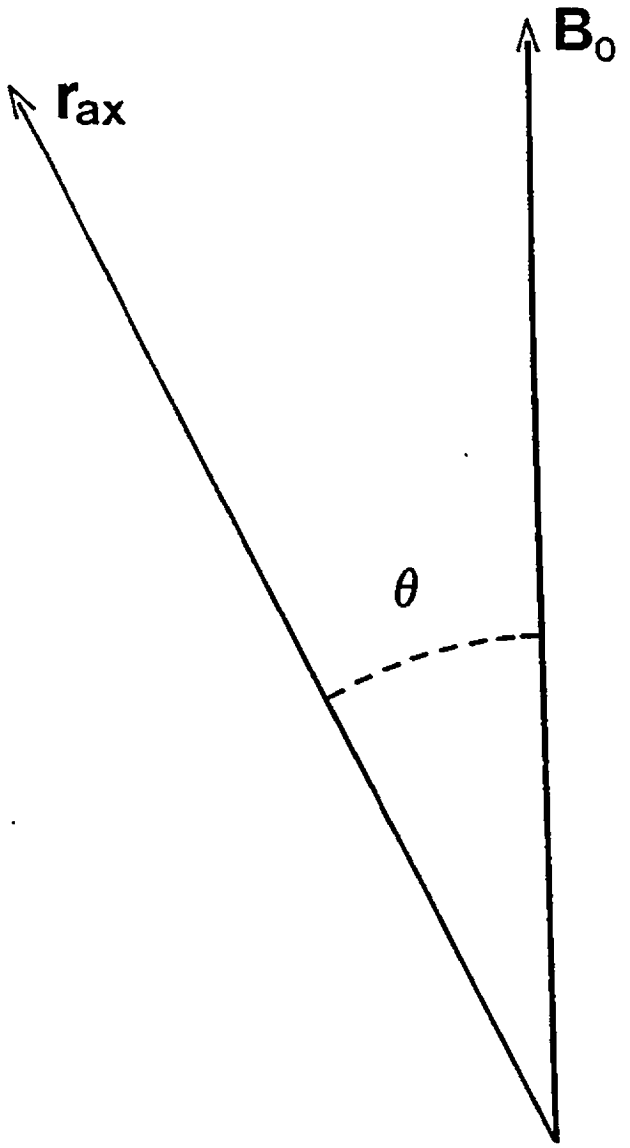

Figure I.2

A "Pake doublet" ^{1}H nmr spectrum for two "isolated" dipolar coupled ^{1}H nuclei with an internuclear separation of 1.58 Å. The spectrum was obtained by computer simulation based on equation I.1.

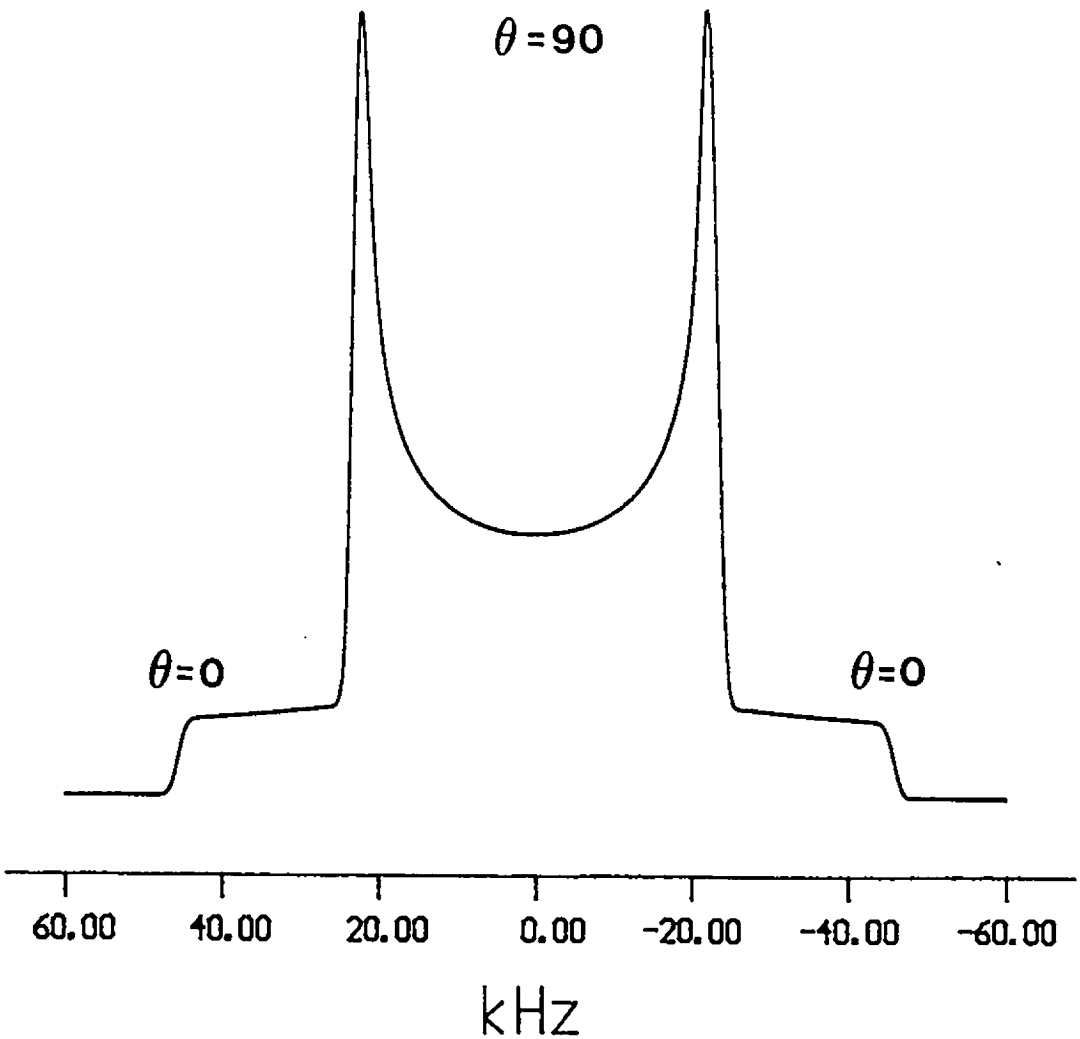

^1H-^1H separation is 1.58 Å. This was an important experimental result in 1948 and as a tribute to his early experiments, this characteristic line shape which is observed for a powder sample containing two "isolated" dipolar coupled spins is often referred to as a "Pake doublet".

Overcoming the anisotropic nature of spin interactions present in solid samples presented a formidable task for nmr experimentalists. It was realized early on that molecular motion often leads to a significant amount of line narrowing in the observed ^1H nmr spectrum of a powdered solid [2,3]. The natural extension of these experiments suggested that mechanical rotation might "fool" the spin system into believing it is in an isotropic environment. Indeed, in 1958, Andrew and his coworkers described the first example where dipolar broadening was reduced in the ^{23}Na nmr spectrum of a single crystal of sodium chloride by rapid sample rotation [4]. They demonstrated that for spin interactions with an angular dependence described in equation I.1, contributions to the nmr spectrum are reduced when the sample is rotated about an axis inclined at 54°44'8" with respect to the static magnetic field, B_o. Shortly thereafter, in 1959, Lowe observed narrowing of the ^{19}F resonance for a single crystal of calcium fluoride which was subjected to rapid rotation at 54°44'8" with respect to the magnetic field, B_o and thus confirmed the applicability of the method to multinuclear spin systems [5]. The term 'magic angle spinning' (mas) evolved

in 1960 while Andrew was presenting his results at a conference when C.J. Gorter inquired about the 'magic' properties of this angle [6].

Although ^{1}H nmr studies of solids in the pre-1970's provided significant advances to the technique as a modality for the study of molecular structure, it became apparent in the early 1970's that the study of heteronuclei such as ^{13}C and ^{15}N by nmr would be desirable. Indeed, early applications of dilute spin nmr spectroscopy to the study of chemical systems in solution indicated the potential utility of this method for obtaining detailed structural information [7]. There were several problems associated with the nmr study of rare spin systems which had to be mastered in order to obtain solution-like nmr spectra from solids. Primarily, the low inherent sensitivity of nuclei such as ^{13}C and ^{15}N made it difficult to obtain useful nmr spectra on continuous wave spectrometers even with selective isotopic enrichment. With the advent of pulsed Fourier transform nmr spectroscopy, problems associated with low natural abundance and small magnetogyric ratio could be reduced by simply accumulating a sufficient number of time domain transients to improve the signal to noise ratio [8]. Soon after, pulse sequences for the observation or elimination of specific nuclear spin interactions began to appear and the routine observation of high-resolution solution nmr spectra for rare spins such as ^{13}C became much simpler [7]. A second major problem associated

with the observation of nmr spectra for rare spins was the inherently longer spin-lattice relaxation times of these nuclei with respect to hydrogen. In the early 1970's, Pines et al. described a pulse sequence for solids which not only enhanced the nmr signal for the dilute spins (e.g. ^{13}C) but also could be repeated at an interval determined by the ^{1}H spin-lattice relaxation time [9]. The experiment, which involves a transfer of magnetization from abundant spins to the rare spins, is termed cross polarization (cp). The final problem to overcome before obtaining high-resolution nmr spectra of dilute spins in solids was how to alleviate the effect of the chemical shift anisotropy (csa). Since the angular dependence of the chemical shift is similar to that of the magnetic dipolar interaction, it too is averaged by mas. Thus, in a most significant experiment, Schaefer and Stejskal combined magic angle sample spinning (mas) with hydrogen/carbon cross polarization (cp) and high-powered hydrogen decoupling to observe the first high-resolution ^{13}C cp/mas nmr spectrum of a powdered solid sample [10].

Since the first reports of high-resolution ^{13}C cp/mas nmr spectra in 1976, the most significant developments in the nmr of solids have involved improvements in nmr instrument design and the ability to routinely perform multinuclear and multi-dimensional nmr experiments under the control of a computer [11]. With the coincident improvements in sensitivity, it is now possible to obtain information on the anisotropic nature

of the dipolar and chemical shift interactions directly from a dilute spin nmr spectrum for a static powdered sample [12]. This is an important result, since in favourable cases, it allows one to determine structural information (i.e., bond lengths) for powdered samples from dilute spin nmr spectra.

The principal objective of this thesis is to illustrate some applications of solid state nmr to the study of molecular systems of chemical and biological importance. The approach taken is multinuclear in nature although it is restricted to the study of spin I=1/2 nuclei - namely, ^{13}C, ^{15}N and ^{31}P. The thesis itself is divided into five main sections. Following this introduction, a brief theoretical description of the relevant spin interactions for spin 1/2 nuclei in solids and the basic nmr techniques used in this report will be presented. The theoretical description is by no means complete and more elaborate discussions can be found in several excellent texts [12-19]. Section III will focus on some particularly useful solid state nmr techniques that can be used to improve the quality of experimental nmr spectra and to assist in the assignment of high-resolution cp/mas nmr spectra. The bulk of the thesis is presented in section IV which is divided into three parts : A, B and C. Each of these three parts is complete in itself and is divided into four subsections : 'Introduction', 'Experimental', 'Results and Discussions' and 'Summary'. Parts A and B are concerned with the application of dipolar-chemical shift nmr spectroscopy to

the study of "isolated spin-pairs" for the characterization of chemical shift tensors. The carbon-nitrogen double bond of benzylideneaniline and related imines will be the focus of part A. Part B will be concerned with the ^{15}N and ^{31}P shielding properties of the first stable compound containing a phosphorus-nitrogen triple bond. In the final part of the applications section (part C), the results of high-resolution ^{13}C and ^{15}N cp/mas nmr studies on several solid tetracycline antibiotics will be presented and related to the structural forms of these compounds in solution. Concluding remarks as to the pertinent new information obtained in the thesis will be summarized in the last section.

The equations, figures and tables have been inserted into the text where they are referred to. They are numbered according to the section in which they appear starting with I.1, II.1, III.1, IV.1 and V.1 for section I, II, III, IV and V, respectively. References are numbered consecutively throughout the thesis and are listed at the end.

II. Basic Solid State NMR Theory

A. The Nuclear Spin Hamiltonian

The Hamiltonian for a general nuclear spin interacting with its environment can be expressed as a sum [12-19] :

$$H = H_Z + H_{RF} + H_{CS} + H_Q + H_D + H_J \qquad [II.1]$$

The first term, H_Z, expresses the interaction of the nuclear spin with the static magnetic field, B_o. H_{RF} corresponds to the interaction of the nuclear spin with a weak external radio-frequency field, B_1, which provides a means for perturbing and studying the spin system. The remaining terms in equation II.1 describe the interaction of the nuclear spin with internal magnetic fields associated with the presence of nearby electrons or other nuclear spins. The magnetic interaction between the nuclear spin and the electrons circulating around the nucleus is described by the chemical shielding term, H_{CS}. H_Q corresponds to the interaction of the electric field gradient with the nuclear quadrupolar moment. The H_D and H_J terms correspond to the interaction of two proximate nuclear spins via through space and via the intervening electrons, respectively. The latter interactions are responsible for the indirect spin-spin coupling of nuclei whereas the former give rise to direct dipolar couplings. All Hamiltonians in this thesis are defined in energy units (Joules). The nature of each of these interactions will be discussed in turn.

A.1 The Zeeman Interaction

Classically, the action of a charged nucleus A spinning about its own axis produces a small magnetic moment, μ_A. The Zeeman interaction of the nuclear magnetic moment with an external magnetic field, B_o, can be written as :

$$H_Z = -\vec{\mu}_A \cdot \vec{B}_o = -(h/2\pi)\ \gamma_A\ \vec{B}_o \cdot \vec{I}_A \qquad [II.2]$$

where γ_A is the gyromagnetic ratio of nucleus A and $\vec{I}_A$ is a spin operator, $\vec{I}_A \equiv (I_{Ax}, I_{Ay}, I_{Az})$. The static external magnetic field is generally chosen to lie along the z-direction and under such conditions $\vec{B}_o \equiv (0,0,B_o)$. Hence, the Zeeman Hamiltonian may be described as :

$$H_Z = -(h/2\pi)\ \gamma_A\ B_o \cdot \vec{I}_{Az} \qquad [II.3]$$

where $\vec{I}_{Az}$ represents the component of the nuclear spin in the z-direction. Solution of the time independent Schrödinger equation ($H_Z|\Psi\rangle = E|\Psi\rangle$) yields a set of energy levels quantized along B_o with quantum number m_I and energies given by :

$$E_{m_I} = -(h/2\pi)\ \gamma_A \cdot m_I \cdot B_o \qquad [II.4]$$

Since the quantum number m_I is restricted to the values $m_I = -I, -I+1, \ldots I$, only two states are available for an isolated spin with I=1/2. The energy required to induce a pure Zeeman transition between these two states is :

$$\nu_o = \omega_o/(2\pi) = \gamma_A\ B_o/(2\pi) \qquad [II.5]$$

where ν_o and ω_o are the Larmor frequency of nucleus A in Hz and $rads^{-1}$, respectively. The values of the Zeeman interaction (in MHz) and the spin properties of the nuclei discussed in this thesis are shown in table II.1 for B_o=4.7 T [20].

Table II.1

NMR properties of the nuclei discussed in this thesis. The Zeeman energies correspond to a static magnetic field strength of B_o=4.7 T.

Isotope	Natural Abundance (%)	Spin I	Gyromagnetic Ratio, γ (10^7 $radT^{-1}s^{-1}$)	Quadrupole Moment, Q (10^{-28} m^2)	NMR Frequency (MHz)
^{1}H	99.985	1/2	26.7522		200.13
^{13}C	1.108	1/2	6.7283		50.32
^{14}N	99.635	1	1.9338	$1.67x10^{-2}$	14.47
^{15}N	0.365	1/2	-2.7126		20.29
^{35}Cl	75.530	3/2	2.6242	$-8.20x10^{-2}$	19.63
^{37}Cl	24.470	3/2	2.1844	$-6.50x10^{-2}$	16.34
^{31}P	100.000	1/2	10.8394		81.03

For a spin system at thermal equilibrium, the Boltzmann law predicts that the population of the energy level associated with each m_I is proportional to $\exp(h\nu_o m_I/kT)$ where k is the Boltzmann constant and T is the absolute temperature. Since the energy of nuclear spins aligned parallel to B_o is slightly lower than the energy for those opposed to the static magnetic field, a net magnetization M_o develops along the z-direction parallel to B_o. For nmr, where ($h\nu_o << kT$) for experimentally accessible temperatures, M_o can be expressed

according to equation II.6, which is known as the Curie law [14]. An implication of equation II.6 is that a spin system

$$M_o = \frac{N(\gamma_A(h/2\pi))^2\, I(I+1))\; B_o}{3kT} \qquad [II.6]$$

with a low "spin temperature" has a greater net magnetization (M_o) than a system with a high "spin temperature". An example of how one can experimentally exploit this fact will be discussed in section II.C. The small excess of spins oriented along the z-direction, M_o, is the source of the observed nmr signal.

A.2 The Effect of RF Pulses

The time dependent Hamiltonian describing the interaction of nuclear spins with a weak radio-frequency field, $B_1(t)$, applied in the transverse plane [19] is :

$$\mathcal{H}_{RF}(t) = -(h/2\pi)\gamma_A\vec{B}_1(t)\cdot\vec{I}_A = -(h/2\pi)\omega_1(I_{Ax}\cos\omega t - I_{Ay}\sin\omega t) \qquad [II.7]$$

where B_1 represents the amplitude of the rf field, $\vec{B}_1(t)$ is given by $B_1(\cos\omega t, -\sin\omega t, 0)$, $\omega_1=\gamma_A B_1$ and ω is the angular frequency of the rf field. The time dependence of $\mathcal{H}_{RF}(t)$ can be removed by expressing the Hamiltonian in a 'rotating reference frame', (x',y',z'), where B_1 rotates along with the laboratory coordinates x and y at an angular frequency ω about the z axis. In this reference frame, $\mathcal{H}_{RF}$ can be written as :

$$\mathcal{H}'_{RF} = -(h/2\pi)\;\gamma_A\; B_1\cdot\vec{I}_{Ax} = -(h/2\pi)\;\omega_1\cdot\vec{I}_{Ax} \qquad [II.8]$$

The similarity of this expression to equation II.3 suggests that the nuclear spin will interact with the rf field in an analogous manner to the interaction of the nuclear spin with the static magnetic field, B_o. That is, when the rf field (B_1) is applied in a pulsed fashion at the Larmor frequency along the x' axis for example, the net magnetization will be flipped an angle θ about the x' axis according to :

$$\theta = \gamma_A \cdot B_1 \cdot t_p \qquad [II.9]$$

where t_p is the length of the pulse and θ is the "flip angle". In the simplest pulse nmr experiment, a $\theta=\pi/2$ pulse applied at the Larmor frequency along the x' transforms the net magnetization originally along the z-direction to the y' axis. The resulting transverse magnetization, which fluctuates at or near the Larmor frequency, induces a small signal along the y' axis which is detected in the form of a 'free induction decay' (FID). The FID is digitized and Fourier transformed to give the conventional intensity versus frequency nmr spectrum. The decay of the FID in the transverse plane and the return to thermal equilibrium with the net magnetization along the z-direction (i.e., $M_z=M_o$) are determined by two characteristic time constants, T_2 and T_1, respectively. The latter determines how often one may pulse the spin system whereas the former is related to the observed line width in the nmr spectrum.

A.3 Chemical Shielding

When a sample is placed into an external magnetic field, B_o, the electrons around each nucleus are induced to circulate around the nucleus about the direction of the applied magnetic field. This gives rise to a small magnetic field which modifies the actual magnetic field that the nucleus experiences. For a nucleus in a symmetrical electronic environment (e.g., a free atom), the small induced magnetic field opposes the static magnetic field and therefore shields the nucleus from B_o. In general, the electronic distribution around any given nucleus in a molecule is unsymmetrical. Under such conditions, the small induced magnetic field is not necessarily parallel to the external magnetic field and can be described [17] as :

$$H_{CS} = -(h/2\pi)\ \gamma_A\ \vec{I}_A \hat{\sigma} \cdot \vec{B}_o \qquad [II.10]$$

where $\hat{\sigma}$ is the rank two chemical shielding tensor. In an arbitrary axis system (x,y,z) associated with the molecular reference frame, the chemical shielding tensor may be represented by nine components :

$$\hat{\sigma} = \begin{pmatrix} \sigma_{xx} & \sigma_{xy} & \sigma_{xz} \\ \sigma_{yx} & \sigma_{yy} & \sigma_{yz} \\ \sigma_{zx} & \sigma_{zy} & \sigma_{zz} \end{pmatrix} \qquad [II.11]$$

This tensor can be expressed as the sum of a symmetric ($\sigma_{ij}=\sigma_{ji}$) and antisymmetric ($\sigma_{ij}\neq\sigma_{ji}$) tensor each of which in principle contributes to the total shielding of the nucleus [17,21-23]. It has been demonstrated that the antisymmetric

contributions are small and influence the nmr spectrum in second order only and therefore shall be neglected [17,21,22]. However, if one wishes to obtain information about the antisymmetric part of the chemical shielding tensor, then a procedure outlined by Haeberlen should be consulted [23]. When only the symmetric part of the chemical shielding tensor is considered, then there are only six unknowns to be determined for complete characterization of the tensor. It is always possible to find an axis system such that $\hat{\sigma}$ is diagonal, equation II.12. This is termed the principal axis

$$\hat{\sigma} = \begin{pmatrix} \sigma_{11} & 0 & 0 \\ 0 & \sigma_{22} & 0 \\ 0 & 0 & \sigma_{33} \end{pmatrix} \qquad [II.12]$$

system (pas) of the chemical shielding tensor and σ_{11}, σ_{22} and σ_{33} are the three principal components. For a rigid chemical system, the pas of each nucleus is specifically related to the molecular frame. Thus, when the magnitudes of the three principal components and their orientation are known in the molecular reference frame, the chemical shielding tensor is completely characterized.

For a solid, the chemical shielding of a nucleus varies with the orientation of the molecule with respect to B_o (figure II.1) and the corresponding resonance frequency is :

$$\nu_\sigma = -\nu_o(\sigma_{11} \sin^2\theta \cos^2\varphi + \sigma_{22} \sin^2\theta \sin^2\varphi + \sigma_{33} \cos^2\theta) \qquad [II.13]$$

Here θ and φ are the polar and azimuthal angles which orient the magnetic field vector (B_o) in the principal axis system of the chemical shielding tensor. For a powdered sample, all

Figure II.1

The angles ϑ and φ define the orientation of the magnetic field vector (B_0) in the principal axis system of the chemical shielding tensor.

Figure II.1

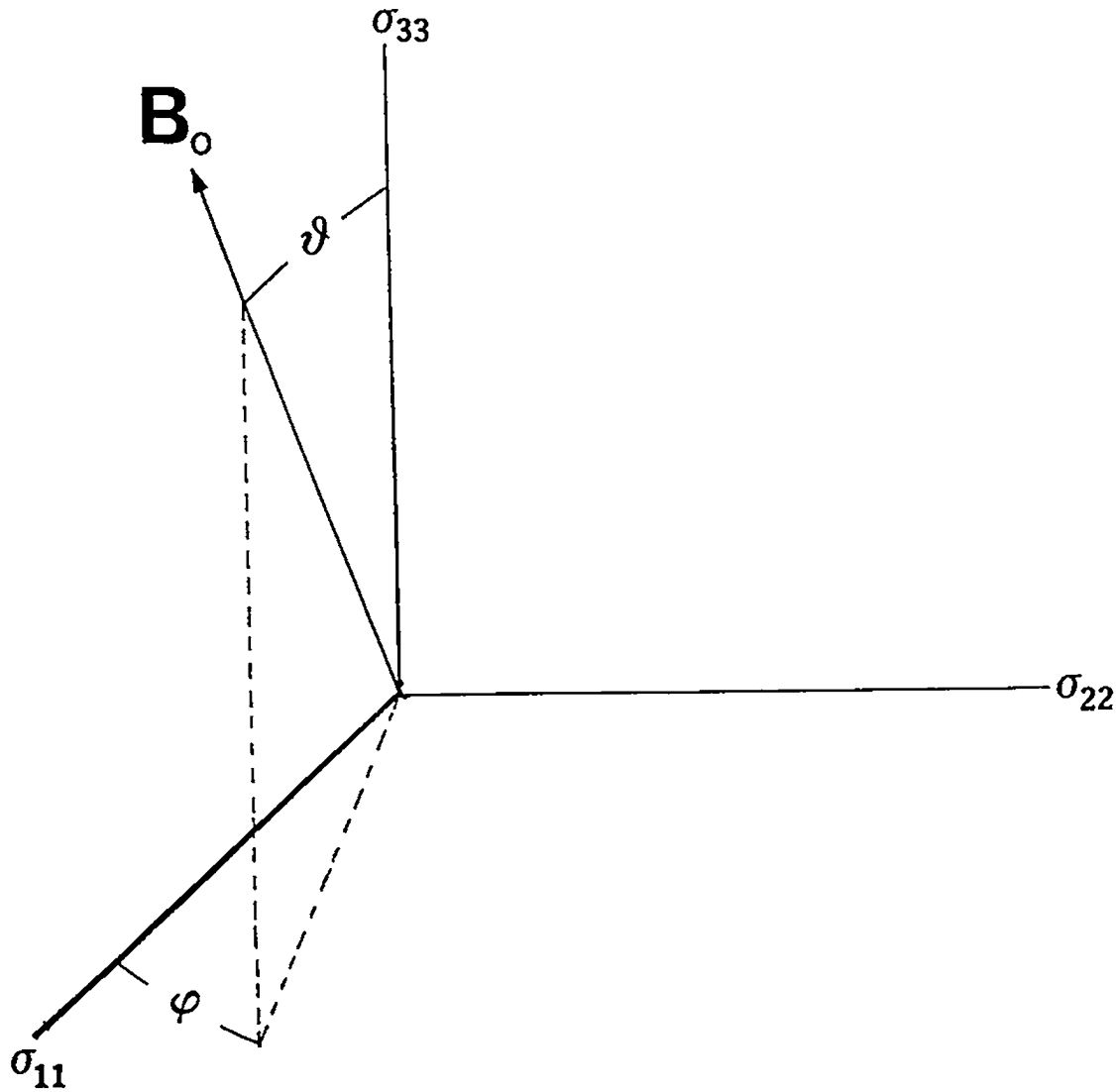

Figure II.2

Chemical shielding powder nmr line shape for (a) axially symmetric and (b) non-axially symmetric anisotropies.

Figure II.2

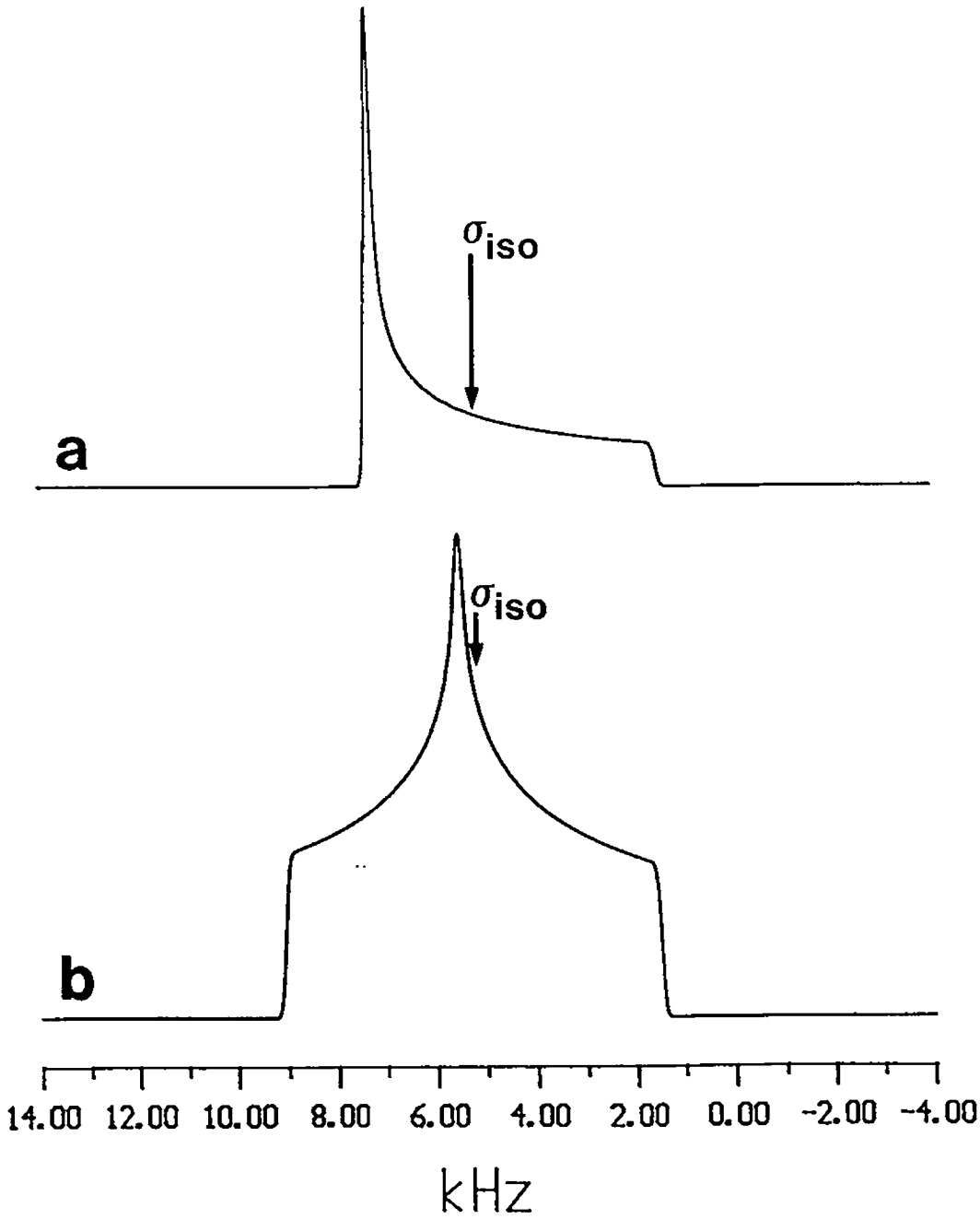

values of θ and φ are possible and the resulting line shape observed in the nmr spectrum of this nucleus is a broad powder pattern. Examples of theoretical powder patterns for axially symmetric ($\sigma_{11}=\sigma_{22}\neq\sigma_{33}$) and non-axially symmetric ($\sigma_{11}\neq\sigma_{22}\neq\sigma_{33}$) chemical shielding tensors of a spin I=1/2 nucleus are shown in figure II.2. The principal components of the shielding tensor are defined as $(\sigma_{33}-\sigma_{iso})\geq(\sigma_{11}-\sigma_{iso})\geq(\sigma_{22}-\sigma_{iso})$ and the breadth of the powder nmr spectrum in the absence of any other internal interaction, $\sigma_{33}-\sigma_{11}$, is defined as the chemical shielding anisotropy, $\Delta\sigma$. For the non-axially symmetric chemical shielding tensor the deviation from axial symmetry can be represented by an asymmetry parameter :

$$\eta_\sigma = (\sigma_{22}-\sigma_{11})/(\sigma_{33}-\sigma_{iso}) \qquad [II.14a]$$

which can take on values between 0 to 1. More elaborate definitions of these parameters can be found elsewhere [12,23].

In solution, random molecular rotations reduce the anisotropic nature of $\hat{\sigma}$ to an isotropic value :

$$\sigma_{iso} = (1/3)\ \mathrm{Tr}\ \hat{\sigma} = (\sigma_{11} + \sigma_{22} + \sigma_{33})/3 \qquad [II.15]$$

A solid state nmr technique that averages the csa to an isotropic value by mechanical rotation will be discussed in section II.C. The value of σ_{iso} represents the average shielding of the nucleus (figure II.2) in question relative to that of a bare nucleus. The absolute magnitudes of chemical shieldings of a nucleus are not easily obtainable [20] and thus it has become normal practice to measure

resonance frequencies relative to that of a particular nucleus in a standard reference sample. The differences between the sample and reference signals are referred to as chemical shifts, δ, and can be calculated in parts per million (ppm) from the expression in equation II.16. The subscripts s and

$$\delta_s = \{(\nu_s - \nu_r)/\nu_r\} \cdot 10^6 \approx (\sigma_r - \sigma_s) \cdot 10^6 \qquad [II.16]$$

r refer to the sample and reference, respectively. The principal components of $\hat{\sigma}$ can also be expressed as chemical shift principal components δ_{11}, δ_{22} and δ_{33} with the convention that $\delta_{11} \geq \delta_{22} \geq \delta_{33}$. It is important to make a clear distinction between absolute shieldings (σ's) and relative chemical shift values (δ's). Thus, a large positive value of δ_{11} corresponds to low shielding and a highly shielded nucleus will have a large positive value of σ_{11}. The asymmetry of the chemical shift tensor, η_δ, can be calculated from the expression :

$$\eta_\delta = (\delta_{22}-\delta_{11})/(\delta_{33}-\delta_{iso}) \qquad [II.14b]$$

The basic theoretical description of chemical shielding can be traced to early papers by Lamb [24] and Ramsey [25]. In 1941, Lamb derived an expression to account for the diamagnetic shielding of a free atom, σ^d, due to the induced magnetic field generated by the circulation of electrons about the nucleus [24]. The diamagnetic term, which is related to ground state wavefunctions, can be calculated accurately for free atoms from theoretical methods [25,26]. Thus, calculated values for σ^d for free atoms with atomic numbers from Z=2 to

Z=86 are available in the literature [25,26] and have indicated that σ^d is invariably positive (i.e., shields the nucleus). For a nucleus in a molecule, the expressions described by Lamb are not valid and therefore an alternative method must be used to estimate σ^d. An empirical approach outlined by Flygare et al. [27] has proven to be reliable for calculating σ^d for nuclei in molecules. Numerous calculations based on this model have [27] indicated that σ^d for a given nucleus does not vary significantly from compound to compound. That is, with the exception of hydrogen, variations in chemical shifts are not due to variations in σ^d.

Ramsey's original formulation of chemical shielding accounted for this fact by introducing a second term, σ^p, into the expression for chemical shielding. In this model, the shielding of the nucleus is described as a sum of two terms as indicated in equation II.17. The paramagnetic term, σ_A^p,

$$\sigma_A = \sigma_A^p + \sigma_A^d \qquad [II.17]$$

which is invariably negative, is related to excited electronic states and corrects for the unsymmetrical electron circulations around a nucleus in a molecule. A variety of approximate computational methods for estimating σ^p based on Ramsey's equations [25] for a nucleus in a molecule have been described and are concisely summarized in ref. 20. Theoretical discussions of the shielding of a nucleus are usually based on reformulations of Ramsey's theory by Saika and Slichter [28] and Pople [29]. These models express the

shielding of a nucleus, A, as a sum of three terms : σ_A^p, σ_A^d and a sum of terms given by σ_A^X which accounts for the effects that electron circulations centred on atoms different from A have on the shielding of the A nucleus. Since Pople and Karplus [29] have demonstrated that contributions from the paramagnetic term centred on the nucleus are primarily responsible for chemical shift variations, the σ_A^X terms are often neglected in qualitative discussions of shieldings. This assumption will be made in the discussions which follow.

The description of Pople and Karplus [29] provides a direct model for examining the relationship of the local electronic environment and the shielding of a nucleus in terms of specific tensor elements, $\sigma_{\alpha\alpha}$. If α, β and γ define an orthogonal reference frame, then for a particular atom, σ^p for each specific tensor element can be described [29] as :

$$\sigma^p_{\alpha\alpha} = -2\ (\mu_o/4\pi)\ \mu_B^2\ \langle r^{-3}\rangle_p \sum_j^{occ} \sum_k^{unocc} (\Delta E_{jk})^{-1}\ (C_{j\beta}\ C_{k\gamma} - C_{j\gamma}\ C_{k\beta}) \qquad [II.18]$$

where μ_o is the permeability constant, μ_B is the Bohr magneton ($eh/4\pi m_e$), $\langle r^{-3}\rangle_p$ is the average inverse cube of the distance of the p electrons from the nucleus, ΔE_{jk} is the one electron excitation energy from the j^{th} occupied molecular orbital (MO) to the k^{th} unoccupied MO and $C_{j\beta}$ is the coefficient of the $2p_\beta$ atomic orbital in the j^{th} MO on atom A. On the basis of this model, the paramagnetic term would be anticipated to increase the closer the p electrons are to the nucleus, the smaller the appropriate ΔE_{jk} and the larger the values of the coefficients

in the MO's associated with the ΔE_{jk} term. Note that electrons localized in s orbitals do not contribute to σ^p for atom A.

The energy term (ΔE_{jk}) consists of contributions from excited states for magnetic-dipole-allowed transitions. For example, one electron transition energies between $n\rightarrow\pi^*$, $n\rightarrow\sigma^*$, $\sigma(p_y)\rightarrow\sigma^*(p_z)$, $\pi\rightarrow\sigma^*$, etc. or the average of a few of these transitions usually dominate the paramagnetic shielding of a particular principal component (σ^p_{11}). It is important to point out that in all cases, the paramagnetic contributions to each specific principal component, $\sigma^p_{\alpha\alpha}$, are associated with electronic excitations which involve MO's that are derived from atomic orbitals in the plane orthogonal to the orientation of the principal axis. For example, σ^p of the least shielded element (σ_{11}) of the ^{13}C chemical shielding tensor of formaldehyde which is oriented parallel to the C=O bond is dominated by a low-lying $n\rightarrow\pi^*$ transition energy [32]. The importance of $\Delta E_{n\rightarrow\pi^*}$ becomes more pronounced when discussed in the context of nitrogen and phosphorus chemical shieldings. In these systems, the presence of a lone pair of electrons on the atoms has a marked influence on the overall chemical shielding properties of the nitrogen and phosphorus nuclei.

Another factor which should be considered when discussing paramagnetic shielding contributions is the symmetry of the local electronic distribution around the nucleus. It has already been stated that σ_p is zero for a spherically symmetric electronic environment as is the case for a free

atom. Consideration of the electronic symmetry in acetylene, H-C≡C-H, indicates that the electrons are free to "circulate" around the bond along the C_∞ axis. Thus, the paramagnetic contribution to the ^{13}C shielding of the C_2H_2 is zero when the molecule is oriented parallel to B_o and a maximum when the C_∞ axis of the molecule is oriented perpendicular to B_o. This simple qualitative description is consistent with the electronic symmetry restrictions of Ramsey's original formulation of chemical shielding [25] and provides further support for the fact that each σ_{ii} is dominated by electron "circulations" in the plane perpendicular to the principal component of the chemical shielding tensor.

Finally, it should be noted that the nuclear site symmetry can impose some restrictions on the number of independent principal values of the chemical shielding tensor [30,31]. For example, if the nuclear site symmetry is C_{3v} as for the carbon nucleus of $CHCl_3$, then only two independent principal components are sufficient to completely describe the shielding tensor. If the nuclear site symmetry is tetrahedral or higher, then the tensor is completely described by a single isotropic value. Note that this latter situation implies that the molecular point group symmetry is at least cubic or higher. The point to be stressed from this discussion is that the chemical shielding anisotropy of a nucleus in a molecule is a distinct reflection or "fingerprint" of the local site symmetry of the atom.

A.4 The Quadrupolar Interaction

Although the focus of this thesis is directed towards the study of spin I=1/2 nuclei, there are several examples throughout this monograph where interactions between a spin 1/2 nucleus, A, and a quadrupolar nucleus, X, are important. In some cases, solid state nmr studies of a spin 1/2 nucleus which is dipolar coupled to a quadrupolar nucleus provide useful information which can be related to the molecular structure. The theoretical aspects of this will be examined in the following two sections, II.B and II.C, of this chapter.

The quadrupolar interaction is only relevant for nuclei with a non-spherical charge distribution and a spin I>1/2 (see table II.1). In tensor notation the quadrupolar Hamiltonian may be represented [14] as :

$$H_Q = \frac{eQ}{6I(2I-1)} \vec{I}_X \hat{V} \cdot \vec{I}_X \qquad [II.19]$$

where eQ is the nuclear quadrupole moment, $\vec{I}_X$ is the spin vector of nucleus X, and $\hat{V}$ is the traceless, symmetric rank two electric field gradient tensor at the nucleus. In its own principal axis system where $\hat{V}$ is diagonal, equation II.19 can be expressed in terms of the nuclear quadrupolar coupling constant, $\chi=(e^2q_{zz}Q)/h$ as :

$$H_Q = \frac{\chi \cdot h}{4I(2I-1)} [3I_{Xz}^2 - I^2 + \eta_Q(I_{Xx}^2 - I_{Xy}^2)] \qquad [II.20]$$

where $V_{ii}=eq_{ii}$ (i=1,2,3) with the convention $|V_{33}| \geq |V_{11}| \geq |V_{22}|$

and η_Q is defined as $(V_{11}-V_{22})/V_{33}$.

The Hamiltonian represented by equation II.20 is only valid in the high-field limit where $H_z >> H_Q$ [33-35]. If the value for $\chi(X)$ for a given X nucleus approaches the Larmor frequency of that same nucleus $\nu_o(X)$, then this condition will not be satisfied. Under these circumstances, the axis of quantization for the quadrupolar nucleus is no longer the z-direction of the rotating frame and thus the eigenfunctions for the quadrupolar nucleus are no longer the normal X spin Zeeman eigenfunctions, $|I,m>$. Although this may appear to be a disadvantage from an nmr view point, there are distinct advantages when the nuclear quadrupolar coupling constant of the X nucleus is large enough such that the high-field approximation is not strictly valid.

A.5 The Direct Dipolar Interaction

The direct dipolar interaction for two isolated spins A and X can be expressed [12,14,17,19] as :

$$H_D = (\mu_o/4\pi)(h/2\pi)^2 \gamma_A\gamma_X \langle\overline{r_{AX}^{-3}}\rangle \vec{I}_A \cdot \hat{D} \cdot \vec{I}_X \qquad [II.21]$$

where $\langle\overline{r_{AX}^{-3}}\rangle$ is the average internuclear separation between the two spins A and X, $\vec{I}_A$ and $\vec{I}_X$ are the spin operators for A and X and $\hat{D}$ is the traceless axially symmetric rank two dipolar coupling tensor. In the principal axis system of the dipolar tensor, r_{AX} is oriented along the z-direction and the dipolar tensor is given in equation II.22.

$$\hat{D} = \begin{pmatrix} 1 & 0 & 0 \\ 0 & 1 & 0 \\ 0 & 0 & -2 \end{pmatrix} \qquad [II.22]$$

The dipolar Hamiltonian may be expressed in spherical polar coordinates [17,19] to give the expression in equation II.23, which is referred to as the "dipolar alphabet". Only the A and B terms are included in this discussion and the remaining expressions of the "dipolar alphabet" can be found in several texts [12,14,17].

$$H_D = (\mu_o/4\pi)(h/2\pi)^2 \gamma_A\gamma_X \langle\overline{r_{AX}^{-3}}\rangle [A+B+C+D+E+F] \qquad [II.23]$$

where $A = -\vec{I}_{A_z}\vec{I}_{X_z}(3\cos^2\theta-1)$

$$B = (1/4)\ [I_{A+}I_{X-} + I_{A-}I_{X+}]\ (3\cos^2\theta-1)$$

In these expressions, I_{A+} and I_{X-} are the "raising" and "lowering" operators for the corresponding A or X nucleus (e.g., $I_+=I_x+iI_y$) and θ is the angle between the internuclear vector r_{AX} and the static magnetic field, B_o (see figure I.1). For two unlike spins A and X where the difference in Zeeman energies is large, only the A-term of the "dipolar alphabet" commutes with the Zeeman operator (equation II.3). Therefore, only this term has to be considered when determining the first order perturbations to the Zeeman energy levels of an "isolated" dipolar coupled two spin system. For a specific orientation of the dipolar vector (r_{AX}) in the magnetic field, the A nucleus resonance frequency can be expressed as :

$$\nu_D(A) = \nu_o(A) + m_x R(3\cos^2\theta - 1) \qquad [II.24]$$

where m_x is the spin quantum number of the X nucleus and R is

the dipolar coupling constant defined in Hz as :

$$R = (\mu_o/4\pi)\ (h/4\pi)\ \gamma_A\gamma_X\ \overline{\langle r_{AX}^{-3}\rangle} \qquad [II.25]$$

Thus, for an oriented single crystal of an "isolated" two spin system where the A nucleus is dipolar coupled to X nucleus of spin I=1/2, the A-spin nmr spectrum consists of two sharp resonance lines. For a powdered sample of this same material, all orientations of r_{AX} relative to B_o are possible and a "Pake doublet" line shape is observed in the nmr spectrum of the A nucleus. For such a heteronuclear spin pair, the dipolar splittings at the discontinuities (θ=90°) and shoulders (θ=0°) are R and 2R, respectively. Conversely, if the X nucleus of the AX spin-pair has a spin I=1, then three overlapping powder patterns are observed in the A spin nmr spectrum. Examples of theoretical ^{13}C dipolar nmr spectra for "isolated" $^{13}C,^{15}N$ and $^{13}C,^{14}N$ spin pairs are shown in figure II.3. Note that for the $^{13}C,^{14}N$ spin pair (figure II.3b), two sets of dipolar splittings are observed at the discontinuities (θ=90°) and shoulders (θ=0°) with magnitudes of R and 2R, respectively. However, the actual value of R for the $^{13}C,^{14}N$ spin pair is reduced by a factor of $\gamma(^{14}N)/\gamma(^{15}N)$ = 0.713 (see table II.1) according to the expression for R given in equation II.25. If the high-field approximation for the quadrupolar nuclei is not satisfied, then other terms of the "dipolar alphabet" begin to contribute to the nmr spectrum and modify the observed dipolar splittings.

Figure II.3

Calculated ^{13}C dipolar nmr spectra for isolated heteronuclear spin pairs assuming zero ^{13}C csa. The spectrum in (a) corresponds to that for two spin I=1/2 nuclei, ^{13}C and ^{15}N whereas in (b) the ^{13}C nucleus is dipolar coupled to an I=1 ^{14}N nucleus. The bond length used to calculate the nmr spectra was 1.40 Å.

Figure II.3

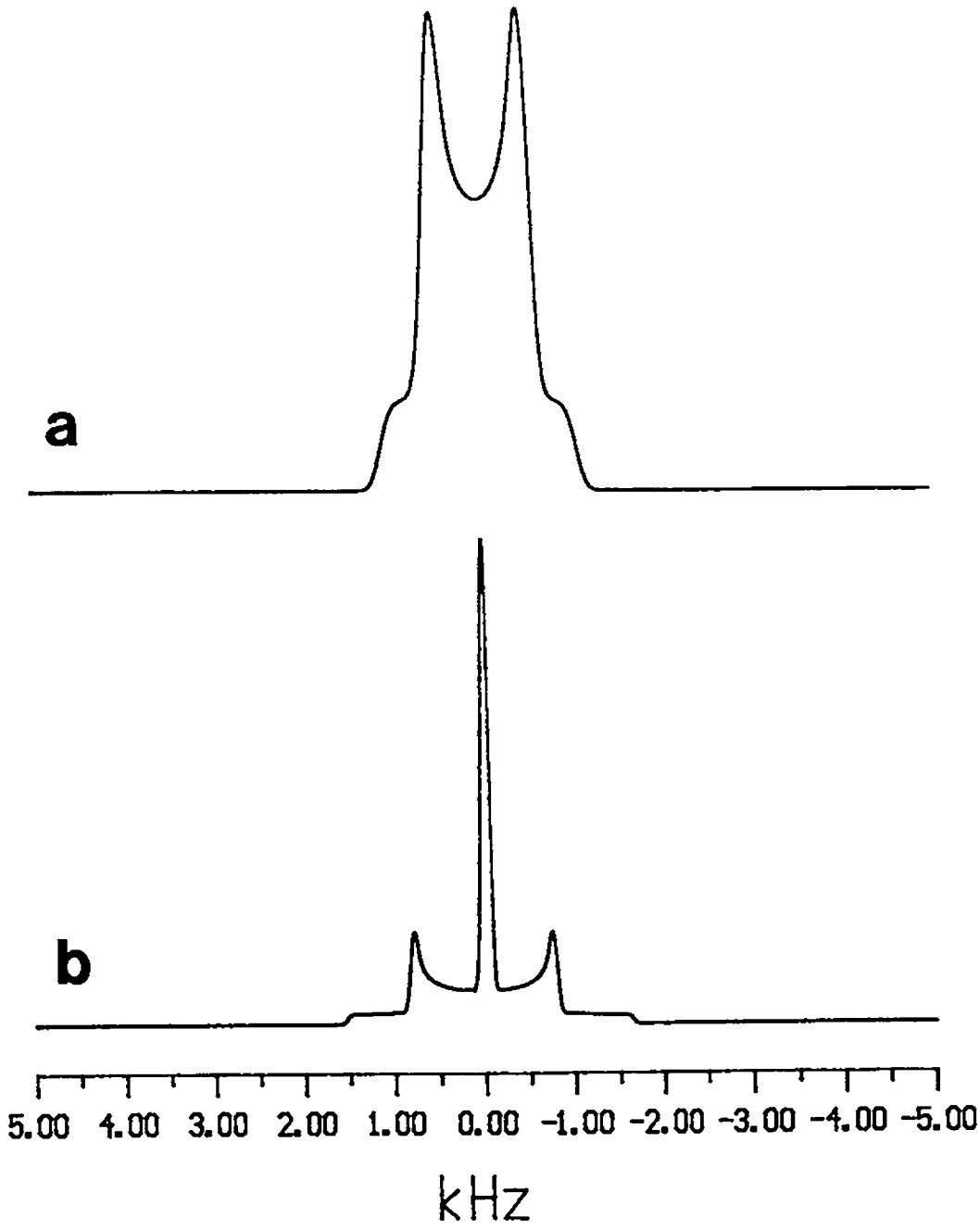

It is important to remember that the dipolar splittings are orientation dependent and that they depend on the inverse cube of the r_{AX} bond length. Thus, in principle, it is possible to obtain structural information from an nmr spectrum of two dipolar coupled nuclei. This may not always be possible since other interactions or molecular motions may interfere with an accurate measurement of R. The principal dipolar interactions of concern to this thesis are those between heteronuclei such as ^{13}C, ^{15}N and ^{31}P. Based on table I.1, equation II.25 and r_{AX} bond lengths between 1.20 Å and 2.0 Å values of R are anticipated to be in the range of approximately several hundred Hz to 1.5 kHz.

Since homonuclear spin interactions are always present in some form for any chemical sample, a closer examination of such spin systems is worthwhile. For a two-spin system of spin I=1/2 nuclei, the B term of the dipolar Hamiltonian also commutes with the Zeeman Hamiltonian. An expression similar to equation II.24 can be derived for the nuclei of the homonuclear spin pair as :

$$\nu_D(A) = \nu_o \pm (3/4)\ R\ (3\cos^2\theta - 1) \qquad [II.26]$$

which is closely related to equation I.1. In this case, the splittings of the discontinuities (θ=90°) and shoulders (θ=0°) in a purely dipolar nmr spectrum of an equivalent spin pair are 3R/2 and 3R, respectively. One further point relating to the nature of term B should be discussed. That is, the B term contains the shift operators I_+ and I_- which alter both nuclear

spin states by ±1. As such, it is often referred to as the "flip-flop" operator and it is particularly important in the study of solids by nmr since it allows nuclear spins to exchange spin information. Thus, it provides a path for spin-lattice relaxation (T_1) of nuclei in solid samples [12].

A.6 The Indirect Dipolar Interaction

The interaction of two proximate nuclear spins, A and X, via the intervening electrons in chemical bonds can be expressed [12,17] as :

$$H_J = (\mu_o/4\pi)(h/2\pi)\ \vec{I}_A \cdot \hat{J} \cdot \vec{I}_X \qquad [II.27]$$

where $\hat{J}$ is the second rank indirect coupling tensor. At present, the information available in the literature on the anisotropic nature of $\hat{J}$ is limited [36-44]. However, it has been generally assumed, with some justification [39,44], that for the one bond spin-spin coupling in a variety of molecular systems, the J tensor is axially symmetric. That is, $J_\parallel$ is oriented along the internuclear vector and $J_\perp$ resides in the plane orthogonal to r_{AX}. The close analogy of $\hat{J}$ to $\hat{D}$ is reflected in the fact that the two tensors transform in a similar manner. Thus, it is not easy to separate these two interactions in an nmr experiment. If the anisotropy in J is defined as $J_\parallel - J_\perp$, then a modified expression for the effective dipolar coupling constant, R', can be expressed as :

$$R' = R - (\Delta J/3) \qquad [II.28]$$

The trace of the J tensor corresponds to the isotropic value, J_{iso} which is observed in solution due to random molecular rotations :

$$J_{iso} = (2J_{\perp} + J_{\parallel})/3 \qquad [II.29]$$

Reliable values of ΔJ are difficult to find in the literature. However, based on a limited number of theoretical [36-38,40-44] and experimental [39,44] results, values of ΔJ are anticipated to be approximately $10 \cdot J_{iso}$ or less. In addition, the anisotropy in J is expected to be negligible for indirect couplings between second row elements (e.g., ^{13}C and ^{15}N) but increases substantially when the indirect coupling involves heavier nuclei [20,39].

B. Chemical Shift-Dipolar NMR of Isolated Spin Pairs - Static Samples

Complete characterization of the chemical shift parameters for a nucleus in a molecule requires a knowledge of both the magnitudes and orientations of the three principal components of the chemical shift tensor (δ_{ii}, i=1,2,3) in the molecular frame of reference. Therefore, in general, six parameters are required; the three principal components and three Euler angles. The traditional approach for obtaining such information has been to study single crystals via solid state nmr spectroscopy and determine the magnitudes and orientation of the three principal components of the chemical shift tensor in the crystal axis system from chemical shift

versus crystal rotation plots [45-49]. A much simpler method is applicable when the nuclei of interest are part of an "isolated" spin pair, AX, and are coupled to one another by the direct dipolar interaction. Using this technique, known as dipolar-chemical shift solid state nmr spectroscopy [50-56], one can obtain the magnitude of the three principal components of the chemical shift tensor and two of the three angles that define the orientation of the chemical shift tensor. This makes the dipolar-chemical shift nmr method particularly useful since it alleviates the problems associated with preparing suitable single crystals and carrying out time consuming nmr studies on them.

For dipolar-chemical shift nmr experiments to be successful, it is important to ensure that the system being investigated is in fact an "isolated spin-pair". Thus, for a heteronuclear spin-pair AX, the magnitudes of the homonuclear dipolar interactions between A nuclei or the X nuclei should be minimal. If a third nmr active spin is present in the sample, for example ^1H, then one must remove all dipolar couplings involving this spin as well. If these conditions can be satisfied in the system of interest, then the Hamiltonian for the A nucleus of an "isolated" AX spin pair can be expressed as :

$$H_A = H_Z + H_{CS} + H_D^{AX} + H_J^{AX} \qquad [II.30]$$

The resonance frequency of the A nucleus which depends on the

mutual orientations of the chemical shift, direct and indirect dipolar tensors can be expressed [50-56] as :

$$\nu_A(m_x) = \nu_o - \nu_\sigma - m_x\nu_D - m_x\nu_J \qquad [II.31]$$

Combining the indirect and direct dipolar terms as in equation II.28 an analytical expression [50-56] for the resonance frequency of the A nucleus in a rigid chemical system is :

$$\begin{aligned}\nu_A(m_x) &= (\gamma_A B_o/2\pi)[1-[\sigma_{11}\sin^2\vartheta\cos^2\varphi + \sigma_{22}\sin^2\vartheta\sin^2\varphi + \sigma_{33}\cos^2\vartheta]] \\ &\quad - m_x R'[1-3(\sin\beta\sin\vartheta\cos(\varphi-\alpha) + \cos\beta\cos\vartheta)^2] \qquad [II.32] \\ &\quad - m_x J_{iso}\end{aligned}$$

The polar angle ϑ represents the orientation of B_o relative to δ_{33}, and the azimuthal angle φ represents the angle between δ_{11} and the projection of B_o onto the δ_{11}-δ_{22} plane as indicated in figure II.4. The Euler angles α and β which orient the dipolar vector in the principal axis system of the chemical shift tensor are a distinct physical property of each molecular system and cannot be controlled by the experimentalist. Note that a minor drawback of this experiment is that one can only determine the orientation of the three principal components of the chemical shift tensor of the A nucleus within a rotation about the dipolar vector.

The spin number of the X nucleus, m_x, determines the number of subspectra observed for the A nucleus. If the X nucleus is a spin 1/2 nucleus, there are two such subspectra and the difference between the discontinuities of these two subspectra are related to the mutual orientations of the dipolar and chemical shift tensors as specified in equation

Figure II.4

The angles α and β define the orientation of the dipolar vector, r_{AX}, in the principal axis system of the chemical shift tensor; θ and φ define the orientation of the magnetic field vector, B_o, in this frame.

Figure II.4

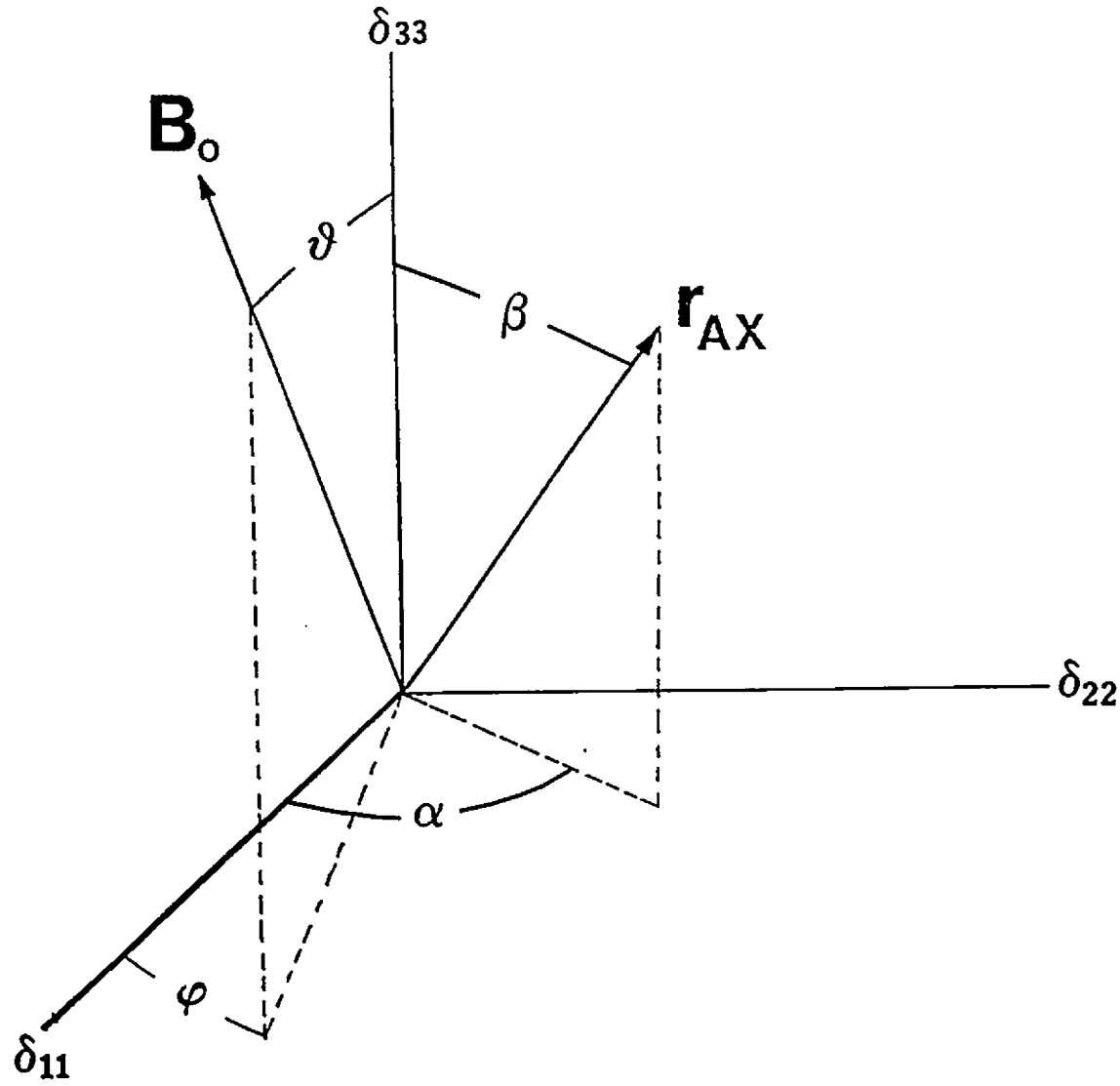

Figure II.5

Typical ^{13}C powder nmr line shapes at 4.7 T for (a) chemical shift anisotropy where δ_{11}=180 ppm, δ_{22}=110 ppm and δ_{33}=30 ppm (b) heteronuclear dipolar coupling of R=1100 Hz for a $^{13}C,^{15}N$ spin-pair and (c) both chemical shift anisotropy and dipolar coupling assuming δ_{33} is perpendicular (β=90) to the dipolar vector, r_{AX}, and δ_{11} (α=0) is approximately parallel to r_{AX}.

Figure II.5

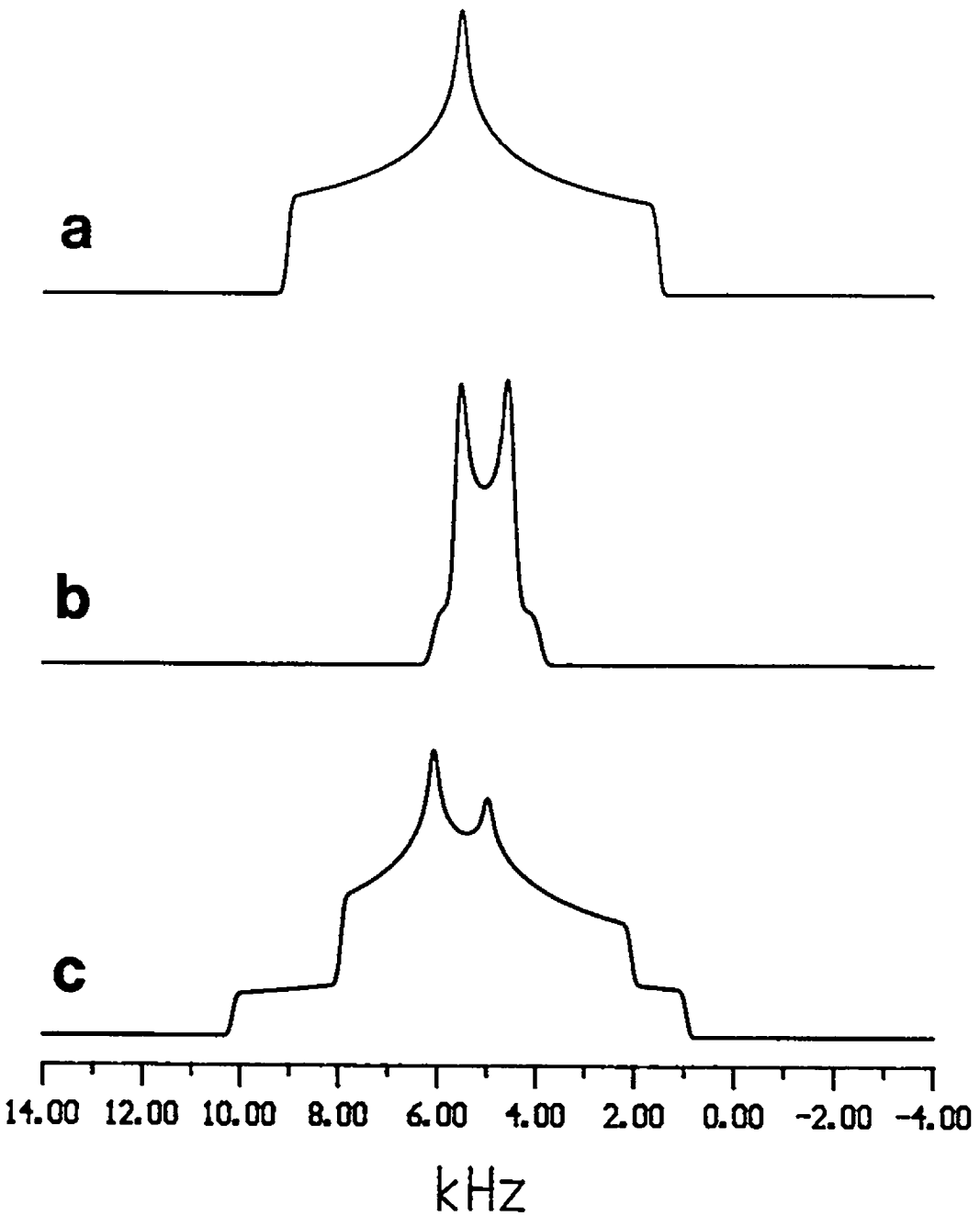

II.32. Thus, one can obtain accurate values for the three principal components of the A chemical shift tensor and the two angles α and β from an nmr spectrum acquired for an A nucleus (I=1/2) directly bonded to a spin 1/2 X nucleus. An example of a dipolar-chemical shift nmr spectrum for such a heteronuclear spin pair is shown for the ^{13}C nucleus of a $^{13}C,^{15}N$ spin-pair in figure II.5. Note that the resultant nmr spectrum for the A spins (figure II.5c) is not merely a superposition of the chemical shift part (figure II.5a) and the dipolar part (figure II.5b) but rather corresponds to the mutual orientations of the two tensors depicted in figure II.4 and described mathematically in equation II.32. The line shape of dipolar-chemical shift nmr spectra are very sensitive to the angles α and β and several examples of this are shown in figure II.6 for the case of two dipole coupled spin I=1/2 nuclei. Thus, the approach used to interpreting such nmr spectra is to estimate the values of α, β, R' and δ_{ii} from an experimental nmr spectrum of the A nucleus and then to simulate the nmr spectrum of the A nucleus based on equation II.32 to refine these parameters. If ΔJ and J_{iso} are assumed to be negligible, then initial estimates of α and β can be obtained from the following expressions :

$$\Delta\nu_{11} = \pm R\,[1 - 3\,(\sin\beta\,\cos\alpha)^2] \qquad [II.33a]$$

$$\Delta\nu_{22} = \pm R\,[1 - 3\,(\sin\beta\,\sin\alpha)^2] \qquad [II.33b]$$

$$\Delta\nu_{33} = \pm R\,[1 - 3\,\cos^2\beta] \qquad [II.33c]$$

where the values of $\Delta\nu_{ii}$ correspond to the dipolar splittings

Figure II.6

The influence of varying the orientation of the ^{13}C chemical shift tensor with respect to r_{AX} on the ^{13}C dipolar-chemical shift nmr spectrum (4.7 T) of two isolated spin I=1/2 nuclei. The chemical shift and dipolar coupling parameters correspond to those used in the calculated nmr spectra of figure II.5 and the angles are (a) α=0°, β=0°, 30°, 60°, 90° and (b) β=90°, α=0°, 30°, 60°, 90°.

Figure II.6a

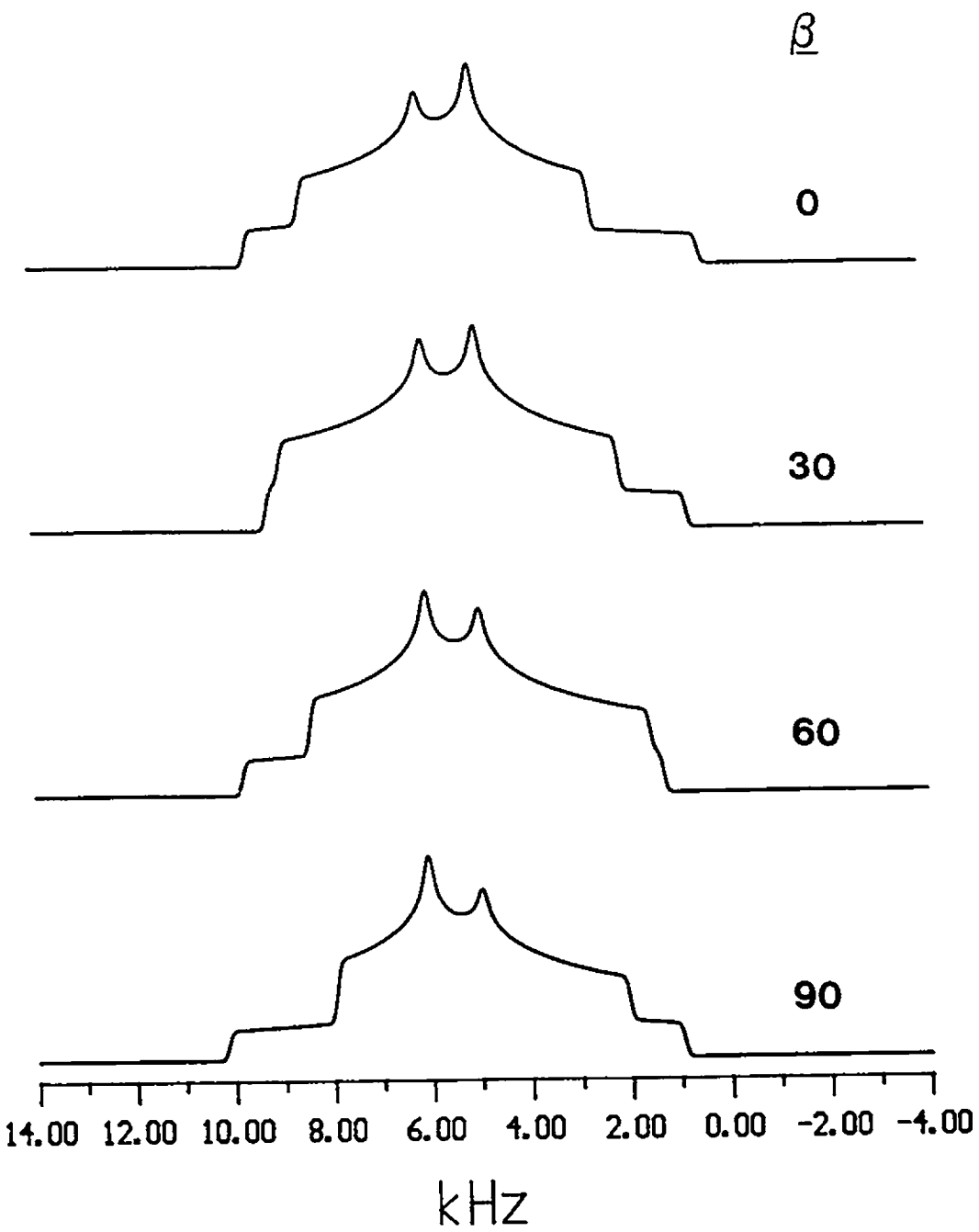

Figure II.6b

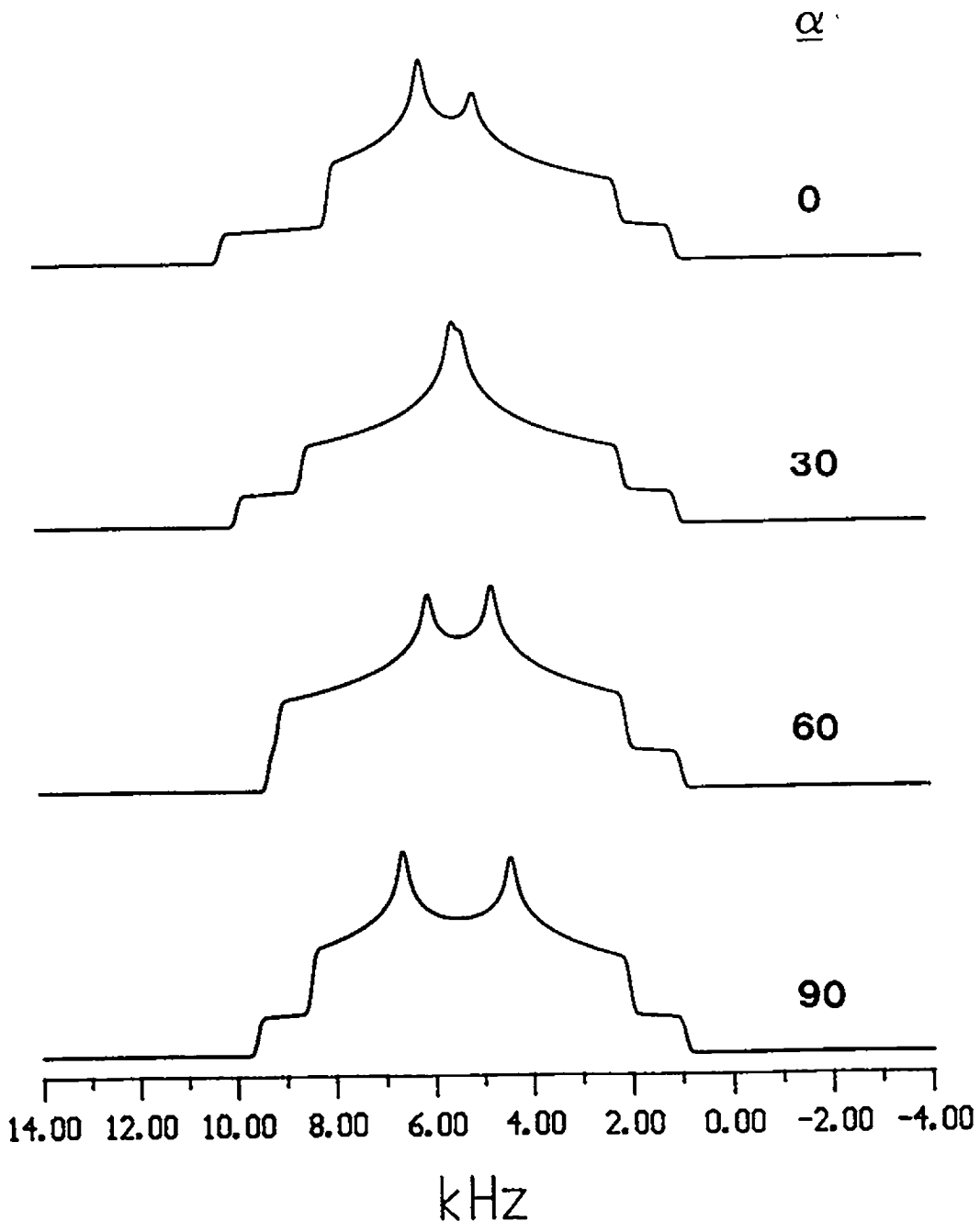

observed in the A nucleus dipolar-chemical shift nmr spectrum.

If an A nucleus is dipolar coupled to a an X nucleus which is quadrupolar with spin I=1, then three subspectra corresponding to m_x=-1,0,+1 are observed in the nmr spectrum of the A nucleus. Note that for this dipolar coupled system, equation II.32 is not strictly valid unless the conditions of the high-field approximation for the X nucleus are satisfied [33-35]. An example of the ^{13}C dipolar-chemical shift nmr spectrum for a $^{13}C,^{14}N$ spin-pair is shown in figure II.7.

If the Larmor frequency of the quadrupolar X-nucleus, $\nu_o(X)$, is much greater than the nuclear quadrupolar coupling constant, $\chi(X)$, then the axis of quantization for the X nucleus is along the applied magnetic field, B_o, and the high-field approximation is valid [33-35]. In the simplest case, that of axial symmetry in the chemical shielding tensor with the dipolar vector directed along the unique axis of the shielding tensor, it has been found that the high-field approximation is satisfied when $\nu_o(X)/\chi(X) > 4$ [35]. When this ratio becomes smaller, the high-field approximation breaks down and the quantum number m_x is no longer strictly valid. Under these circumstances an orientation-dependent mixing of the normal X spin Zeeman eigenfunctions, $|I,m>$, occurs and it is these "mixed" spin eigenfunctions that should be used to calculate the resonance frequency of the A spins. In this case, it is useful to define the orientation of all the relevant nuclear spin interactions relative to the

Figure II.7

Typical ^{13}C powder nmr line shapes at 4.7 T for (a) chemical shift anisotropy where δ_{11}=180 ppm, δ_{22}=110 ppm and δ_{33}=30 ppm, (b) heteronuclear dipolar coupling of R=796 Hz for a ^{13}C,^{14}N spin pair and (c) both chemical shift anisotropy and dipolar coupling assuming δ_{33} is parallel (β=0°) to the dipolar vector, r_{AX}, and δ_{11} is perpendicular to r_{AX} (α=90°). Spectra were calculated assuming that the high-field limit is valid for the ^{14}N nucleus.

Figure II.7

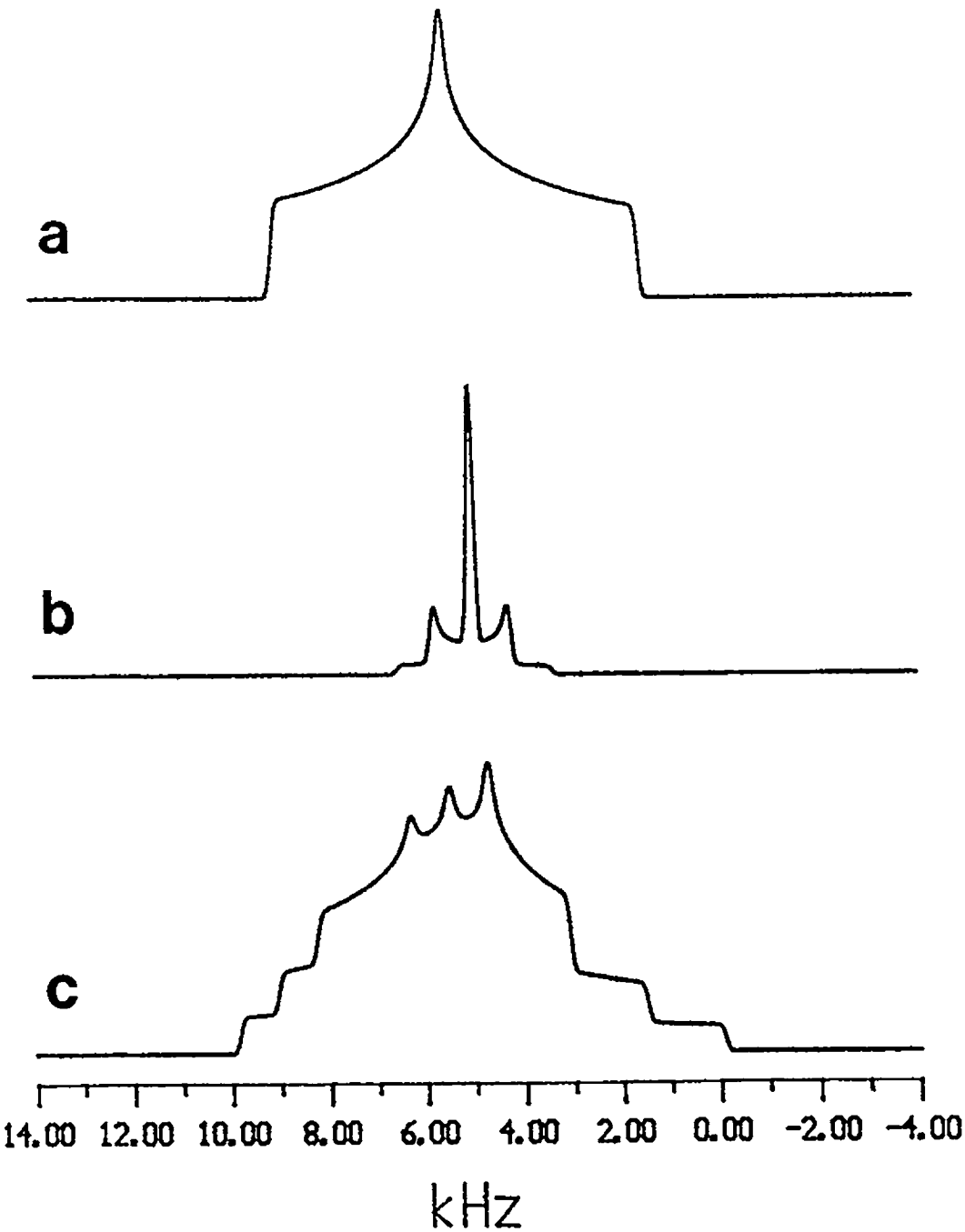

principal axis system of the electric field gradient (efg) as shown in figure II.8. The angles ξ and Ω are used to define the orientation of the magnetic field vector, B_o, in the principal axis system of the X nucleus efg and are not shown in figure II.8. They are similar to the angles ϑ and φ shown in figure II.4. The orientation of the dipolar vector in this frame is defined by the angles α^D and β^D. The angles α^{CS}, β^{CS} and γ^{CS} represent the orientational angles of the principal axis system of the chemical shift tensor of the A nucleus in the principal axis system of the X nucleus electric field gradient. The interactions to be considered for such a heteronuclear spin-pair are the same as those in equation II.31. However, the expressions for ν_σ and ν_D have to be modified to account for the change in reference frames. The chemical shift tensor may be expressed in the electric field gradient tensor frame by a rotational transformation [17,52] of the form :

$$\hat{\sigma}'(\alpha^{CS},\beta^{CS},\gamma^{CS}) = R(\alpha^{CS},\beta^{CS},\gamma^{CS})\ \hat{\sigma}\ R^{-1}(\alpha^{CS},\beta^{CS},\gamma^{CS}) \qquad [II.34]$$

The expression for the frequencies associated with the chemical shift can then be obtained from :

$$\sin\vartheta\cos\varphi = \cos\gamma^{CS}\cos\beta^{CS}\sin\xi\cos(\Omega - \alpha^{CS}) + \sin\gamma^{CS}\sin\xi \sin(\Omega - \alpha^{CS}) - \cos\gamma^{CS}\sin\beta^{CS}\cos\xi \qquad [II.35a]$$

$$\sin\vartheta\sin\varphi = -\sin\gamma^{CS}\cos\beta^{CS}\sin\xi\cos(\Omega - \alpha^{CS}) + \cos\gamma^{CS}\sin\xi \sin(\Omega - \alpha^{CS}) + \sin\gamma^{CS}\sin\beta^{CS}\cos\xi \qquad [II.35b]$$

$$\cos\vartheta = \sin\beta^{CS}\sin\xi\cos(\Omega - \alpha^{CS}) + \cos\beta^{CS}\cos\xi \qquad [II.35c]$$

by substitution in equation II.32. Olivieri et al. have

Figure II.8

The angles α^D and β^D define the orientation of the dipolar vector, r_{AX}, in the principal axis system of the electric field gradient of the X nucleus; α^{CS}, β^{CS} and γ^{CS} define the orientation of the A nucleus chemical shift tensor in this reference frame; the orientation of the magnetic field vector, B_o, in this reference frame is not shown.

Figure II.8

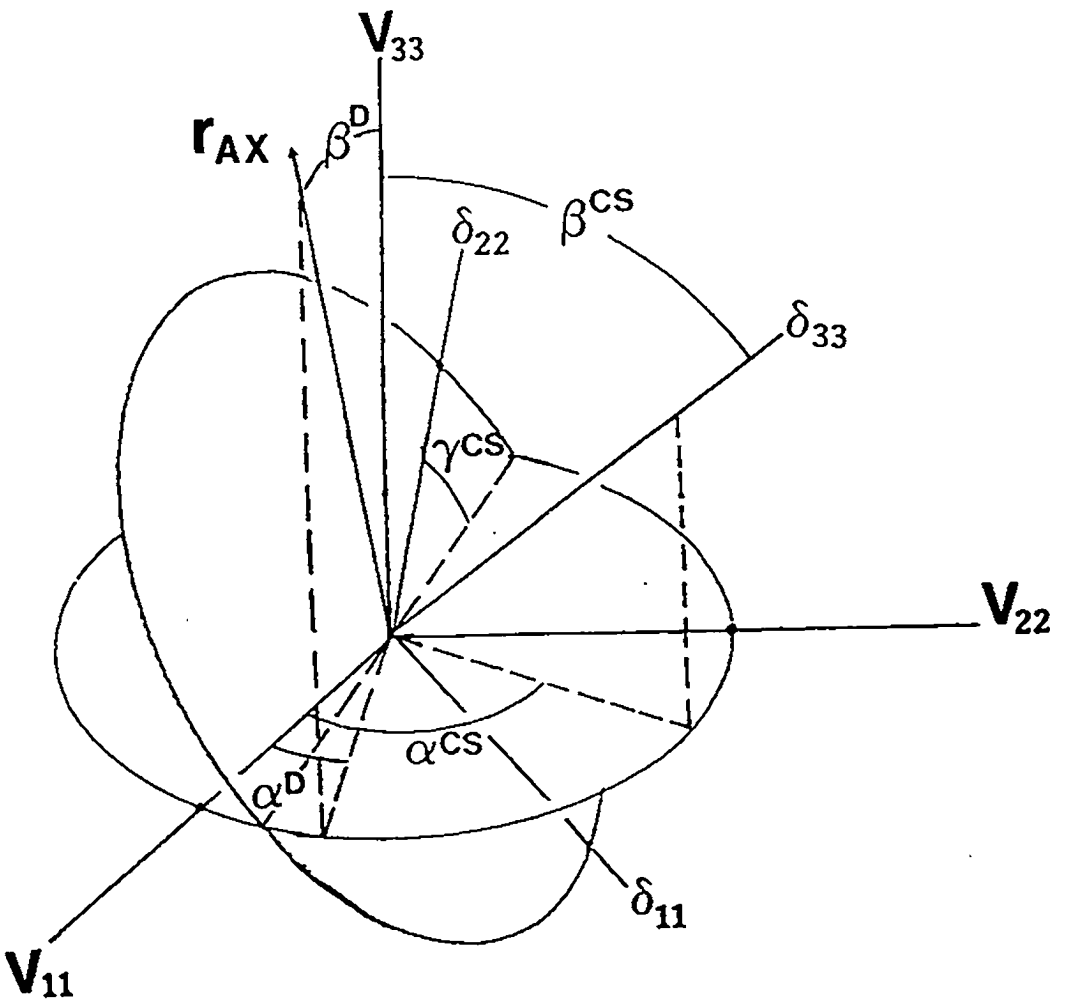

described a perturbation treatment for a $^{13}C,^{14}N$ spin pair where they derived an analytical expression for the heteronuclear dipolar interaction in the electric field gradient tensor frame [58]. Combining their equations with the angular representation in figure II.8 gives :

$$\nu_D(0) = \frac{3R'\chi(X)}{2\nu_o(X)} [\cos\xi\ \cos\beta^D + \sin\xi\ \sin\beta^D\ \cos(\Omega - \alpha^D)]$$
$$\{3\cos\xi\ \cos\beta^D - (3\cos^2\xi + \eta_Q\sin^2\xi\ \cos2\Omega)[\cos\xi\ \cos\beta^D +$$
$$\sin\xi\ \sin\beta^D\ \cos(\Omega - \alpha^D)] + \eta_Q(\sin\beta^D\ \sin\xi\ \cos(\Omega + \alpha^D) \quad [II.36a]$$

$$\nu_D(+1) = -(\nu_D(0)/2) - R'\{1-3[\cos\xi\ \cos\beta^D + \sin\xi\ \sin\beta^D$$
$$\cos(\Omega - \alpha^D)]^2\} \quad [II.36b]$$

$$\nu_D(-1) = -(\nu_D(0)/2) + R'\{1-3[\cos\xi\ \cos\beta^D + \sin\xi\ \sin\beta^D$$
$$\cos(\Omega - \alpha^D)]^2\} \quad [II.36c]$$

Substituting these expressions along with the chemical shift terms in equations II.35a,b,c in equation II.31 provides a fully operative equation which is completely general for an A nucleus of spin I=1/2 dipole coupled to an X nucleus of spin I=1. That is, the revised equation II.31 is applicable when the conditions of the high-field approximation are not satisfied. In analogy to the angles α and β defined in figure II.4, the angles α^D, β^D, α^{CS}, β^{CS} and γ^{CS} are physical constants which are characteristic for each particular molecular system.

C. High Resolution Solid State NMR of Dilute Spin I=1/2 Nuclei - Rotating Samples

In order to obtain a high-resolution nmr spectrum for the dilute spin I=1/2 nuclei (A) in a solid sample, the anisotropic nature of the spin interactions associated with the A-nuclei and with other nuclei of the sample (X and I) must be reduced. The definition of a dilute spin system as referred to in this thesis is one for which the homonuclear A-spin dipolar interactions are small (e.g. < 0.5 kHz). This is readily satisfied for ^{15}N and ^{13}C in almost any organic molecule since the natural abundance of these spins is very low (see table II.1). For ^{31}P, where the natural abundance is 100 %, homonuclear interactions are usually sufficiently small to make ^{31}P a "dilute" spin system for solid state nmr. Noted exceptions to this classification occur if two ^{31}P nuclei are bonded together or if selective isotopic enrichment has modified the natural spin properties of the system. Thus, for a "dilute" spin system, the Hamiltonians describing the A-spin and I-spin interactions (where I is an abundant nucleus such as hydrogen) can be written as :

$$H_A = H_Z + H_{CS} + H_D^{AI} + H_J^{AI} + H_D^{AX} \qquad [II.37a]$$

$$H_I = H_Z + H_{CS} + H_D^{II} + H_J^{II} + H_D^{IA} + H_D^{IX} \qquad [II.37b]$$

The experimental nmr methods used to reduce the magnitude of the corresponding interaction energies will be examined in turn.

High-power hydrogen decoupling with a second radio-frequency field, B_2, applied at the hydrogen Larmor frequency causes a coherent averaging of the A-I, I-I and X-I dipolar interactions if the amplitude of the field is of comparable size to the interaction energies. Typically, 50-100 Watts of continuous rf power is necessary to obtain decoupling fields of 50 kHz (i.e., an ^1H $\pi/2$ pulse length of 5 μs). The heating that results from the application of such a field (B_2) imposes an upper limit of approximately 2 seconds on the acquisition times for dilute spin nmr spectra obtained with decoupling. Several other methods for decoupling are available such as the coherent averaging multiple pulse techniques WAHUHA, MREV-8 and others [12,59-64]. Although these are useful in some cases, at present the general effectiveness of such pulse sequences for decoupling hydrogen in typical chemical systems is limited.

In addition to removing the dipolar interactions involving hydrogens, the decoupling field (B_2) can also be used to enhance the nmr signal of the dilute spins (A) by a technique known as cross polarization (cp). This was first applied to the nmr study of naturally abundant ^{13}C in solid samples by Pines et al. in 1972 [9] and the details of cross polarization dynamics can be obtained from numerous sources in the literature [9,12,65-72,74]. The basic objective of any cp technique is to transfer polarization from the abundant I-spins (usually hydrogen) to the dilute A-spins under

investigation. Consideration of equation II.6 suggests that if one can manipulate the spin system such that the exchange of Zeeman energy between the A and I spins could occur, then thermodynamically the hydrogen nuclei which have a low spin temperature and a large magnetization reservoir could effectively "cool" the dilute spin A nuclei by transferring magnetization to them. The most common technique which creates a situation for the exchange of Zeeman energy between the A and I nuclei is referred to as the Hartmann-Hahn matching condition [65]. This can be expressed as :

$$\omega_{1,A} = \omega_{2,I} \qquad \text{[II.38a]}$$

$$\gamma_A \cdot B_{1,A} = \gamma_I \cdot B_{2,I} \qquad \text{[II.38b]}$$

and indicates that in their respective rotating frames, both the A and I nuclei precess with the same frequency. The mechanism and kinetics of this method of cross polarization depend mainly on the magnitude of the direct dipolar interactions between the A and I spins. This has been discussed in detail by Jelinski and Melchoir [71] and the experimental implications of the cross polarization dynamics between the A and I nuclei will be examined in section III.B.

One possible pulse sequence for performing a cp nmr experiment is indicated in figure II.9. First, a high-power $\pi/2$ pulse is applied with the rf field B_2 at the hydrogen Larmor frequency to establish transverse magnetization for the I-nuclei in the static magnetic field, B_o. Immediately following this pulse, both the B_1 and B_2 rf fields for the A

and I spins are turned on simultaneously. The B_2 rf field is applied along an axis which is phase shifted by $\pi/2$ relative to the first rf pulse (e.g., along the y' axis if the first pulse was applied along the x' axis) and causes the I-spin net magnetization to precess about that axis. This is termed spin-locking and the return of the I-spin magnetization to thermal equilibrium ($M_z=M_o$) is characterized by a specific relaxation time, $T_{1\rho,I}$. The A spin rf field, B_1, allows the A-nuclei to 'contact' the magnetization reservoir of the I-nuclei under the Hartmann-Hahn matching conditions for a period t_c. The final part of this pulse sequence, involves turning off the A-spin rf field and observing the resulting FID of the dilute spins with high-power hydrogen decoupling. Note that it is always necessary to wait a short period of time, t_d, to allow the electronic circuits to recover from the influence of the high-power pulses. The whole sequence can then be repeated to obtain a sufficient number of transients to give the desired signal to noise ratio in the Fourier transformed frequency domain nmr spectrum.

There are several distinct advantages relating to the use of the cp technique shown in figure II.9. First, since the source of the dilute spin magnetization arises from the abundant spins (e.g., hydrogens), the repetition rate is governed by the ^1H spin-lattice relaxation time (T_{1I}) and not the spin-lattice relaxation time of the A-nuclei (T_{1A}). This is advantageous, since T_{1A} are generally [12,71,72] much longer

Figure II.9

Timing diagram for a cross polarization pulse sequence. The relative phases of the hydrogen pulses are indicated. Typical times for the various delays in the cp nmr experiment are : (1) $\pi/2$ pulse lengths, t_p=2-7 μs; (2) contact (spin-lock) time, t_c=1-12 ms; (3) dead time, t_d=20-60 μs; (4) acquisition time, t_{aq}=1-2000 ms; (5) recycle time, t_r=3-200 s.

Figure II.9

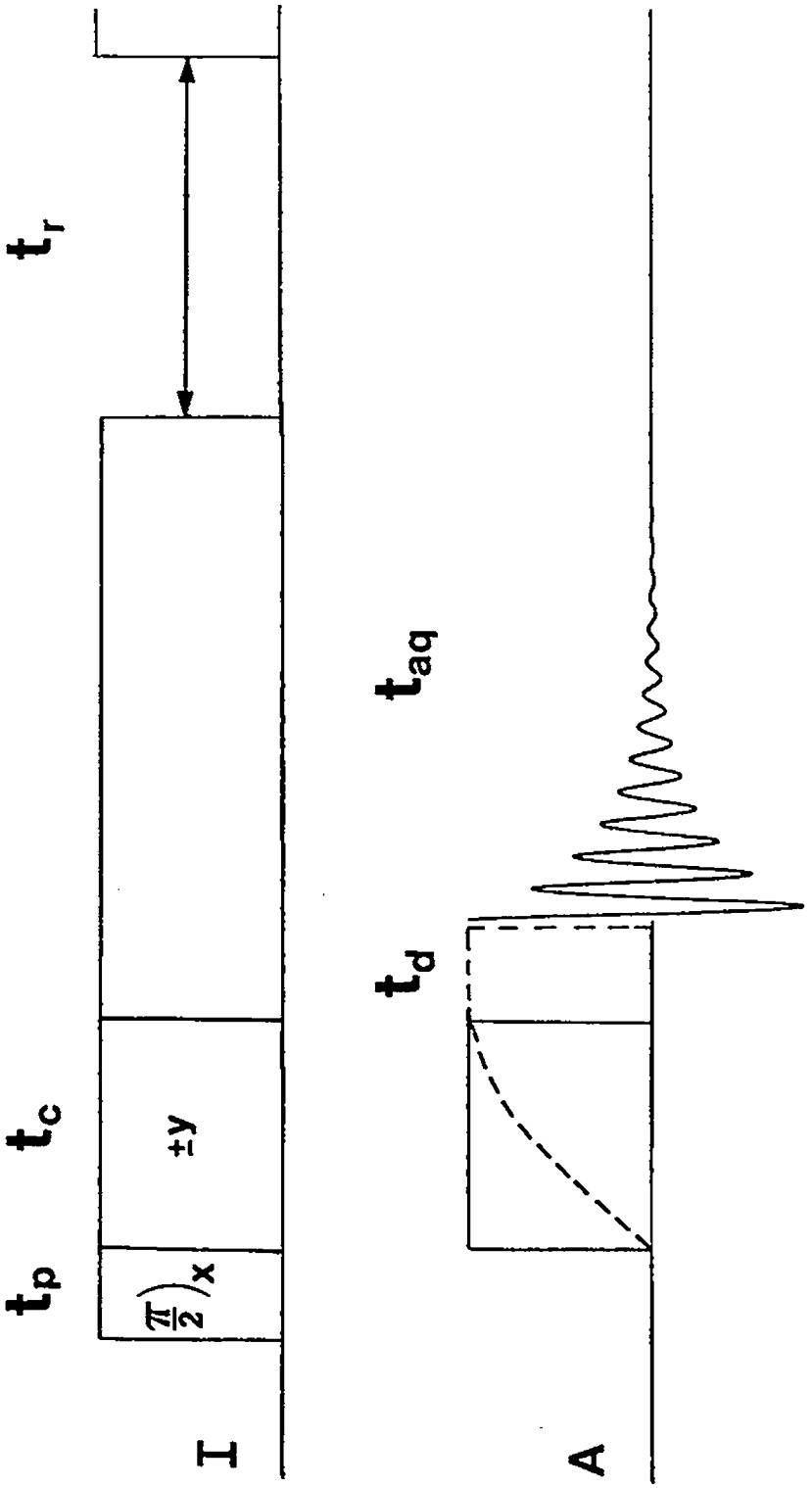

than T_{1I} and therefore one can obtain more FIDs in a given time period using cp than with simple single pulse acquisition of the A-nuclei. In addition, the equilibrium magnetization established for the A-nuclei after a single contact with the I-spins is enhanced by a factor of approximately (γ_I/γ_A) as compared to the nmr signal observed with a single pulse applied to the A nuclei of the sample after $5xT_{1A}$. This results in an enhancement factor of approximately 4 (16 in time) for ^{13}C nuclei and a factor of 10 (100 in time) for ^{15}N nuclei if the abundant spins are hydrogens. Finally, if the I-spins are characterized by a long $T_{1\rho,I}$, then it is possible to re-contact the A-spins with the I-spin reservoir before repeating the sequence. Although this can result in an even greater signal enhancement for the A nuclei, it is generally not used in practice since it requires the decoupling field to be on at high-power levels for unacceptably long periods of time.

An example of an ^{15}N nmr spectrum acquired at B_o=4.7 T with the pulse sequence shown in figure II.9 is presented in figure II.10a for a static powdered sample of ^{15}N enriched 4-methoxy-1-naphthonitrile. The breadth of the nmr spectrum results from the ^{15}N chemical shift anisotropy, $\Delta\delta$, which is slightly non-axially symmetric (η_δ = 0.12, $\Delta\delta$ = 396 ppm). In order to obtain a high-resolution ^{15}N nmr spectrum for such a solid sample, the influence of the chemical shift anisotropy must be removed.

Figure II.10

Nitrogen-15 nmr spectra of a solid powdered sample of 20% ^{15}N enriched 4-methoxy-1-naphthonitrile at 4.7 T. The nmr spectrum in (a) was acquired without sample rotation whereas that in (b) was acquired with magic angle spinning at 2.9 kHz. The contact time for the experimental nmr spectra was 9 ms and the recycle time was 7 s. The nmr spectrum in (c) was calculated based on the computer simulation routine of Clayden et al. [82].

Figure II.10

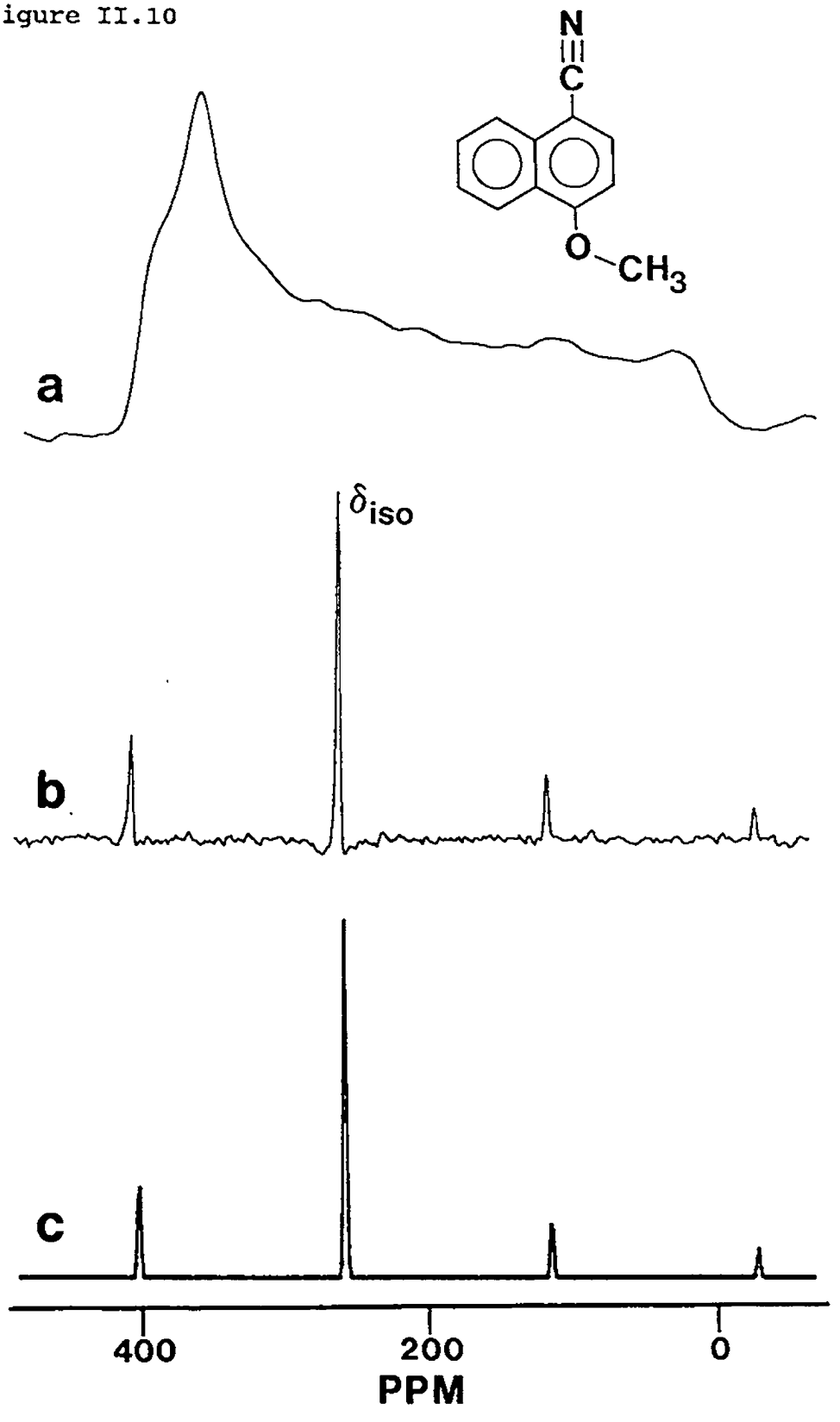

Andrew et al. described a method whereby rapid mechanical rotation of the sample at an angle inclined (β_r) relative to the magnetic field, B_o, (figure II.11) scales the traceless part of second rank tensor interactions ($\hat{\sigma}$, $\hat{V}$, $\hat{D}$, $\hat{J}$) by a factor of $1/2(3\cos^2\beta_r-1)$ [4,6]. If the angle β_r is set to 54°44'8" (the "magic angle"), and the sample spinning speed (ν_r) is large compared to the internal interaction energies, then the dipolar and first order quadrupolar interactions are averaged to zero and the indirect and shielding interactions are averaged to their isotropic values. Thus, when this method is combined with cross polarization and high-power hydrogen decoupling one observes a sharp resonance signal for each chemically distinct A-nucleus in analogy to a high-resolution solution nmr spectrum. The isotropic chemical shifts (δ_{iso}) observed in dilute spin cp/mas nmr spectra of solids are usually comparable to the corresponding values observed in solution nmr studies. For example, ^{13}C chemical shifts are usually within ± 3 ppm as compared to the corresponding values observed in solution nmr whereas differences for ^{31}P and ^{15}N may be slightly larger due to intermolecular interactions. This is generally valid unless the molecule of interest has a significantly different conformation and/or structure in solution as compared to the solid state [73]. Note as well, that additional peaks may arise in the solid state cp/mas nmr spectrum due to crystallographic nonequivalence of the nuclei being

Figure II.11

The angle β_r defines the inclination of the sample spinning axis relative to the static magnetic field, B_o.

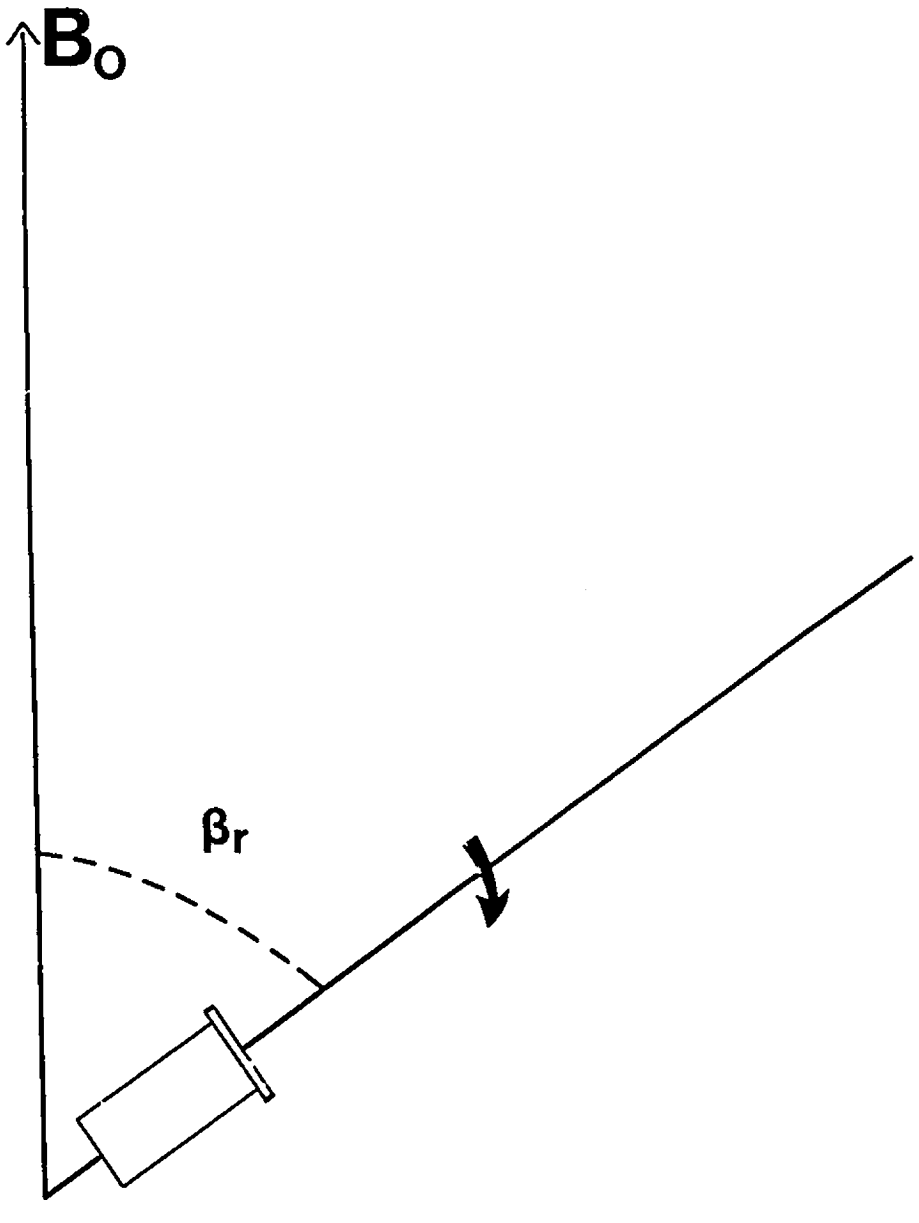

investigated and/or by the presence of one or more polymorphs [74]. Finally, if the nucleus being observed is indirectly coupled to another nucleus X, then the isotropic J may or may not be observed depending on the magnitude of J_{iso} relative to the inherent line width of the dilute spin nmr resonance signal.

The line widths in high-resolution solid state nmr spectra of dilute spins are related to several experimental parameters as well as the nature of the solid sample [75-77]. Typically nmr line widths (at half height) observed with the use of a double air-bearing solid state nmr probe on highly crystalline samples are approximately 0.2-2 ppm. For inhomogeneous samples such as glasses or polymers on the other hand, line widths on the order of 2-9 ppm are often observed in the dilute spin nmr spectrum. Alla and Lippmaa have demonstrated that this change in observed line broadening between crystalline and inhomogeneous samples is related to the anisotropy of the magnetic susceptibility rather than volume susceptibility effects [77a]. In addition, several authors have noted that for every degree of missetting of the magic angle, the observed line width in the dilute spin cp/mas nmr spectrum will increase by approximately 2% of the static line width [75-77]. Therefore, nuclei which have large chemical shift anisotropies will have line widths which are particularly sensitive to the setting of the magic angle. It is usual then, to adjust the angle to the correct position

prior to acquiring a high-resolution cp/mas nmr spectrum.

The most common methods for setting the magic angle involve the use the ^{13}C resonance signal of the aromatic carbons of hexamethylbenzene (HMB) [77] or by observing the ^{79}Br (I = 3/2) nmr signal of solid KBr [78]. For HMB, the limiting line width for both the aromatic and methyl carbons in the ^{13}C cp/mas (ν_r=3-4 kHz) nmr spectrum at 50.32 MHz (B_o=4.7 T) is approximately 38 ± 5 Hz provided the decoupler field strength is in excess of 35 kHz [77a]. For KBr, this author has observed that for a properly shimmed cp/mas nmr probe, the correct setting of the magic angle can be established by the observation of rotational spin-echoes [78] for a period of approximately 14 ms in the time domain ^{79}Br nmr signal at spinning speeds of 3-4 kHz. Note that these are both external methods for adjusting the magic angle and unless the HMB or KBr are included in the actual rotor being used for the mas nmr experiment, they do not guarantee that the sample being investigated will spin at exactly the magic angle. A more elaborate means of monitoring the actual setting of the angle β_r using lasers has been described by Ernst and coworkers [79].

When the sample spinning speed (ν_r) is less than the chemical shift anisotropy ($\Delta\delta$) in Hz, one observes an array of spinning sidebands at multiples of the rotor frequency ($n \cdot \nu_r$) in the resulting dilute spin nmr spectrum. For example, four spinning sidebands are apparent in the ^{15}N cp/mas

nmr spectrum obtained for 4-methoxy-1-naphthonitrile at a sample spinning speed of 2.9 kHz (figure II.10b). In the absence of dipolar couplings, the intensity and the distribution of the spinning sidebands about the isotropic value in the dilute spin nmr spectrum are a reflection of the dilute spin chemical shift anisotropy. Thus, in principle, one can obtain information about the anisotropic nature of the chemical shifts by interpreting the spinning sideband intensities. Several methods have been described to extract the three principal components of the chemical shift tensor from such a "slow spinning" dilute spin nmr spectrum [80-82]. The simplest method involves a graphical procedure outlined by Herzfeld and Berger [80]. In this method, the intensity of several spinning sidebands ($I \pm N$) are compared to the intensity of the isotropic resonance (I_o) and these values are then used to plot a series of contours that have been calculated by Herzfeld and Berger using numerical methods. The intersection point of the various contours can then be used to extract two parameters (μ and ρ) which can be related to the chemical shift anisotropy [80]. This method has the advantage that only a small number of sidebands ($N \pm 3$) are required to obtain reasonable estimates of the three principal components of the chemical shift tensor. However, for nearly axially symmetric chemical shift tensors, the results of this analysis are not very reliable. An alternative approach presented by Maricq and Waugh relies on a moment analysis of

the sideband intensities [81]. A principal drawback of this method is that significant errors in the three principal components of the shift tensor are observed unless the intensities of all of the sidebands are included in the calculation. A more recent approach presented by Clayden and his coworkers, involves computer simulation of the dilute spin nmr spectrum followed by an optimization routine which minimizes the errors between the calculated and experimental intensities of several sidebands [82]. Although this method is suitable for small chemical shift anisotropies, this author has found it to be unreliable for larger values of $\Delta\delta$. The simulated ^{15}N cp/mas nmr spectrum based on the method of Clayden et al. [82] is shown in figure II.10c for the ^{15}N enriched sample of 4-methoxy-1-naphthonitrile. The chemical shift tensor parameters obtained from this simulation, $\Delta\delta$=396 ppm and η_δ=0.12, were found to be very similar to those observed in static ^{15}N nmr spectrum (figure II.10a).

Normally the dipolar interactions between unlike or like spins A and X are sufficiently small (i.e., < 0.5 kHz) that even moderate magic angle spinning speeds are sufficient to average these to zero. An exception to this occurs when the nucleus of interest, A, is dipolar coupled to a quadrupolar nucleus, X. In this case, the cp/mas nmr spectra of dilute spins which are directly bonded to a quadrupolar nucleus often show characteristic splittings in their isotropic resonance signals [83-91]. An example of this effect is illustrated in

figure II.12 for the ^{31}P cp/mas nmr spectrum of the inorganic salt, $[(C_6H_5)_3P=N=P(C_6H_5)_3]^+ (NO_2)^-$. The first point to note regarding this cp/mas nmr spectrum is that there are two sets of ^{31}P isotropic resonances. This provides an example of the influence of crystallographic nonequivalence on solid state nmr spectra of dilute spins. In addition, each isotropic ^{31}P resonance signal shows a broadened asymmetric doublet of splitting ~100 Hz. Similar splitting patterns are not observed in ^{31}P cp/mas nmr spectrum when ^{14}N is replaced by an ^{15}N nucleus (I=1/2) or in compounds where the ^{14}N quadrupolar coupling constant is small. The splittings result from a break down of the high-field approximation for the quadrupolar nucleus. That is, the Larmor frequency of the quadrupolar nucleus is not large compared to the nuclear quadrupolar coupling constant, χ, and thus the dipolar interaction between the dilute spin of interest and the ^{14}N nuclei contains terms with an angular dependence other than $(3\cos^2\theta_{AX}-1)$ which are not completely averaged by magic angle spinning at 54°44'8".

Similar to nuclear shielding, the magnitude of the electric field gradient at the ^{14}N nucleus is also very sensitive to the symmetry of the local electronic environment. For example, a nitrogen nucleus in a tetrahedral environment would be expected to have a small electric field gradient compared to that of a dicoordinate nitrogen involved in a double bond. Typical values for the ^{14}N nuclear quadrupolar coupling constant, χ, are on the order of 1-5 MHz [12] while

Figure II.12

The phosphorus-31 cp/mas nmr spectrum of the inorganic salt $[(C_6H_5)_3P{=}N{=}P(C_6H_5)_3]^+ (NO_2)^-$. The sample spinning speed was 2.52 kHz.

Figure II.12

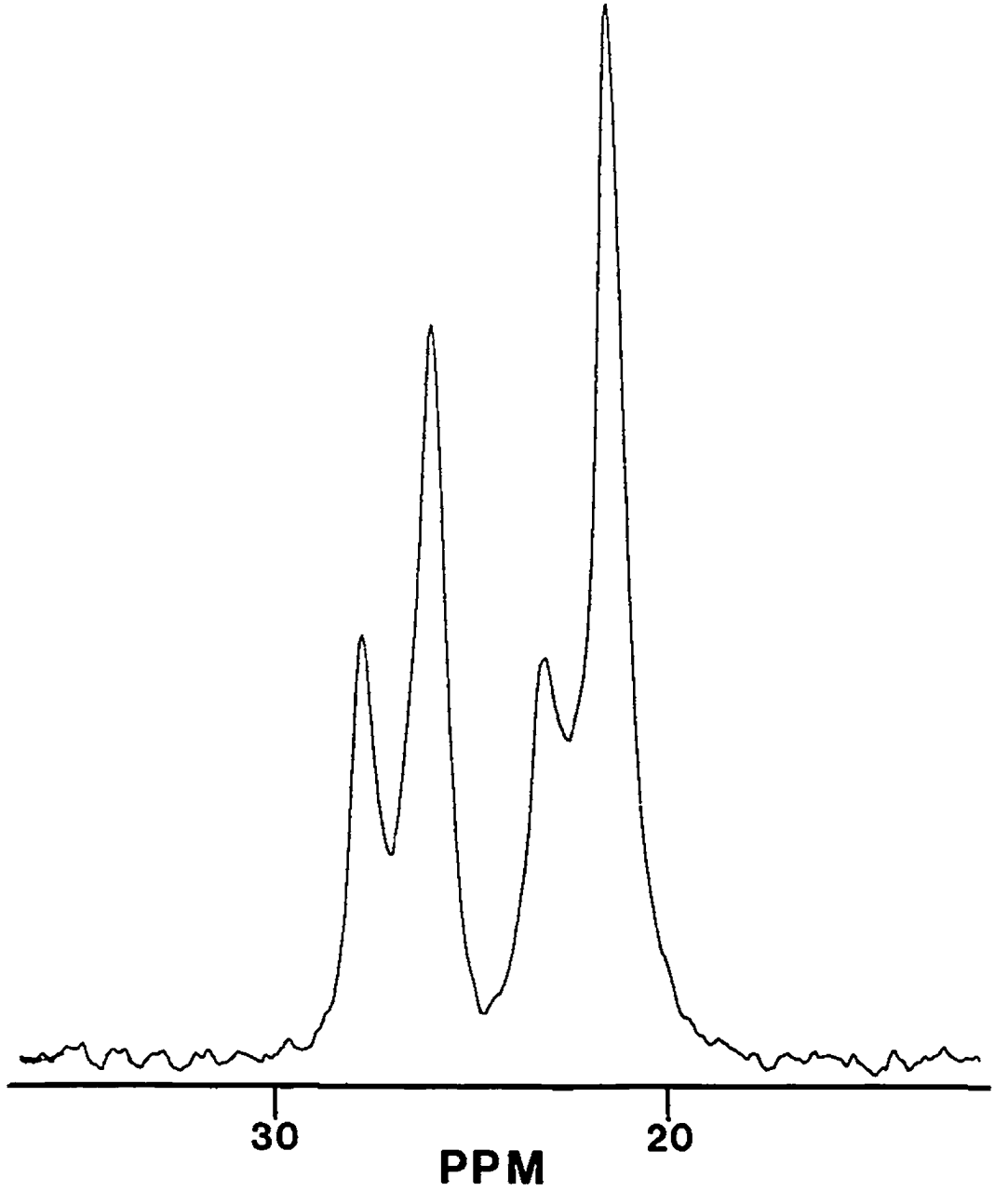

at B_o=4.7 T, the Larmor frequency for ^{14}N is 14.47 MHz. A theoretical procedure for calculating the mas line shapes of a ^{13}C nucleus dipolar coupled to an ^{14}N nucleus where the high-field approximation is not valid has been presented by Hexem [88]. The method is generally applicable to the case of any spin I=1/2 nucleus dipolar coupled to a spin I=1 nucleus and assumes that the indirect dipolar coupling is negligible. The resulting mas nmr spectrum calculated for the spin I=1/2 nucleus is the sum of three first order dipolar coupled powder patterns which have been substantially scaled by magic angle rotation. Two of these residual powder patterns are superimposed and are separated from the third to give the approximate 2:1 asymmetric doublet pattern seen in figure II.12.

The splitting of the asymmetric doublet in the dilute spin nmr spectrum is expected to increase with (1) an increase in the ^{14}N quadrupolar coupling constant; (2) a decrease in the size of Bo; (3) an increase in the A-X dipolar interaction (i.e., shorter r_{AX}). A computer simulation routine developed by Hexem is useful for calculating and interpreting dilute spin mas nmr spectra of these systems [88]. Examples of calculations using Hexem's method for the ^{13}C mas line shape of a $^{13}C,^{14}N$ spin pair with various ratios of the ^{14}N Zeeman energy to the ^{14}N quadrupolar coupling constant are shown in figure II.13a for a particular orientation of the nitrogen electric field gradient. As anticipated, the splitting of the

Figure II.13

Calculated ^{13}C mas line shapes at 4.7 T for a $^{13}C,^{14}N$ spin-pair. The nmr spectra in (a) were calculated by assuming that V_{33} is oriented along the dipolar vector, the asymmetry parameter η_Q=0.5 and r_{AX} is 1.40 Å. The ratio of ν_o/χ is indicated on each cp/mas nmr spectrum and the calculated splittings of the asymmetric doublet are -72 Hz, -119 Hz, -286 Hz and +286 Hz for a ratio of ν_o/χ of 10, 6, 2.5 and -2.5, respectively. The simulated nmr spectra in (b) were calculated by assuming that χ=-4 MHz, $\alpha^D=\gamma^D=0°$ and the bond length is 1.40 Å. The value of β^D is indicated on each ^{13}C mas nmr spectrum and the calculated splittings were determined to be +198 Hz, +136 Hz, +36 Hz and -49 Hz for values of β^D=0°, 30°, 54.7356° and 90°, respectively.

Figure II.13a

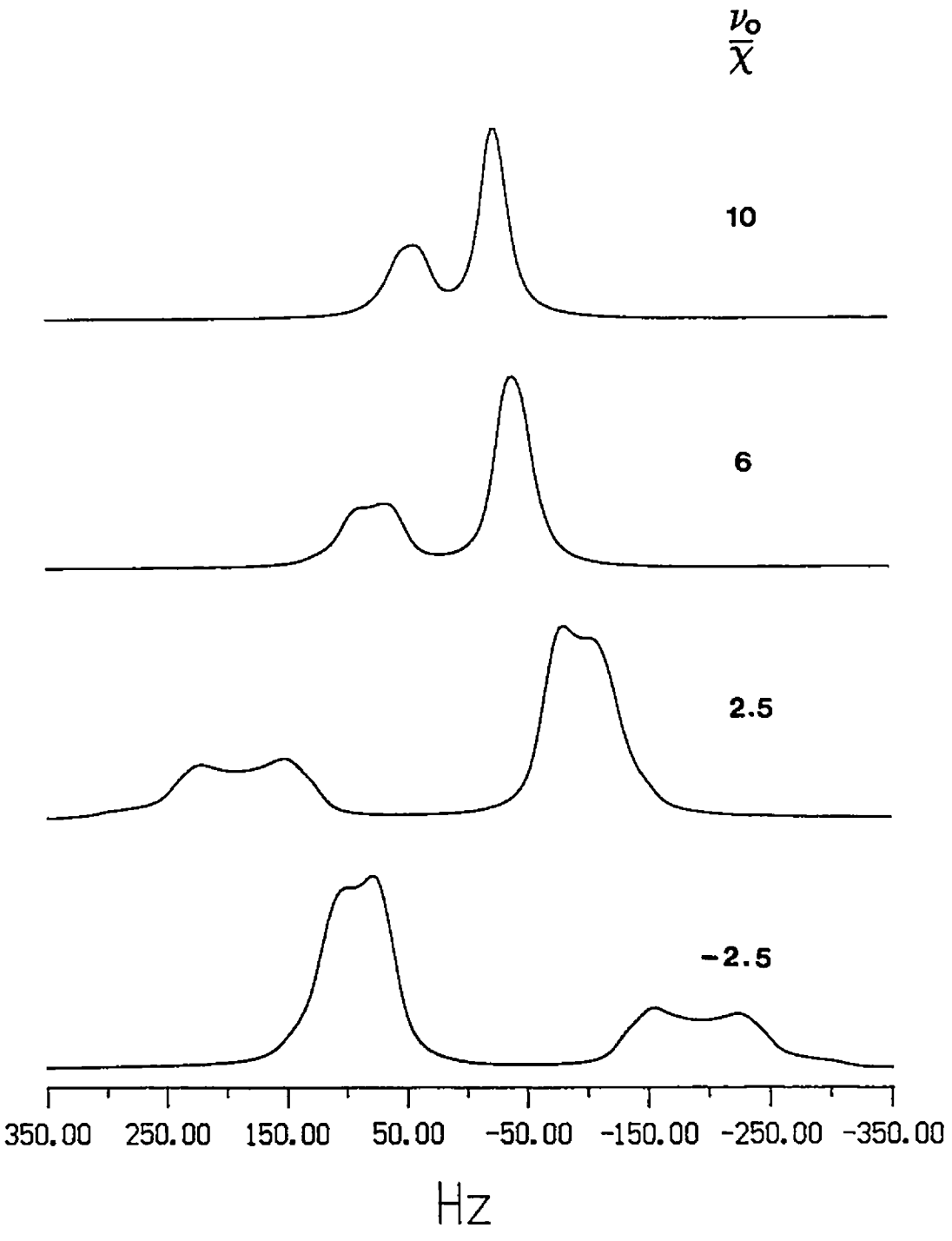

Figure II.13b

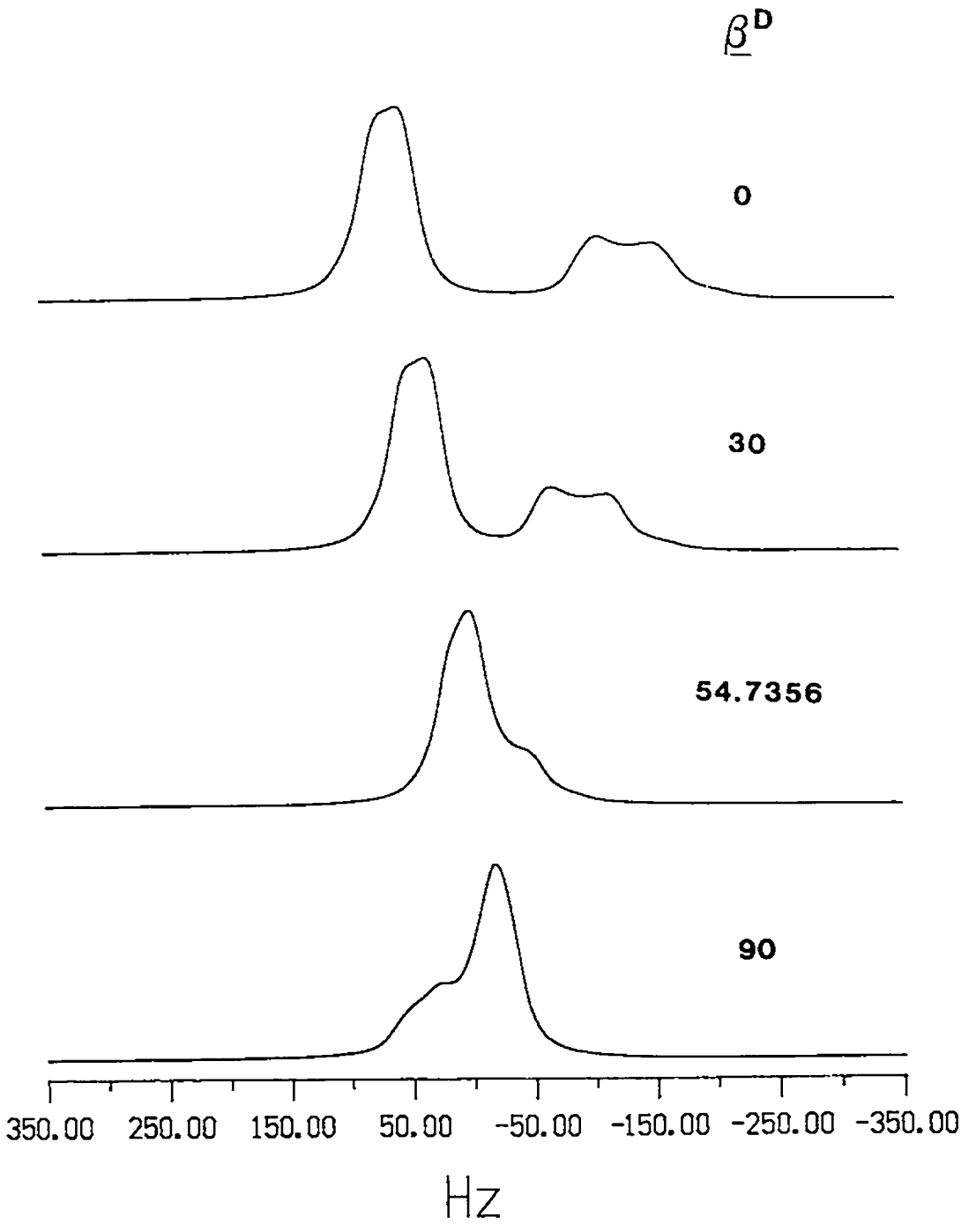

asymmetric doublet decreases substantially as the size of Zeeman interaction increases relative to χ (^{14}N). Note that the nmr spectrum of the dilute spin reverses in shape when the magnitude of χ is negative. The influence of the size of r_{AX} on the dilute spin nmr spectrum is not as marked as the influence of the magnitude of χ. However, the relative orientation of r_{AX} and the electric field gradient can have a significant effect on the observed splittings in the ^{13}C line shape as indicated in figure II.13b. For an orientation where the principal component of the ^{14}N efg (V_{33}) relative to r_{AX} is at the magic angle, the splitting is very small and may not even be observed depending on the experimental line width of the dilute spin nmr spectrum. In addition, variations in β^D can also lead to a reversal in the ^{13}C line shape.

In some cases, the nature of the splittings observed in dilute spin I=1/2 nmr spectra can be used to obtain structural and or electronic information. For example, if the orientation and magnitude of the electric field gradient tensor of a nucleus in a particular molecule are known, then simulations of the dilute spin nmr spectrum may allow one to estimate the bond length (r_{AX}) between the dilute spin A and the quadrupolar nucleus X. On the other hand, if r_{AX} is known it may be possible to obtain information about the nature of the quadrupolar coupling constant. This information can be very important, for example, if one wishes to analyze a dipolar-chemical shift nmr spectrum of a spin I=1/2 nucleus

dipolar coupled to a quadrupolar X nucleus. Finally, the observed splittings can be very useful in the assignment of high-resolution nmr spectra of nuclei such as ^{13}C where many lines are observed for typical organic solids.

III. Some General Experimental Techniques for the NMR Study of Solids

The focus of this section relates to the description of some experimental nmr techniques for the study of solid samples which either (1) improve the quality of the solid state nmr spectra or (2) provide a means for assigning high-resolution nmr spectra of solids. The experimental aspects of solid state nmr have been thoroughly discussed in several texts and monographs, most of which have already been referred to [12,71,72,74,92-94]. The approach taken here is of a semi-quantitative nature with the principal objective being an understanding of the difficulties associated with studying solid samples and how to overcome these problems when performing the nmr experiment.

A. Hahn Echo NMR Spectroscopy of Solids

The anisotropic nature associated with spin interactions in solids impose stringent demands on the nmr spectrometer in order to observe "broad line" nmr spectra of static powdered samples. For example, heteronuclei such as ^{15}N and ^{31}P have chemical shielding anisotropies that range upwards of 1000 ppm which, at 4.7 T, corresponds to a frequency distribution of approximately 20 kHz for ^{15}N and over 80 kHz for ^{31}P. Two important considerations when attempting to study such anisotropic line shapes are : (1) the rf pulse power that one can deliver to the spin system and (2) the finite recovery

times of rf tuned circuits in the probe and receiver. The first problem relates to the fact that one must be able to "flip" all spins by the same amount (equation II.9) if the simple rotating frame approach to nmr interactions is to be valid. Thus, for a ^{31}P nucleus with a chemical shift anisotropy of over 80 kHz (≈1000 ppm) at 4.7 T, not even a $\pi/2$ pulse width of 4 μs (i.e., $(\gamma B_1/2\pi)$=62,500 kHz) would be able to provide uniform excitation across the entire frequency range of the nmr spectrum. It is important to point out that it is <u>not</u> the power of the rf amplifier that determines the effective flip angle but more importantly how efficiently the nmr probe can use this power. Thus, with improvements in nmr probe design, $\pi/2$ pulse lengths of 2-3 μs for heteronuclei are becoming available [11,95-98]. Even with such improvements, the "dead times" associated with the various tuned circuits in the nmr spectrometer are usually sufficiently long (20-60 μs) following an excitation pulse that the first few points on the FID cannot be recorded. For very broad line nmr spectra, a loss of the information in the first few points causes significant distortions in the powder nmr line shape [101]. An example which demonstrates the effect of a 20 μs pre-acquisition delay on the ^{119}Sn (I=1/2, ν_o=74.63 MHz) static cp nmr spectrum of 2,2-dibutyl-1,3,2-dioxastannolane is shown in figure III.1a. The total breadth of this cp nmr spectrum which is dominated by the tin chemical shift anisotropy is over 60 kHz. The distortions in the line shape are obvious

Figure III.1

The ^{119}Sn cp nmr spectrum of a static powdered sample of 2,2-dibutyl-1,3,2-dioxastannolane obtained with (a) the basic cp pulse sequence (figure II.9) with a pre-acquisition delay of t_d=20 μs and (b) the Hahn-echo cp sequence (figure III.2) with a τ delay of 50 μs. ^{119}Sn $\pi/2$ and π pulse lengths were 3.2 μs and 6.4 μs, respectively. Note the clear definition of the ^{119}Sn chemical shift anisotropy line shape in (b) as compared to (a).

Figure III.1

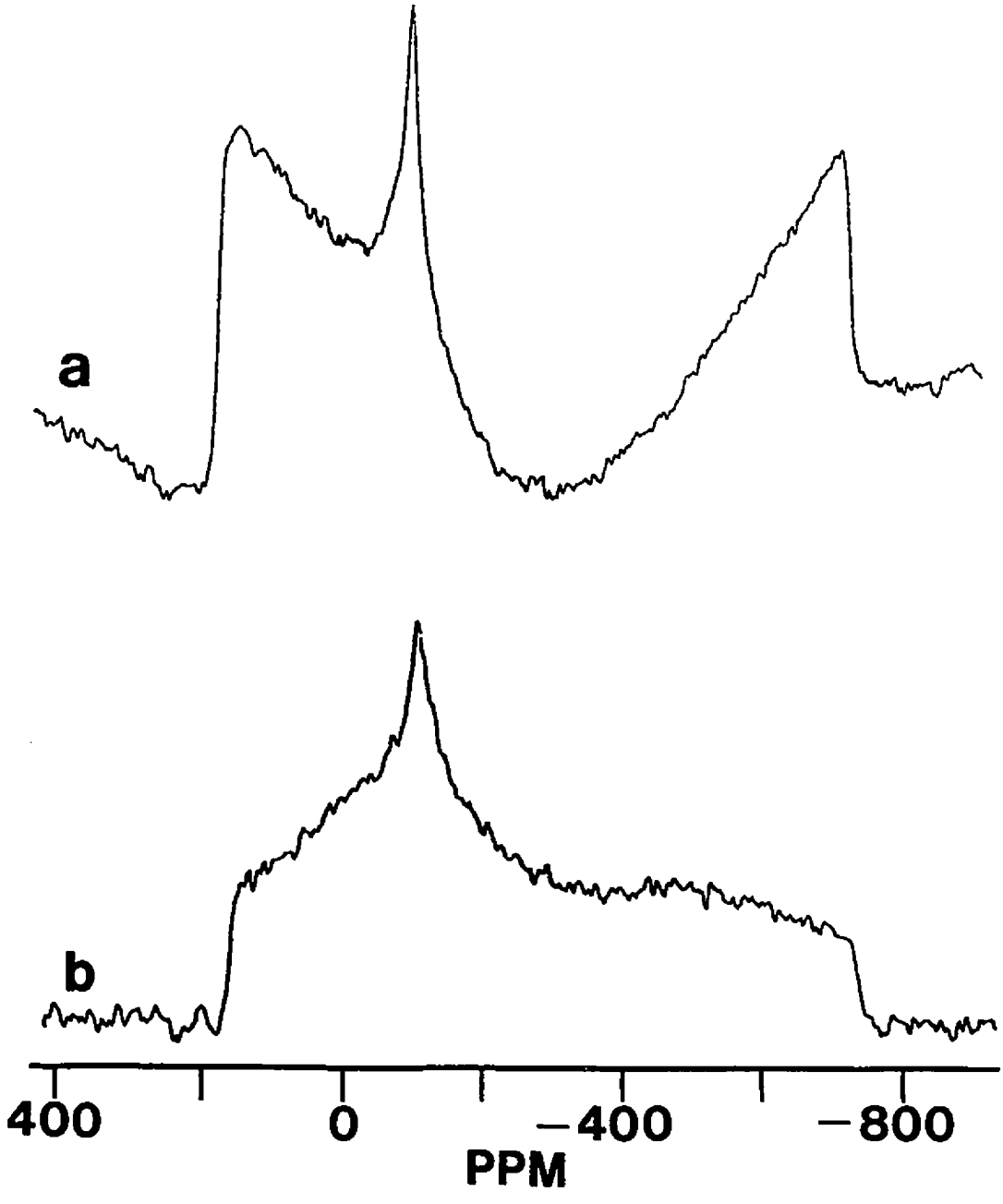

and thus obtaining accurate values for the three principal components of the ^{119}Sn chemical shift tensor is difficult.

Since the inherent "dead times" of the nmr spectrometer cannot be easily rectified so that the observation of the FID can start immediately after the excitation pulse, an alternative approach must be considered. The simplest method to overcome finite recovery times was first applied to solids by Stoll, Vega and Vaughan [99] and involves the use of a Hahn-echo pulse sequence [100] for observing the A-spins. The timing diagram for such a sequence incorporated into the basic cp sequence is shown in figure III.2. Basically, this technique involves the addition of a π pulse (in the transverse plane) to the A-spins at a time τ after the end of the contact pulse. Acquisition of the A-spin nmr signal then occurs at a time τ after the π pulse with high-power hydrogen decoupling. With a judicious choice of τ, an echo signal will occur at a time greater than the recovery time of the instrument and in the absence of other internal interactions a line shape with minimal distortions will be obtained for the dilute spin being investigated. An example of a Hahn-echo ^{119}Sn cp nmr spectrum (τ=50 μs) for a static powder sample of 2,2-dibutyl-1,3,2-dioxastannolane is shown in figure III.1b. Comparison of the two nmr spectra in figure III.1 clearly demonstrates the improvements that can be obtained by observing the first few points of the FID.

Figure III.2

The timing diagram for the cross polarization Hahn-echo spectroscopy of powdered solids. Typical pulse lengths correspond to those indicated in figure II.9. Values for the τ delay are normally between 40 μs and 150 μs. The FID signals for the two quadrature channels are indicated and the zero crossing (ZC) and echo maximum (EM) are labelled.

Figure III.2

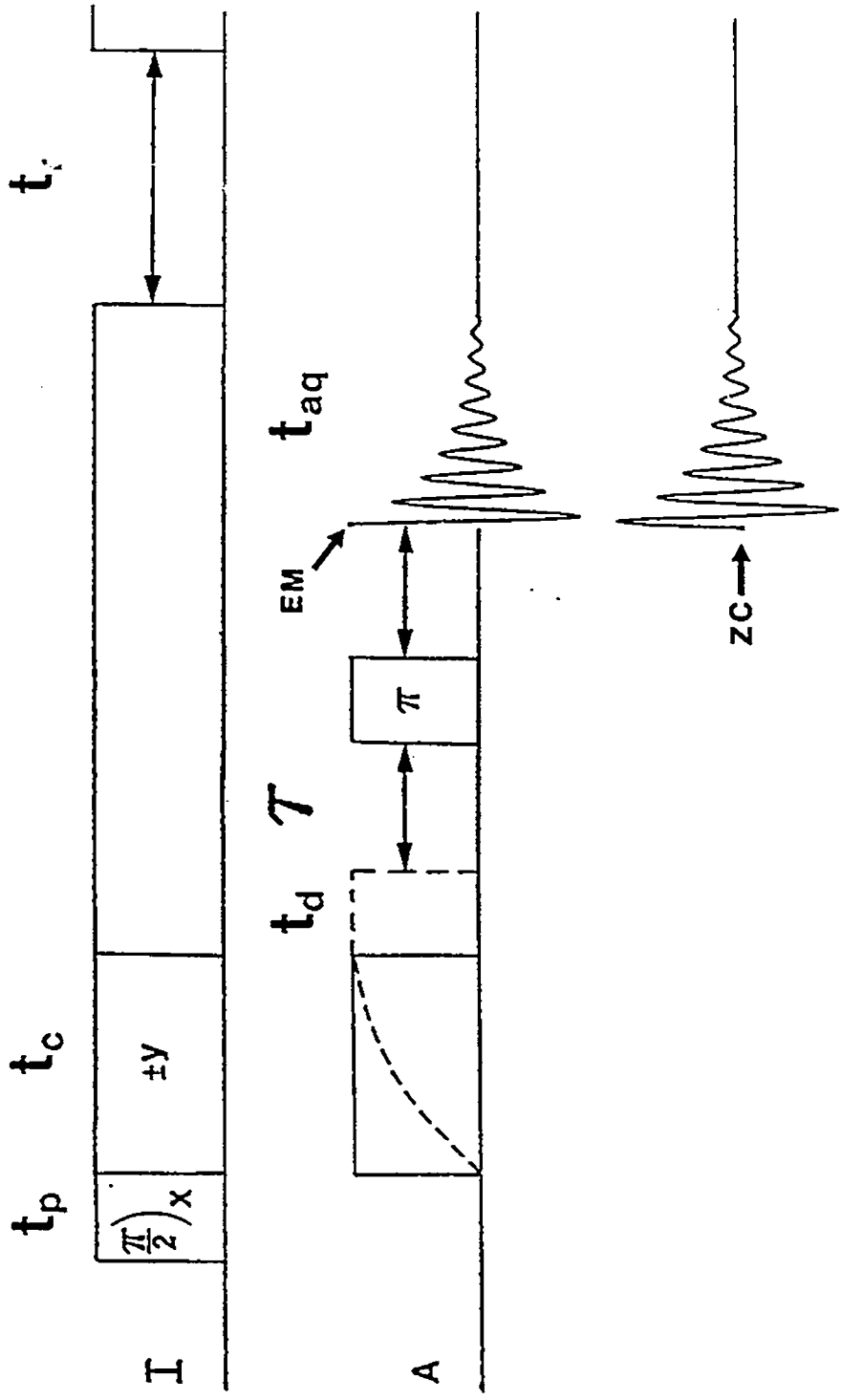

It is important to point out that the Hahn-echo sequence will only "refocus" the spin interactions which have linear dependence on I_z [17,19]. This is advantageous since problems associated with inhomogeneity of the static magnetic field (B_o) and imperfect pulses will be minimized. In addition, the heteronuclear dipolar interaction and the chemical shielding interaction are both described by Hamiltonians which are first order in I_z and therefore the spin echo technique is applicable to the study of "isolated" heteronuclear spin pairs. This is an important result since the general utility of the dipolar-chemical shift nmr method relies on obtaining accurate values for the dipolar splittings ($\Delta\nu_{II}$) from the dilute spin nmr spectrum. Conversely, homonuclear dipolar interactions have a second order dependence on I_z and are not influenced by the application of the π pulse. If present, they can modulate the echo amplitude and therefore lead to distortions in the nmr spectrum of the dilute spin being investigated. Fortunately, for the majority of organic and inorganic solids, the homonuclear spin interaction energies are small and should not influence the general applicability of the Hahn-echo method.

Rance and Byrd have presented a detailed discussion of the experimental aspects associated with acquiring Hahn-echo nmr spectra for dilute spin 1/2 nuclei in solids [101]. Before attempting this experiment, it is important to consider the spin-spin relaxation time (T_2) of the A-nuclei being

examined. If the T_2 is short as compared to the inherent recovery time of the nmr spectrometer, t_d, then the Hahn-echo method will not provide useful nmr spectra. Since most modern high-resolution solid state nmr spectrometers have natural "dead times" of approximately 20-60 μs, typical values for the τ delay are on the order of 40-100 μs. Shorter τ values, on the order of 10-30 μs, can be obtained on some nmr instruments by (i) opening the audio frequency filter to the maximum value to alleviate acoustic ringing effects and/or (ii) adding resistors to the tuned rf circuit of the nmr probe to reduce the ring-down time [98]. The choice of the echo maximum can be done by determining the point where the FID signal is a maximum in one channel and zero in the other quadrature channel as indicated in figure III.2. In some cases this can be done by simply examining the FID but in others, one may require the use of an interpolation scheme such as the one outlined by Rance and Byrd [101]. It is important to note that the proper choice of the echo maximum is <u>critical</u> if one wants to obtain the minimum amount of distortion in the resulting dilute spin nmr spectrum. Finally, it is important to phase cycle the various pulses in the Hahn-echo experiment. This will help reduce distortions related to incomplete rf excitation and rf pulse imperfections. The phase cycle scheme described by Rance and Byrd [101] has been shown to give excellent results and this author highly recommends such a scheme in practice. In summary, the Hahn-echo nmr technique

reduces the distortions in the dilute spin static nmr spectra arising from the finite dead time of the nmr spectrometer. The solid state nmr experimentalist should, however, be aware that it is much more difficult to deal with inadequate rf pulse power. Therefore, this author stresses a well established fact [11,12,17,19], that high power rf pulses are essential to the implementation of modern day solid state pulse nmr techniques.

B. Optimization of the Cross Polarization Experiment

In order to obtain reliable chemical shift parameters from a dilute spin nmr spectrum of a static powdered solid, it is essential to have sufficient signal to noise (S/N) so that the discontinuities and shoulders are well defined. The S/N ratio of an nmr spectrum is dependent upon a number of instrumental and experimental parameters. For example, the S/N ratio for a particular nucleus increases with the use of higher applied magnetic fields, B_o; also, improvements in S/N can be realized by making a suitable choice of rf pulse lengths (i.e., flip angles) and recycle times. Of paramount importance to improving the S/N ratio when studying dilute spins in solids by cross polarization, is the judicious choice of the contact time, t_c. In general, the optimum value of t_c varies for every different dilute spin in the solid sample being investigated. However, for carbon-13 nuclei in typical organic solids, it has been demonstrated that the value of t_c

is usually relatively constant for the carbon nucleus of a given functional group [68].

The best value of t_c to use for the dilute spin A-nuclei in a cp nmr experiment is primarily determined by the relative contributions of two competing processes : (1) the A-nuclei cross polarization rate, R_{AI}, which is characterized by a relaxation time T_{AI} and (2) the I-nuclei rotating frame spin-lattice relaxation time, $T_{1\rho,I}$. The first of these times, T_{AI}, corresponds to the time required for the A nuclei to fully polarize (i.e., M_A proportional to γ_I/γ_A) under the Hartmann-Hahn matching condition. The time T_{AI} is related [102] to the A-I heteronuclear second moment which for a solid powdered sample can be expressed as :

$$M_{2,AI} = (1/2\ \gamma_A\gamma_I\ (h/2\pi)\ (\mu_o/4\pi))^2 \sum_j [(3\cos^2\theta_{AI_j}-1)^2/r^6_{AI_j}] \quad [III.1]$$

The sum is over all I_j nuclei which have a direct dipolar coupling to the A-nuclei being investigated. The strong dependence of $M_{2,AI}$ on the A-I internuclear separation implies that the directly bonded I-nuclei (e.g., hydrogens) will dominate the cross polarization rate, $R_{AI} = (1/T_{AI})$. On this basis, one would anticipate that R_{AI} would increase with the number of I-nuclei attached to the dilute spin being investigated. In addition, since the second moment, $M_{2,AI}$ is closely related to the magnitude of the local dipolar interactions, R_{AI} will be smaller for systems where molecular motion causes averaging of the heteronuclear dipolar interaction. For example, the hydrogen/carbon cross

polarization rates for ^{13}C nuclei of typical organic solids would be expected to increase in the order :

CH_3 (static) > CH_2R_2 > CHR_3 ≈ CH_3 (rotating) >> CR_4

Indeed, this simple qualitative description is consistent with experimental solid state ^{13}C cp/mas nmr results for a large number of organic solids [68].

The enhancement of the dilute spin nmr signal as governed by T_{AI} competes with the process of rotating frame spin lattice relaxation whereby the I-spins return to equilibrium along the z-direction (i.e., $M_z=M_o$) with a time constant, $T_{1\rho,I}$. The time $T_{1\rho,I}$ is related to molecular motions which occur at or near the frequency of the rf field used to establish the spin-locking condition for the I-nuclei. If the I-nuclei are hydrogens where typical decoupler rf field strengths for solid samples are on the order of 40-70 kHz, then hydrogen $T_{1\rho}$ values are sensitive to molecular motions in the tens of kHz regime.

A simple method to experimentally determine the balance between T_{IA} and $T_{1\rho}$ is to perform a series of nmr experiments on the sample of interest with a variety of contact times, t_c. Normally, this type of experiment is carried out on a spinning sample (mas) since it is easier to observe a variation in the signal intensity of a narrow resonance signal as compared to the broad line nmr signal observed for a static powder. Unless the magic angle spinning speed approaches the magnitude of the AI dipolar interactions in Hz, the influence of mas on the cross polarization dynamics is negligible.

However, when $M_{2,AI}$ is small relative to the spinning speed, it has been demonstrated that mas can modulate the dipolar interaction and hence modulate the observed dilute spin nmr signal intensity [68]. This is normally not observed for rigid systems with directly bonded hydrogens but can often be encountered if molecular motions are present or if the nucleus of interest is located at a site with only remote contacts to hydrogen [68]. For the general case, the observed relative intensities of a particular A-spin resonance signal in the dilute spin cp/mas nmr spectra can be numerically fit to the expression [103] :

$$I=(I_o/T_{AI})\{(\exp(-t_c/T_{1\rho,I})-\exp(-t_c/T_{AI}))/((1/T_{AI})-(1/T_{1\rho,I}))\} \quad [III.2]$$

where I is the observed signal intensity for each t_c and I_o is the maximum signal intensity which corresponds to the optimum value of the contact time, $t_{c,o}$. Two illustrative examples as applied to ^{15}N cp/mas nmr are shown in figure III.3. The plots in this figure represent the observed ^{15}N resonance signal intensity versus the contact time for the isotropic resonance signal (δ_{iso}) of two 20% ^{15}N enriched samples of 1-methoxy-4-(N-phenylaminomethyl)naphthalene. The only difference between the two samples is that one of them has a hydrogen bonded to the nitrogen (figure III.3a) whereas the other one has a deuterium (I=1) bonded to the nitrogen (figure III.3b). Numerical optimization of the plotted intensities as a function of the contact times by a simplex procedure [103,104] provides values for T_{AI}, $T_{1\rho,I}$ and I_o.

Figure III.3

Plots of the ^{15}N isotropic signal intensity versus hydrogen/nitrogen contact time for magic angle spinning samples of (a) normal and (b) N-deuterated 1-methoxy-4-(N-phenylamino-methyl) naphthalene. The curves represent the best fit lines of the experimental data to equation III.2 which were obtained by simplex optimization. The optimum values of the contact times, $t_{c,o}$, are labelled.

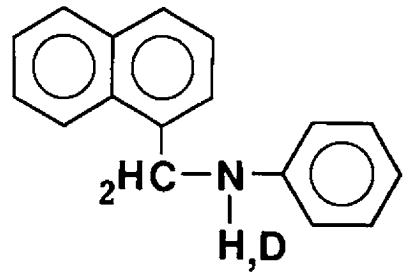

Figure III.3

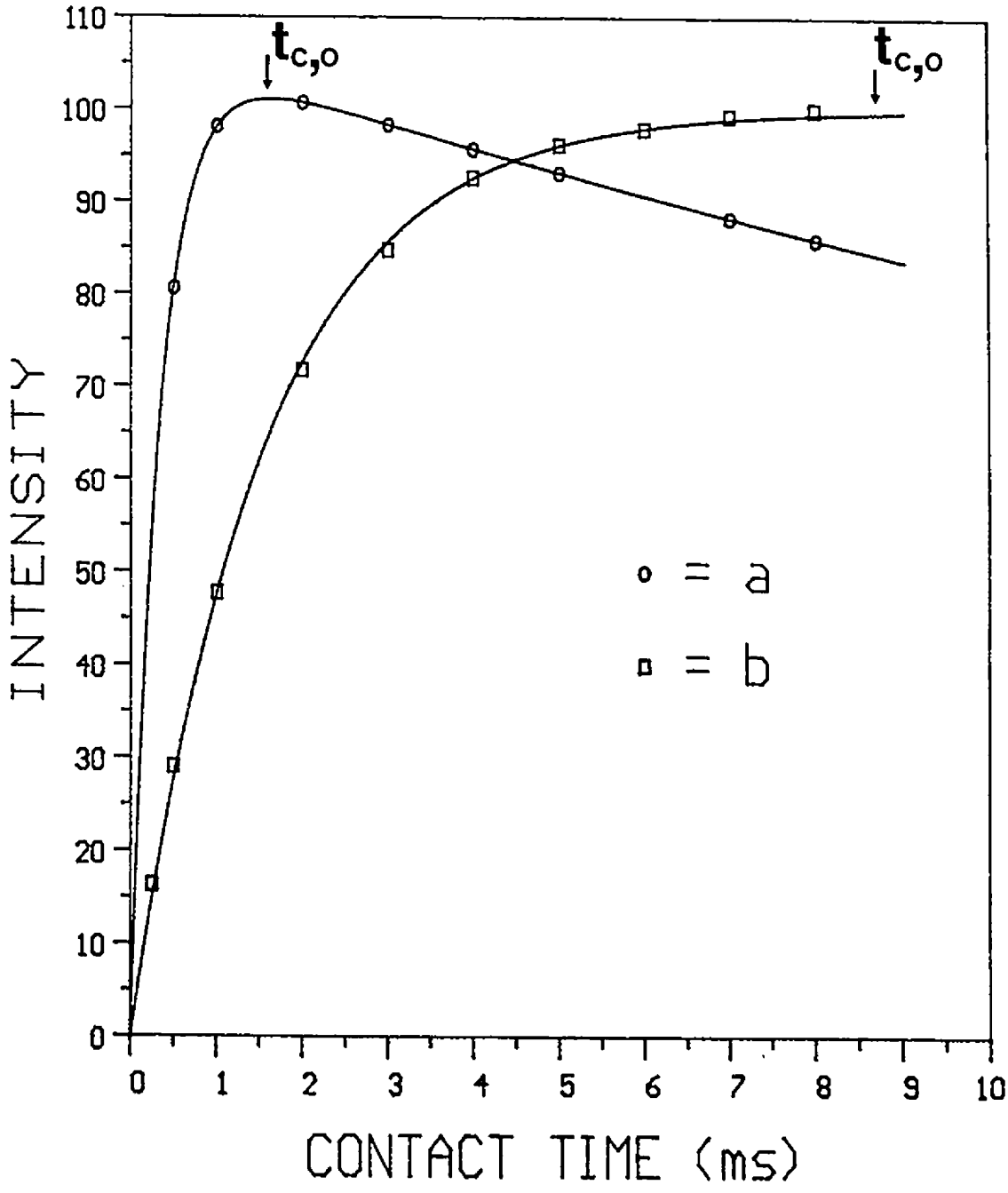
110
100
90
80
70
60
50
40
30
20
10
0
INTENSITY
$t_{c,o}$
$t_{c,o}$
o = a
□ = b
0
1
2
3
4
5
6
7
8
9
10
CONTACT TIME (ms)

The optimum value for the contact time, $t_{c,o}$, can be obtained readily from inspection of the plots in figure III.3 and is located at the maximum relative signal intensity as indicated. Typical data that is obtained from the use of the simplex optimization procedure on the experimental results for the two samples of 1-methoxy-4-(N-phenylaminomethyl)naphthalene is presented in table III.1.

Table III.1

Hydrogen/nitrogen-15 cross polarization data for normal and deuterated 1-methoxy-4-(N-phenylaminomethyl)naphthalene. The experimental ^{15}N nmr spectra were recorded at a spinning speed of 2.5 kHz with high-power hydrogen decoupling.

Parameter	Normal	Deuterated
I_o	105.6	100.1
T_{AI} (ms)	0.34	1.55
$T_{1\rho,I}$ (ms)	37.0	1.83E6
$t_{c,o}$ (ms)	1.50	> 8.0

Consideration of the data in table III.1 provides support for the conclusion that the directly bonded hydrogens dominate T_{AI}.

For example, the N-deuterated sample has a cross polarization relaxation time, T_{AI}, which is approximately five times as long as the corresponding value observed for the sample with a hydrogen bonded to the nitrogen nucleus of this molecule. The $T_{1\rho,I}$ values of the two samples are also very different which indicates that the N-H bond is probably involved in independent motions as compared to the rest of the molecule. The optimum contact times, $t_{c,o}$, are typical for ^{15}N nuclei which normally has values of $t_{c,o}$ in the range of 0.5-12 ms. Thus, if one is going to perform an nmr experiment on a dilute spin in a static sample, the value of $t_{c,o}$ should be determined prior to acquiring the static nmr spectrum. Finally, it has been demonstrated that for ^{13}C cp/mas nmr the optimum value of t_c for typical organic solids is usually between 1-3 ms [68]. If values for t_c in this range are used in the nmr experiment, the intensities in the ^{13}C cp/mas nmr are often closely related to the atomic ratios in the sample [68]. This is an important result since it allows one to perform a crude quantitative analysis of a solid sample in order to estimate the purity. For solid samples whose structural integrity is not maintained in solution, this information may be critical for characterizing the material.

A modification to the basic cp nmr experiment is useful if the hydrogen $T_{1\rho}$ is long compared to the sum of the contact time and acquisition time. An example of such a situation is apparent for the hydrogen $T_{1\rho}$ of deuterated 1-methoxy-4-(N-

phenylaminomethyl)naphthalene shown in figure III.3b. Under these conditions, a substantial portion of the hydrogen magnetization remains at the end of the acquisition period. Tegenfeldt and Haeberlen have described a pulse sequence which is similar to that of the normal cp experiment (figure II.9) with the addition of a $\pi/2$ pulse to the I-nuclei at the end of the observation period [105]. This pulse is of opposite phase with respect to the initial I-spin $\pi/2$ pulse and returns the I-magnetization to the z-axis (i.e., along B_o). The experiment is appropriately called the FLIPBACK pulse sequence and can be used to increase the S/N ratio of the dilute spin nmr spectrum for chemical systems which have long I-nuclei spin-lattice relaxation times [105]. It should be noted that the use of this pulse sequence will never decrease the S/N ratio in the resulting cp nmr spectrum as compared to a single or multiple contact cross polarization experiment.

C. The Dipolar Dephasing Experiment

Alla and Lippmaa were the first to describe and use the dipolar dephasing pulse sequence shown in figure III.4 for the study of dilute spins [106]. The initial part of this sequence generates the enhanced nmr signal for the dilute spins during the contact time, t_c, as previously discussed. When the decoupling field for the I-nuclei is turned off, the A-I dipolar Hamiltonian evolves for a period of time, τ_{DD}, referred to as the dipolar dephasing delay. During the

Figure III.4

The timing diagram for the dipolar dephasing pulse sequence. The dipolar dephasing delay, τ_{DD}, is indicated.

Figure III.4

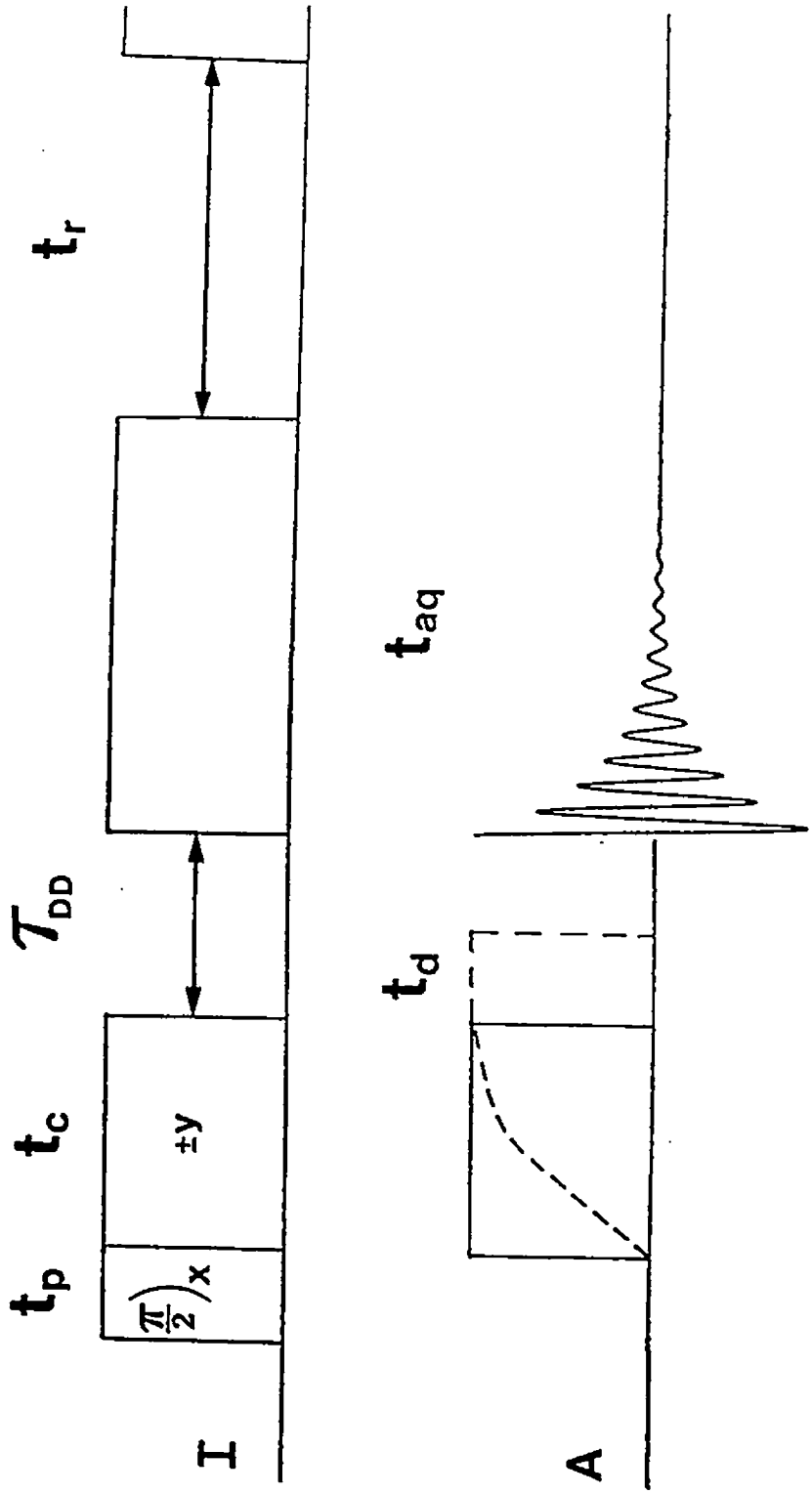

interval τ_{DD}, the spin order of the dilute nuclei rapidly dephases due to the influence of the chemical shift anisotropy and the heteronuclear dipolar interactions. At the end of the interval τ_{DD}, the decoupler field for the I-spins is turned on and therefore stops the evolution of the A-I dipolar Hamiltonian during acquisition while maintaining the influence of the chemical shift interaction. Thus, the dipolar dephasing experiment allows one to measure the time required for a polarized dilute spin to lose its magnetization after the I-spin lock is turned off. The analogy of this to the measurement of the ^{13}C spin-spin relaxation time (T_2) is noted.

The resulting nmr spectrum observed for the dilute spins with the application of the pulse sequence in figure III.4 depends on the magnitude of the local dipolar interactions with the I-nuclei. For strongly dipolar coupled A-I spin systems such as CH, NH, CH_2 and NH_2, the decay of spin order is very efficient and this leads to very weak signals in the nmr spectrum for these nuclei with τ_{DD} times greater than 40 μs [68c,106-114]. For weakly coupled spin systems such as rotating methyl groups or nonprotonated moieties (e.g., CR_4, NR_3), the local dipolar interactions with the I-nuclei are small and therefore the spin order developed for these nuclei during the contact time will be maintained throughout the dipolar dephasing delay. Thus, the cp/mas spectra acquired for typical organic solids with the dipolar dephasing pulse scheme will contain resonance signals for those dilute spins

in a quaternary environment (i.e, no directly bonded hydrogens) or those involved in a significant amount of molecular motion. Because of this property, the technique is often referred to as the non-quaternary suppression pulse (NQS) sequence.

A variety of dephasing delay times (τ_{DD}) have been reported for the study of ^{13}C nuclei in solid materials [68c, 106-114]. According to Opella and Frey, τ_{DD} times of approximately 40 μs are usually sufficient to suppress the ^{13}C resonance signals for carbon nuclei of methine and methylene groups. For ^{15}N nuclei, the heteronuclear dipolar interactions involving hydrogens are usually smaller than those for ^{13}C and thus one would anticipate that slightly larger values of τ_{DD} would be appropriate. To date there has not been a comprehensive study to address this issue in detail. This author has found that τ_{DD} for ^{15}N dipolar dephasing nmr experiments are approximately 80-200 μs for complete suppression of ^{15}N nmr signals for nitrogens with bonded hydrogens.

The simplification of the dilute spin nmr spectrum obtained with the dipolar dephasing pulse sequence usually results in the immediate assignment of several resonances to particular dilute spins in the sample being investigated. This is advantageous since the suppression of indirect spin-spin couplings (J_{iso}) between ^{13}C and ^{1}H in ^{13}C cp/mas nmr spectra makes the assignment of the resonance signals more

complicated. In addition to simplifying the assignment of dilute spin cp/mas nmr spectra, the dipolar dephasing experiment can also be used to obtain specific structural information in the solid state. For example, with ^{15}N cp/mas nmr one could readily distinguish between the protonated and nonprotonated forms of tertiary amines (i.e., NR_3 versus $HN^{+}R_3$) on the basis of ^{15}N cp/mas experiments performed with the dipolar dephasing pulse sequence. In this case, only the non-protonated form of the tertiary amine would give rise to an ^{15}N resonance signal in the cp/mas nmr spectrum acquired with the dipolar dephasing pulse sequence. Experimental examples will be given for the tetracycline antibiotics in section IV.C.

IV. Applications of Solid State NMR

A. Characterization of the Carbon-13 and Nitrogen-15 Chemical Shift Tensors of the Carbon-Nitrogen Double Bond in Benzylideneaniline and Related Imines.

A.1 Introduction

In the past ten to fifteen years information about the anisotropic nature of the chemical shift has become available for carbon nuclei [12,48,55b,56,115-126] and to a lesser extent for nitrogen nuclei [12,20,53,55b,56,115-117,119,122, 127-130] in a variety of molecular environments. Generally, the principal components of the chemical shift tensor for any given functional group are reasonably constant or typical for that particular functional group [12,20, 115,117,120b,124, 125]. For example, in a series of ten relatively unstrained molecules containing olefinic carbons, Orendt et al. [125] found that the most shielded component of the ^{13}C chemical shift tensor, δ_{33}, varied between 5 ppm and 51 ppm; similarly, the intermediate component, δ_{22}, varied between 86 ppm and 152 ppm and the least shielded component, δ_{11}, varied between 214 ppm and 288 ppm. In this same series of molecules the isotropic chemical shift, δ_{iso}, has a smaller range, 116 ppm to 149 ppm. Potentially more information regarding substituent effects, steric effects and other structural parameters on the chemical shielding at a nuclear site is available from the

three principal components of the shift tensor than from the isotropic chemical shift, particularly if the orientation of the principal axis system of the tensor can be determined. Thus, it is desirable to characterize chemical shift tensors for molecular systems containing as many different bonding environments as possible. One system, which has not previously been studied by solid state nmr, is the carbon-nitrogen linkage of the imine bond. In order to determine the orientation of the ^{13}C and ^{15}N chemical shift tensors in the imine fragment, samples of a representative compound, benzylideneaniline (1a), were prepared. This compound was

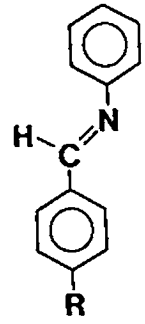

Compound	R
1a	H
1b	OCH_3
1c	NO_2

chosen since it is easy to prepare with selective isotopic enrichment (e.g., ^{13}C or ^{15}N) at either or both of the imine carbon or nitrogen. The "isolated" spin-pairs (e.g., $^{13}C,^{14}N$ and $^{13}C,^{15}N$) may then be investigated by ^{13}C and ^{15}N dipolar-chemical shift nmr spectroscopy to fully characterize both chemical shift tensors. A further advantage of this compound is that x-ray diffraction results indicate that 1a crystallizes in the monoclinic space group $P2_1/c$ with four crystallographically equivalent molecules per unit cell [131].

This is important since difficulties in analyzing powder nmr spectra where crystallographic nonequivalence is present are avoided [55a]. The results reported in this section of the thesis represent the first example where both the orientation and magnitude of the carbon and nitrogen chemical shift tensors of a "localized" imine bond have been determined. A previous study on all-trans-retinylidenebutyl-[^{15}N]-imine [132] provided only the magnitude of the imine nitrogen chemical shift tensor. Both carbon and nitrogen chemical shift tensors determined for 1a will be compared to recent experimental results on the oxime moiety [55b] as well as with other chemical systems containing carbon or nitrogen involved in a double bond.

The second part of the discussion of the imine system will focus on the variation of the three principal components of the ^{15}N chemical shift tensors in several related compounds. Specifically, the nitrogen shielding properties of two substituted benzylideneanilines 1b and 1c , three naphthylideneanilines (2) and two salicylideneanilines (3) will be examined. The compounds indicated in 1 and 2 provide an opportunity to examine the influence of substituents on the magnitudes of the three principal components of the ^{15}N chemical shift tensor whereas the compounds indicated in 3 provide an opportunity to examine the influence of hydrogen bonding on the ^{15}N chemical shift tensor.

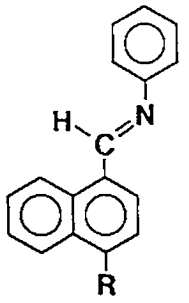

Compound	R
2a	H
2b	OCH_3
2c	CN

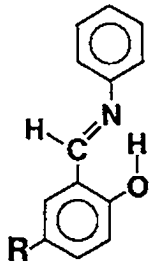

Compound	R
3a	H
3b	Cl

A.2 Experimental

The benzylideneaniline (1), naphthylideneaniline (2) and salicylideneaniline (3) samples were prepared by refluxing an equimolar mixture of the appropriate aldehyde and aniline in toluene using a Dean Stark apparatus for the removal of water. For 1a, the benzaldehyde-^{13}C (99.6 %) and aniline-^{15}N (95 %) were procured commercially (MSD Isotopes, Montrèal, Canada). The $^{13}C{=}^{15}N$ and $^{13}C{=}^{14}N$ samples of 1a were prepared solely from the respective isotopically enriched materials whereas a separate sample of $^{12}C{=}^{15}N$ 1a enriched with 20 % ^{15}N was prepared by mixing aniline-^{15}N with aniline prior to the reaction. The naphthaldehydes used for the preparation of the compounds in 2 were synthesized by Mr. J. Hilborn, Dalhousie University. Salicylaldehyde and 4-chlorosalicylaldehyde were

purchased from the Aldrich Chemical Company. Before preparing ^{15}N enriched samples of 1, 2 and 3, natural abundance samples were synthesized. Carbon-13 nmr spectra of chloroform solutions indicated that with the exception of 2a and 2b, all samples were very pure. The impure samples of 2a and 2b were further purified by column chromatography on silica gel (3 parts methanol:1 part ethyl acetate).

Carbon-13 and ^{15}N solid state nmr spectra were recorded at 50.32 MHz and 20.30 MHz respectively using a Bruker MSL-200 spectrometer (B_o=4.7 T). Samples (~300 mg) were ground to a fine powder and packed into rotors (7 mm o.d., 18 mm long) made from either aluminum oxide or zirconium oxide. Nmr spectra were acquired at 293 K under the conditions of the Hartmann-Hahn match and with high-power hydrogen decoupling. The $\pi/2$ pulse widths were in the range 3.5-6.5 μs for ^{13}C, ^{15}N and ^{1}H. All cp nmr spectra were recorded using the FLIPBACK pulse sequence [105] with recycle times of 7-80 s. The contact times for the ^{15}N nuclei of the various imines studied were optimized from mas nmr experiments (ν_r = 2-4 kHz). Typical values of $t_{c,o}$ for compounds 1, 2 and 3 were found to be 4-6 ms. These optimum values for t_c were then used for acquisition of the respective stat'c ^{15}N nmr spectra. The acquisition time for all cp/mas nmr spectra was approximately 50-200 ms; the corresponding times for the static samples were 15-35 ms. For the static samples of 1a, sensitivity enhancements corresponding to 50 Hz and 100 Hz of line

broadening were applied to the ^{13}C nmr spectra and ^{15}N nmr spectra respectively prior to Fourier transformation. For the remaining samples, sensitivity enhancements were applied as determined from the acquisition time (i.e., $(AT)^{-1}$).

Carbon-13 chemical shifts were referenced with respect to tetramethylsilane by setting the observed chemical shift of the methylene carbon of external adamantane at 38.56 ppm [133]. Adamantane was also used to establish the Hartmann-Hahn matching condition. Doubly enriched ammonium nitrate was used to optimize the Hartmann-Hahn matching condition for the ^{15}N cp nmr experiments. Nitrogen-15 chemical shifts were referenced with respect to $NH_3(\ell)$, 0 ppm (293 K). This was accomplished by setting the observed ^{15}N chemical shift of the ammonium ion signal of external ammonium nitrate at 23.8 ppm.

The theoretical powder nmr spectra were calculated using the interpolation scheme of Alderman et al. [134] based on the equations II.31-II.36. The simulation routine was modified by Mr. B. Power to include the calculation of the ^{13}C static nmr spectrum based on equations II.32, II.35 and II.36. The simulation routine can also include the effects of an isotropic and anisotropic J tensor. However, for 1a the isotropic $^1J(^{13}C,^{15}N)$ coupling is only -7.2 Hz [135]; therefore, it was assumed that the anisotropy in J is small and it was subsequently neglected in all simulations. The theoretical spectra were convoluted with a Gaussian line broadening function, $g(\nu)$, for an improved fit to the experimental nmr

spectra. Calculations of the ^{13}C-^{14}N cp/mas nmr spectra were carried out using the method of Hexem et al. [88]. The simulation routine for calculating these ^{13}C nmr spectra was supplied by Professor S.J. Opella, University of Pennsylvania. All computations were performed on a VAX 8800 computer.

A.3 Results and Discussion

Dipolar-Chemical Shift NMR Experiments on Benzylideneaniline

The static ^{13}C nmr spectrum for the doubly isotopically enriched $^{13}C,^{15}N$ sample of 1a is shown in figure IV.1a. The shape of this nmr spectrum is typical for an isolated $^{13}C,^{15}N$ spin pair with an asymmetry parameter of the carbon chemical shift anisotropy approaching unity. Initial estimates of the three principal components of the carbon chemical shift tensor were obtained from the static ^{13}C nmr spectrum for the $^{13}C,^{14}N$ sample of 1a (*vide infra*). The magnitude of the dipolar interaction constant, R, for the $^{13}C,^{15}N$ pair was calculated to be -1606 Hz based on the r_{CN} bond length, 1.24 ± 0.02 Å, determined by x-ray diffraction experiments [131]. The first attempts to simulate the static ^{13}C nmr spectrum for the $^{13}C,^{15}N$ spin pair allowed the magnitudes of the three principal components and the values of the Euler angles α and β to vary while constraining the bond length to 1.24 Å. After numerous computer simulations, the values of α and β were determined to be 75 ± 7° and 76 ± 7°, respectively. The simulated ^{13}C static nmr spectrum based on these values of α and β is shown

Figure IV.1

The (a) experimental and (b) calculated ^{13}C nmr spectra of a solid powder sample of 1a where both the imine carbon and nitrogen are ^{13}C (99.6%) and ^{15}N (95%) enriched, respectively. The spectrum results mainly from the carbon involved in the imine bond with only a small contribution from the other twelve carbons in the molecule.

Figure IV.1

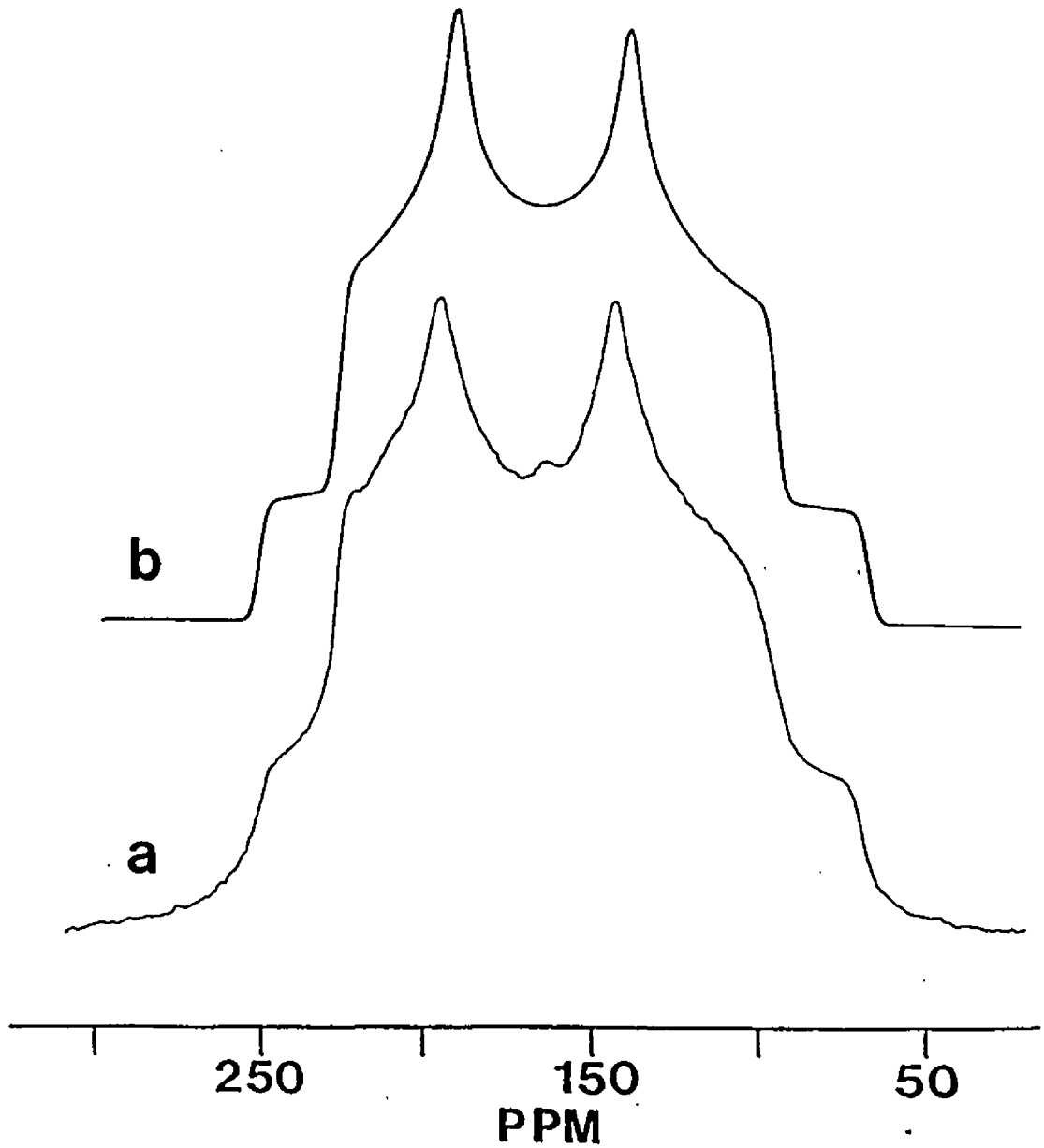

in figure IV.1b and the ^{13}C chemical shift parameters derived from figure IV.1 are indicated in table IV.1.

Table IV.1

Carbon-13 and Nitrogen-15 Chemical Shift Parameters and Dipolar Coupling Constants for the Imine Bond.

Nucleus	R	δ_{11}	δ_{22}	δ_{33}	δ_{iso}	α	β	$\Delta\delta$	η_σ
^{13}C-^{15}N	1606	235	167	79	160	75	76	156	0.88
^{15}N-^{13}C	1606	610	321	65	332	42	78	545	0.92

	R	$\chi(^{14}N)$	η_Q	α^D	β^D	α^{CS}	β^{CS}	γ^{CS}
^{13}C-^{14}N	1145	-4.45	0.64	90	49.5	0	76	46

Further simulations of the ^{13}C nmr line shape which allowed the bond length to vary indicated that for every change of 0.01 Å in the bond length the value of α changed by 1° and that of β changed by 2°. For example, if β is restricted to be 90° (i.e., δ_{33} is perpendicular to the HCN plane), then the value of r_{CN} determined from the calculated ^{13}C nmr spectrum is 1.32 Å (R'=-1332 Hz) and the value of α is 83°. Although this value of r_{CN} is 0.08 Å longer than the value reported from x-ray

diffraction experiments [131], it should not be rejected without a proper consideration of the possible sources of error associated with the dipolar-chemical shift nmr technique.

Derivation of bond lengths from observed dipolar coupling constants in nmr spectra is often complicated by contributions from effects other than the direct dipolar interaction. Since both nuclei being investigated in this system are second row elements, the influence of anisotropy in J is anticipated to be negligible [20]. Molecular motion such as librations may reduce the static value of R; however, for a rigid system such as benzylideneaniline motional effects are expected to be small. Cross-relaxation has been shown to reduce the magnitude of the observed dipolar splittings [136]; however, when this effect is present, it is made obvious by the characteristic "hump" in the line shape at orientations close to the magic angle but causes only a small distortion on rest of the line shape. The presence of one or more of these effects will tend to reduce the observed value of R, leading to longer derived bond lengths. Consequently, bond lengths derived from dipolar coupling constants obtained from nmr spectra should be considered as upper limits. Furthermore, as R and the angles α and β are highly covariant (equation II.32), the values quoted for these angles will also correspond to lower limits. Thus, for the imine carbon of benzylideneaniline, the value for β is 76°, where it should be

understood that if the influence of motional averaging is taken into account β will increase.

For the $^{13}C,^{14}N$ sample of 1a the basic features of the static ^{13}C nmr spectrum are quite different (figure IV.2a). In this case, the ^{13}C spins are dipole coupled to a spin 1 nucleus and three subspectra are discernible in figure IV.2a. Also, the magnitude of the dipolar coupling constant is decreased by a factor $\gamma(^{14}N)/\gamma(^{15}N)$, 0.7129, such that R is 1145 Hz. Initial attempts to simulate this nmr spectrum were made using the parameters previously described for the $^{13}C,^{15}N$ sample of 1a (see table IV.1) under the condition of the high-field approximation [33-35]. The resulting calculated ^{13}C static nmr spectrum under these circumstances is shown in figure IV.2b. Close examination of figure IV.2 indicates that there are significant differences between the experimental and calculated ^{13}C nmr spectra when the dipolar coupling constant is restricted to 1145 Hz. In particular, the dipolar splittings at both the δ_{11} and δ_{33} regions of the experimental nmr spectrum are equal (figure IV.2a) whereas the calculated ^{13}C nmr spectrum predicts unequal splittings (figure IV.2b). When the value of R was allowed to vary, an adequate fit between the experimental and calculated nmr spectra was found when the bond length was increased to r_{CN}=1.29 Å. In this case, the values of α and β were determined to be 80° and 85°, respectively. It should be noted that this result is in disagreement with the x-ray results [131] and the

Figure IV.2

The (a) experimental and (b) calculated ^{13}C nmr spectra of a solid powder sample of 1a where the imine carbon is enriched with 13C (99.6%). The high-filed approximation was assumed for the ^{14}N nucleus when calculating spectrum (b). The * indicates the low-frequency shoulder due to the natural abundance contributions from the other twelve carbons in 1a.

Figure IV.2

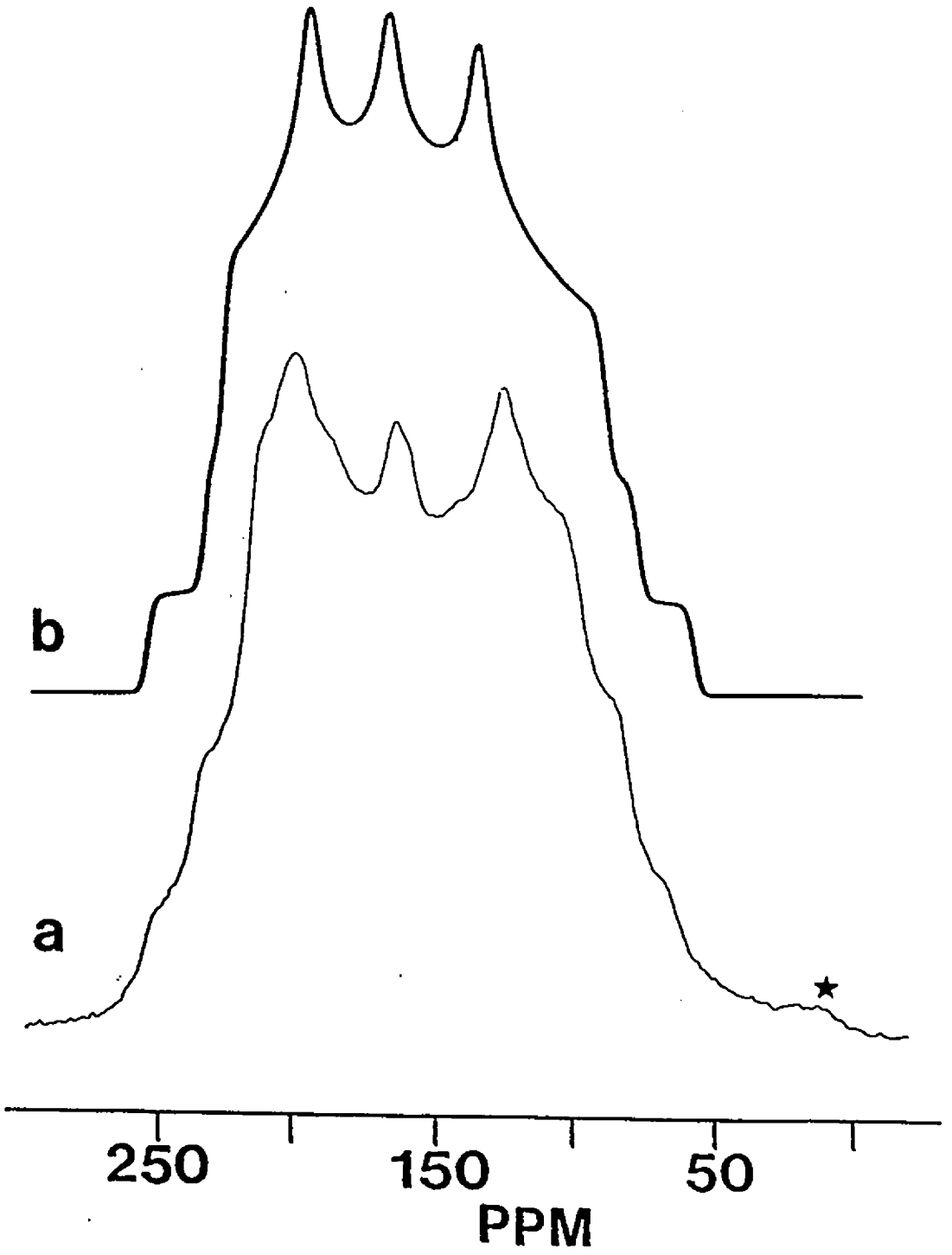

forementioned arguments; therefore, it was concluded that the high-field approximation is not strictly valid at B_o=4.7 T for the ^{14}N nuclei of the imine bond of 1a.

In order to circumvent the high-field approximation, precise information on the magnitude and orientation of the ^{14}N efg tensor is required. Unfortunately, data of this type is currently unavailable in the literature for 1a. However, information on the ^{14}N efg tensor has been reported for two closely related compounds. NQR results exist for the "enol" form of salicylideneaniline (3a) [137], providing the magnitude of $|\chi|$, 4.026 MHz, and η_Q, 0.238. The orientation of the ^{14}N efg tensor is not available for this compound. One would expect the values of $|\chi|$ and η_Q to be somewhat larger in 1a, as the intramolecular hydrogen bonding in 3a may reduce these quantities. Microwave data exist for the parent imine, methyleneimine (H_2C=NH) [138], although only the inertial axes values of the ^{14}N efg tensor are reported. There is insufficient information to determine the components of the efg tensor in the principal axis system, which is essential to the analysis of the ^{13}C static nmr spectrum for the ^{13}C,^{14}N spin-pair. Gerber and Huber [139] performed high-level ab initio calculations of the ^{14}N efg tensor in a series of simple molecules, including methyleneimine. Their results were reported in the inertial axis system, allowing direct comparison to microwave data, and included off-diagonal elements, often not available by experiment. Diagonalization

of the complete ^{14}N efg tensor in the inertial axis system provides χ, η_Q and the orientation of the ^{14}N efg principal axis system with respect to the inertial axes [140]. The calculated inertial axes values for the ^{14}N efg tensor for methyleneimine [139] are in excellent agreement with experiment [138], and indicate that in the principal axis system χ=-4.445 MHz and η_Q=0.64, with V_{33} oriented 53.9° off the inertial "a" axis. This places the principal component of the ^{14}N efg tensor 49.5° (β^D) from the N-C bond in the symmetry plane of the molecule, or approximately along the direction of the nitrogen lone pair.

The validity of these theoretical results for the ^{14}N efg can be tested by performing a ^{13}C cp/mas nmr experiment on 1a and observing the nature of the resulting asymmetric doublet. Using the ^{14}N theoretical results described above the splitting of the ^{13}C isotropic resonance signal was calculated [88] to be approximately 104 Hz. The corresponding splitting observed in the ^{13}C cp/mas nmr spectrum for 1a was 90 ± 20 Hz, in good agreement with the calculations. It should be noted that variation of χ and η_Q by amounts of ± 1.0 MHz and ± 0.3, respectively, caused changes in the calculated splittings by ± 50 Hz. Although the splitting of 90 Hz may at first appear small considering $|\chi|$ is over 4 MHz, the orientation of V_{33} is almost 50° from the dipolar vector, close to the magic angle. Thus, the theoretical ^{14}N parameters derived from the results of Gerber and Huber [139] were assumed to be a reasonable

model for 1a.

The ^{14}N efg tensor for methyleneimine derived from the theoretical data was then used to calculate the ^{13}C static nmr spectrum for the $^{13}C,^{14}N$ spin-pair of 1a according to equations II.31, 35 and 36. The result of this calculation is shown in figure IV.3b together with the experimental ^{13}C nmr spectrum (figure IV.3a); comparison indicates extremely good agreement between the experimental and simulated ^{13}C nmr spectra assuming the bond length is r_{CN}=1.24 Å. The orientation of the ^{13}C chemical shift tensor is equivalent to that used to generate figure IV.2b, where the values of α^{CS}, β^{CS} and γ^{CS} are 0°, 76° and 46°, respectively. The angles α^{D} and β^{D} were determined to be 90° and 49.5°, respectively, based on both the cp/mas and static best-fit simulations. The only significant difference between the calculated and experimental line shapes in figure IV.3 occurs at the low frequency peak in the δ_{22} region. The extra intensity of this peak in the experimental line shape is probably due to contributions from natural abundance ^{13}C nuclei at the 12 other carbon sites in 1a. A small shoulder at approximately 0 ppm also arises from these sites (labelled by * in figure IV.3a).

In summary, the orientation of the ^{13}C chemical shift tensor has been determined via the effect of $^{13}C,^{15}N$ and $^{13}C,^{14}N$ dipolar coupling on the ^{13}C static nmr line shapes. The $^{13}C,^{15}N$ spin pair analysis provided two of the three angles needed to unambiguously orient the ^{13}C chemical shift

Figure IV.3

The (a) experimental and (b) calculated ^{13}C nmr spectra of a solid powder sample of 1a where the imine carbon is enriched with ^{13}C (99.6%). The theoretical ^{14}N efg parameters for methyleneimine (table IV.1) were used in the calculation. The * indicates the low-frequency shoulder due to the natural abundance contributions from the other twelve carbons in 1a.

Figure IV.3

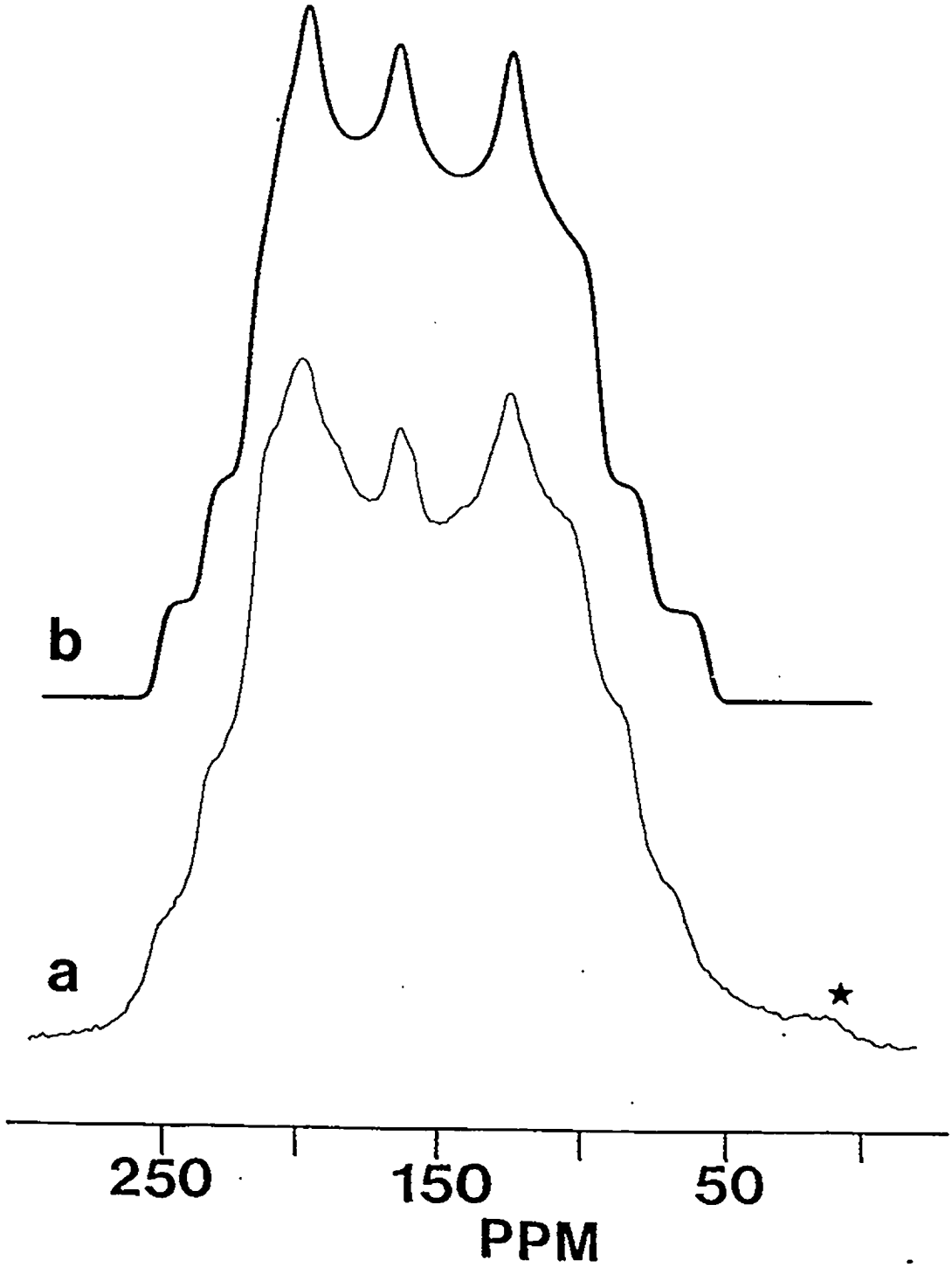

tensor in the molecular frame of reference. The third angle was determined by consideration of the influence of the ^{14}N quadrupolar interaction on the $^{13}C,^{14}N$ dipolar coupling which in turn is manifested in the observed ^{13}C nmr powder pattern. The magnitude and orientation of the ^{14}N efg tensor was approximated using theoretical results for methyleneimine, which should be reasonable within $\pm$ 0.5 MHz for χ and $\pm$ 0.2 for η_Q. These ^{14}N efg parameters successfully modelled the asymmetric doublet observed for the imine carbon of 1a in ^{13}C cp/mas nmr spectra. The estimated errors in the principal components of the carbon chemical shift tensor are $\pm$ 2 ppm, while the errors in α^{CS}, β^{CS} and γ^{CS} should be less than $\pm$ 4°. The calculations indicated that the line shape is extremely sensitive both to the values of these angles and to the sign of χ for ^{14}N. Thus, it can be concluded that the sign of χ is negative in benzylideneaniline, a fact not normally accessible by NQR experiments [141].

The chemical shift anisotropy for the imine carbon of 1a (156 ppm) is somewhat smaller than the values observed for olefinic carbons (typically 200 ppm) [48,120,121,125], carbons of ketones or aldehydes (typically 195 ppm) [48,120,121] or thioketones (approx. 335 ppm) [32]. The only other compound containing the $RR'C{=}NR''$ functional group for which the carbon chemical shift anisotropy has been reported is E-acetophenone oxime [55b] where $\Delta\delta$ is 196.5 ppm. The asymmetry parameter observed for the imine carbon of 1a, η_σ=0.88, resembles that

of the carbon of the olefins, oximes and the amide group in peptides [142] much more closely than ketones, aldehydes or thioketones.

Intuitively, one would expect that the orientation of the carbon chemical shift tensor of 1a would be similar to other double bonded systems such as ketones, olefins and particularly the oximes. Theoretical calculations at both semiempirical [143] and ab initio levels [120,144-148] predict that the most shielded component, δ_{33}, should be oriented perpendicular to the RHC=X plane. In fact, this is observed in simple olefins and symmetrical ketones (and thioketones) where β=90° and the δ_{33} component is perpendicular to the olefinic and the carbonyl (thiocarbonyl) planes, respectively [32,48,121,125]. For 1a β=76 $\pm$ 4°; however, it is important to note that both the N-aryl and C-aryl rings are twisted out of the imine plane by 55° and 10°, respectively [131].

The orientation of the δ_{11} and δ_{22} principal components of the ^{13}C chemical shift tensor of 1a would be expected to be quite similar to those observed for E-acetophenone oxime [55b]. In the latter compound δ_{22} was found to deviate by about 20° from the C=N bonding axis; similar deviations have been reported for δ_{22} of the ^{13}C shift tensor of acetophenone [149]. For 1a, δ_{22} was found to deviate by about 15° from the C=N bond and the least shielded component, δ_{11}, was found to be oriented approximately perpendicular to the C=N bond in analogy to results for the C=C and C=O fragments. Comparison

of the orientational parameters derived for the imine carbon of 1a with those of theoretical calculations on methyleneimine [144] indicates good agreement between experiment and theory. The theoretical results predict that the least shielded component is approximately perpendicular to the C,N dipolar vector (i.e., α=85.8°), and that the most shielded principal component, δ_{33}, is oriented perpendicular to the HCN plane (i.e., β=90°). Given the differences in symmetry and complexity of the two systems the slight deviations of the Euler angles α and β are not surprising.

Finally, it is interesting to attempt to correlate the observed shielding components with electronic transition energies available from ultraviolet spectroscopy. For formaldehyde, benzophenone and thiobenzophenone, Kempf et al. [32] have demonstrated that in these RR'C=X systems, variations in the shielding component directed approximately parallel to the C=X double bond are dominated by the $n\rightarrow\pi^*$ transition energy. That is, as the energy difference decreases, this component becomes more paramagnetic and the chemical shielding decreases (i.e., δ_{11} of this principal component becomes more positive). For the ketone, aldehyde and imine moieties the δ_{22} component of the ^{13}C chemical shift tensor is approximately parallel to the double bond as already discussed whereas in thiobenzophenone the least shielded component, δ_{11}, is oriented parallel to the double bond [32]. The observed value of δ_{22} in 1a and the reported value for the

$n \rightarrow \pi^*$ transition energy (32000 cm^{-1}) [150] are consistent with this qualitative relationship between δ_{22} and $\Delta E^{-1}_{n \rightarrow \pi^*}$ proposed previously [32].

The static ^{15}N nmr spectrum of the doubly isotopically enriched $^{13}C,^{15}N$ sample of 1a is shown in figure IV.4a. A sample of singly ^{15}N enriched 1a provided the three principal components of the ^{15}N chemical shift tensor (see table IV.1). Employing these values with a constraint on the dipolar coupling constant, R, -1606 Hz, the optimum values of α and β were determined to be 42° and 78°, respectively. The calculated ^{15}N static nmr spectrum utilizing these parameters is shown in figure IV.4b. The estimated errors associated with α and β are ± 2° and those for the three principal components of the ^{15}N chemical shift tensor are ± 2 ppm.

The principal components of the ^{15}N chemical shift tensor in 1a are in good agreement with the values previously reported for all-trans-retinylidenebutyl-[^{15}N]-imine [132] (δ_{11}=653 ppm, δ_{22}=339 ppm and δ_{33}=40 ppm; original data has been referenced to $^{15}NH_3(\ell)$). The values for δ_{11}, δ_{22} and δ_{33} in the two compounds only differ by 43, 18 and -25 ppm respectively; therefore, the orientation of the ^{15}N chemical shift tensor in the two compounds is expected to be very similar. On the basis of the data in table IV.1 it is apparent that the most shielded component of the ^{15}N chemical shift tensor is approximately perpendicular to the imine plane (β=78°). The twist of the N-aryl (55°) out of the imine carbon-nitrogen

Figure IV.4

The (a) experimental and (b) calculated ^{15}N nmr spectra of a solid powdered sample of 1a where the imine nitrogen and carbon are both enriched with ^{15}N (95 %) and ^{13}C (99.6 %), respectively.

Figure IV.4

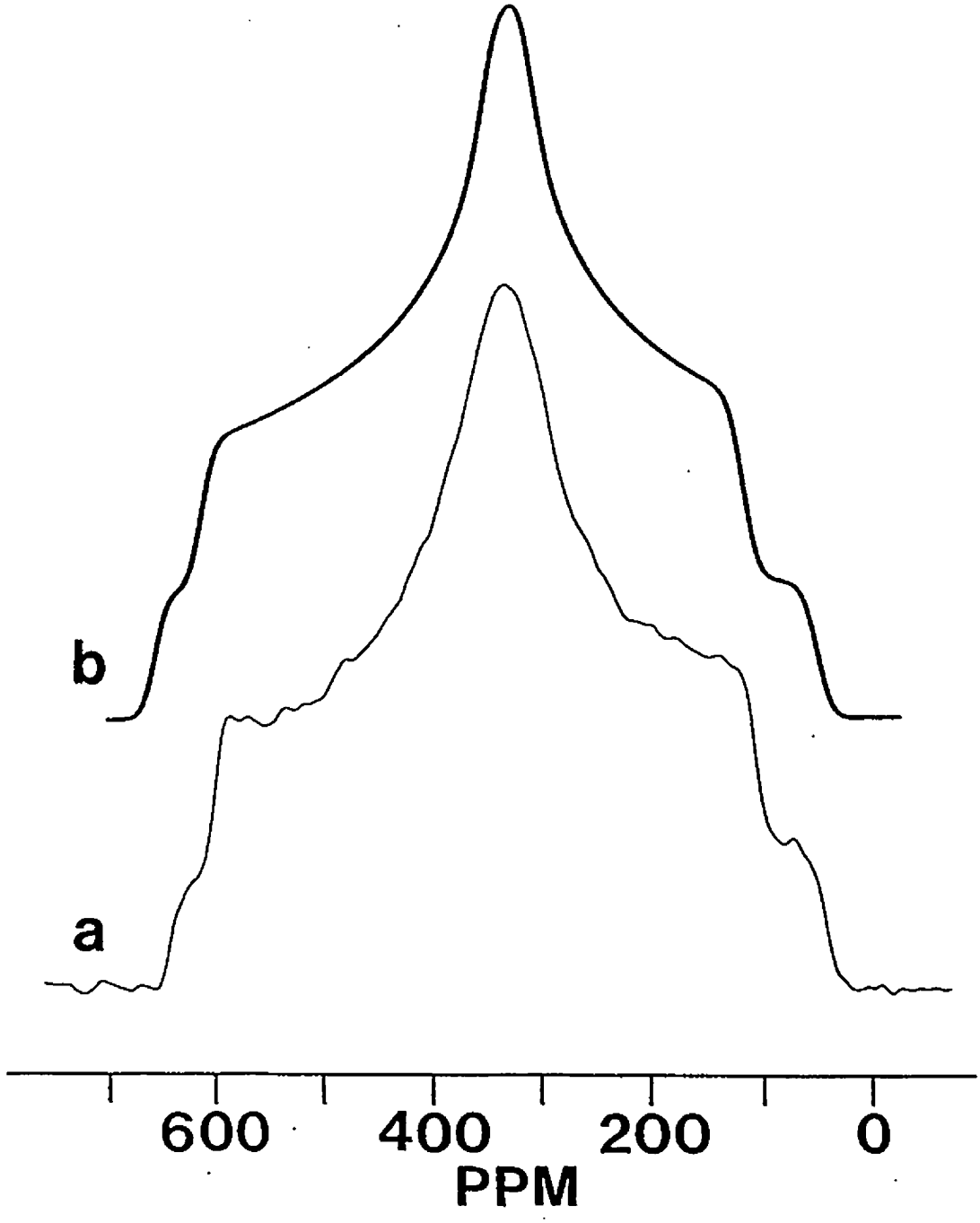

bond plane is probably responsible for the observation that $\beta<90°$. The value of α, 42°, indicates that the approximate orientation of the least shielded component of the nitrogen shift tensor is either along the N-C_{ipso} (N-aryl) bond axis or parallel to the orientation of the nitrogen lone-pair. For molecules containing dicoordinate nitrogen atoms, ab initio molecular orbital calculations consistently predict that the intermediate component of the shift tensor, δ_{22}, is approximately parallel to the orientation of the nitrogen lone-pair [144,146,151]. On this basis, it is concluded that δ_{11} of the ^{15}N chemical shift tensor of benzylideneaniline is oriented approximately along the N-C_{ipso} (N-aryl) bond axis. The theoretical calculations of the ^{15}N shielding tensor tend to overestimate the paramagnetic contribution to the shielding of the least shielded principal component, δ_{11}, of the imine nitrogen. For example, the calculations predict that δ_{11} of methyleneimine is over 150 ppm greater than the corresponding value for 1a. Similar results have been reported for theoretical and experimental ^{15}N chemical shift anisotropies of trans-azobenzene [55a].

The general orientation of the nitrogen shift tensor determined for 1a is in good agreement with that obtained by dipolar-chemical shift nmr experiments on two related molecules, E-acetophenone oxime and trans-azobenzene [55]. For the oxime, $\alpha=52 \pm 2°$ and $\beta=90 \pm 2°$; similarly, for the two crystallographically nonequivalent molecules of trans-

azobenzene, α=37 ± 5°, β=83 ± 5° (site 1) and α=46 ± 5°, β=78 ± 5° (site 2).

Finally, it is interesting to once again attempt to correlate variations in the chemical shift with electronic transition energies. For a dicoordinate nitrogen, variations in the principal component of the shielding tensor which is in the RN=X plane but perpendicular to the orientation of the nitrogen lone-pair are associated with changes in the $n\rightarrow\pi^*$ transition energy [20]. For 1a, trans-azobenzene [55a], E-acetophenone oxime [55b] and the "bent" nitrosyl ligand [152] the least shielded principal component of the ^{15}N tensors (δ_{11}) is oriented in this manner. The $n\rightarrow\pi^*$ transition energy increases in the following order [20,152] :

$$N{=}O < RN{=}NR' < RN{=}CR'R'' < HON{=}CRR'$$

Thus, one would anticipate that the oxime moiety would have the most shielded δ_{11} principal component and the nitrosyl ligand the least shielded δ_{11} principal component of their respective ^{15}N chemical shift tensors. When referenced to external liquid ammonia (293 K) the chemical shifts of the δ_{11} component are 1239 ppm [152], 1032 ppm [55a], 611 ppm and 560 ppm [55b] for the nitrogen of the nitrosyl ligand, trans-azobenzene, benzylideneaniline and E-acetophenone oxime, respectively. Although there are obviously factors other than the $n\rightarrow\pi^*$ transition energy which are responsible for variations in δ_{11}, the basic qualitative feature of decreased shielding of the δ_{11} principal component with

decreased energy of the n→π* transition is apparent.

Variation of the Nitrogen Chemical Shift Parameters in Several Compounds Containing an Imine Moiety

The nitrogen-15 chemical shift anisotropies obtained from static cp ^{15}N nmr spectra of the imines depicted in 1, 2 and 3 are shown in table IV.2. For the remainder of this section, it will be assumed that the orientation of the ^{15}N chemical shift tensors in 1, 2 and 3 does not vary substantially. That is, δ_{33} is approximately perpendicular to the HCN plane, δ_{22} is oriented in the direction of the nitrogen lone-pair and δ_{11} is oriented slightly off the N-C_{ipso} (N-aryl) bond axis.

The influence of varying the substituents of the aryl rings of aromatic imines on ^{1}H, ^{13}C and ^{15}N nmr parameters (e.g., δ_{iso} and J_{iso}) in solution has been well studied [153-157]. Two investigations have focused specifically on the three benzylideneaniline derivatives depicted in 1 [153,155]. The principal conclusions of this work were : (1) the influence of para substituents on the C-aryl ring on the imine carbon chemical shift is small and is opposite in direction to what would be anticipated based on the nature of the substituents; (2) substituents on the N-aryl ring do not systematically influence the imine hydrogen or carbon chemical shifts; (3) the ^{15}N chemical shifts provide evidence that the C-aryl ring is conjugated with the imine C,N double bond.

Table IV.2

Nitrogen-15 chemical shift parameters of several compounds containing an imine moiety. All chemical shifts are in ppm.

Compound		δ_{11}	δ_{22}	δ_{33}	δ_{iso}	$\Delta\delta$	η_σ
1a		610	321	65	332.0	545	0.92
1b	site I	594	313	43	316.7	551	0.97
	site II	615	321	22	319.6	593	0.99
1c	site I	628	332	43	334.5	585	0.98
	site II	674	343	2	339.6	672	0.98
2a		612	327	45	328.2	567	0.99
2b		595	321	65	327.0	530	0.95
2c	site I	632	309	74	338.3	558	0.81
	site II	647	334	50	343.6	597	0.94
	site III	660	334	45	346.3	615	0.92
3a		537	318	48	301.0	489	0.86
3b		514	308	17	279.7	497	0.78

The normal approach to account for substituent effects in aromatic systems is to consider the influence of the substituent on the nature of the electronic charge at various nuclear sites. This is most easily visualized with the aid of resonance structures. Thus, for the p-methoxy derivative

of benzylideneaniline (1b), the resonance contributor of most importance was postulated to be 1bi [153,155]. The empirical

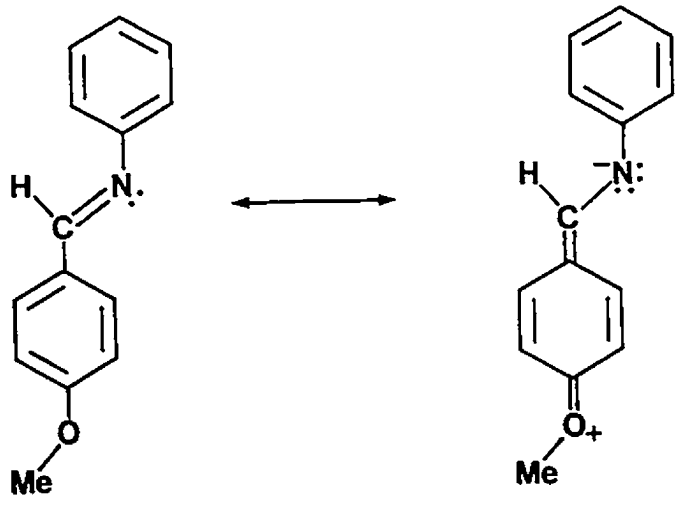

1b 1bi

validity of these "charge" effects were manifested in the ^{15}N isotropic chemical shifts reported by Buchanan and Dawson for compounds 1a, 1b and 1c dissolved in $CDCl_3$ [153]. For example, the resonance form 1bi suggests that the imine nitrogen will have a slightly negative charge associated with the presence of the electron donating methoxy substituent on the para position of the C-aryl ring. Thus, one would anticipate that the ^{15}N resonance frequency of 1b would occur at a lower frequency (i.e., greater shielding and lower δ_{iso}) than the corresponding value for the parent compound, 1a. In fact, the observed ^{15}N chemical shift for 1b was over 8.5 ppm to low frequency of 1a [153]. Similar arguments for electron withdrawing para substituents on the C-aryl ring such as a nitro group (1c) indicate that the nitrogen of the imine bond

in this situation will have a slight positive charge relative to the parent imine, 1a. The ^{15}N chemical shift in $CDCl_3$ for 1c was reported to be over 12 ppm to high frequency of the corresponding value in 1a [153] supporting this simple qualitative description.

For solid imines where the ^{15}N chemical shift is anisotropic, a slightly different approach must be taken to interpret the influence of resonance forms such as 1bi on each of the three principal components of the shift tensor. According to equation II.18, each of the quantities $\langle r^{-3} \rangle_p$, ΔE_{jk} and $C_{j\beta}$ can, in principle, effect the shielding properties of each δ_{ii}. Sardashti and Maciel have recently interpreted para substituent effects on the three principal components of the ^{15}N chemical shift tensors of several benzonitriles [122] in terms of variations in the atomic orbital coefficients, $C_{j\beta}$. This type of approach will be used for the interpretation of substituent effects in the imine systems depicted in 1 and 2.

In order to determine how resonance contributors such as 1bi will influence each $\sigma^p_{\alpha\alpha}$, it is necessary to consider which molecular orbitals of the imine system are associated with each δ_{ii}. Pople's expression for σ^p (equation II.18) indicates explicitly that each $\sigma^p_{\alpha\alpha}$ is related to energy transitions which are restricted by the atomic orbital coefficients $C_{j\beta}$ to MO's in the plane perpendicular to each principal axis. Here, the "y" direction is perpendicular to the HCN plane and the "z" axis is in the direction of the nitrogen lone pair of

electrons. For the nitrogen of the C,N bond of the imine moiety, δ_{33} is oriented approximately along the $2p_y$ atomic orbital direction and the pertinent electronic excitations are those involving $2p_x$ and $2p_z$ atomic orbitals in σ, n and σ^* MO's. The intermediate principal component, δ_{22}, is associated with $2p_x$ and $2p_y$ atomic orbitals involved in σ, σ^*, π_y and π_y^* MO's. The contributions of σ^P to the least shielded principal component, δ_{11}, is dependent on the $2p_y$ and $2p_z$ atomic orbitals involved in σ, σ^*, n, π_y and π_y^* MO's.

Consideration of the resonance contributor 1bi indicates that electron donating substituents on the para positions would be anticipated to increase the effective negative charge along the $2p_y$ atomic orbital direction. On this basis, one might expect that the principal components of the nitrogen shift tensor which are oriented perpendicular to this axis would show significant variations depending on the nature of the para substituent present. For example, in terms of the resonance contributor 1bi, the p-methoxy group present in 1b has the effect of lowering the $2p_y$ atomic orbital coefficient in the π_y^* MO and increasing $C_{j\beta}$ for the π_y MO. Assuming that the larger paramagnetic contribution to δ_{11} is associated with the $n \rightarrow \pi_y^*$ transition energy (i.e., $\Delta E_{n\rightarrow\pi_y^*} < \Delta E_{n\rightarrow\sigma^*} \leq E_{\pi_y\rightarrow\sigma^*}$), variations in σ_{11}^P are related to :

$$\sigma_{11}^P \propto C_n \cdot C_{\pi_y^*}$$

Since $C_{\pi_y^*}$ is anticipated to decrease with the presence of an

electron donating group at the para position of the C-aryl ring, the nitrogen δ_{11} value of 1b should decrease relative to the corresponding value for 1a. Conversely, the presence of an electron withdrawing group at the para position of the C-aryl ring as for 1c will increase the effective positive charge at the nitrogen thereby increasing the $2p_y$ orbital coefficient in π_y^*. In this case, the δ_{11} principal component would be expected to increase relative to the corresponding value for the unsubstituted imine. For 1b (site 1), 1a and 1c (site 1) δ_{11} increases from 594 ppm to 610 ppm to 628 ppm and this observation is consistent with the qualitative arguments based on $C_{j\beta}$. For the naphthylideneanilines 2b, 2a and 2c (site II), the values for δ_{11} also increase from 595 ppm to 612 ppm to 647 ppm, respectively. Since δ_{22} of the imine nitrogen shift tensor is also associated with transition energies involving the π_y^* MO, it too should follow a similar trend in shieldings as observed for the least shielded principal component. In this case, however, the associated energy, $\Delta E_{\sigma\rightarrow\pi_y^*}$, is anticipated to be larger than $\Delta E_{n\rightarrow\pi_y^*}$, and therefore smaller variations in δ_{22} would be expected. For 1b (site 1), 1a and 1c (site 1), the observed values of δ_{22} increase from 313 ppm to 321 ppm to 332 ppm. Analogous results were observed for the naphthylideneanilines indicated in table IV.2. The apparent discrepancies concerning site II of 1b and 1c and sites I and III of 2c will be discussed later.

The salicylideneanilines (3) provide an interesting opportunity to examine the effects of hydrogen bonding on the imine ^{15}N chemical shift tensor. High-resolution ^{13}C and ^{1}H solution nmr experiments [158] have been used to investigate compounds similar to 3 although no ^{15}N nmr experiments have been reported to date. Variable temperature nuclear quadrupole resonance (nqr) experiments on 3 have been used to study the thermochromic and photochromic behaviour associated with the ^{1}H transfer from the oxygen on the C-aryl ring to the imine nitrogen [159]. At room temperatures, the solids studied in this report are present exclusively as the O-protonated moieties depicted in 3.

Allen and Roberts [160] have reported a solution nmr study of hydrogen bonding effects on a series of ^{15}N enriched benzylideneanilines. Their ^{15}N nmr results indicated that the isotropic chemical shifts are highly dependent on the choice of solvent [160]. For example, the ^{15}N chemical shifts (δ_{iso}) for the imines investigated were observed to decrease by approximately 8 to 28 ppm upon changing the solvent from chloroform to trifluoroethanol or trifluoroacetic acid [160]. Consideration of the structure of 3 in the solid state [161] indicates that intramolecular interactions of the hydrogen of the C-aryl ring hydroxy group with the nitrogen lone-pair would be anticipated. On this basis, one would expect that this type of interaction would tend to stabilize the nitrogen lone pair and therefore increase the $n \rightarrow \pi^*$ transition energy.

Since δ_{11} of the imine ^{15}N chemical shift tensor is dependent on this transition energy, a significantly decreased value of δ_{11} for both 3a and 3b as compared to 1 would be anticipated. Comparison of the δ_{11} values in table IV.2 indicates that indeed δ_{11} of the ^{15}N chemical shift tensors of 3a and 3b are more shielded than the corresponding values in 1a by 75 ppm and 96 ppm, respectively. This provides further support that δ_{11} of the nitrogen shift tensor in the imine system is highly dependent on the $n\rightarrow\pi^*$ transition energy.

Finally, it is interesting to point out the utility of ^{15}N cp/mas nmr for studying crystallographic and polymorphic effects in solid imines. It has been demonstrated in the past by numerous x-ray diffraction experiments that substituted benzylideneanilines often crystallize in several different forms [131,162,163]. For example, Nakai et al. [163] have characterized triclinic, monoclinic and orthorhombic forms of p-dimethylaminobenzylidene-p-nitroaniline. The principal differences between these three forms are the twist angle of the N-aryl ring and the length of the C,N imine bond. For the solids studied here, three of the eight compounds show some type of solid state effect in their respective ^{15}N nmr spectra. For example, the ^{15}N cp/mas nmr spectrum 1c consists of two well resolved resonance lines (≈5 ppm separation) as indicated in figure IV.5. Subsequent analysis of single crystals of this material obtained from methanol, provided the reason for

Figure IV.5

A ^{15}N cp/mas spectrum for compound 1c obtained at a spinning speed of 2.0 kHz.

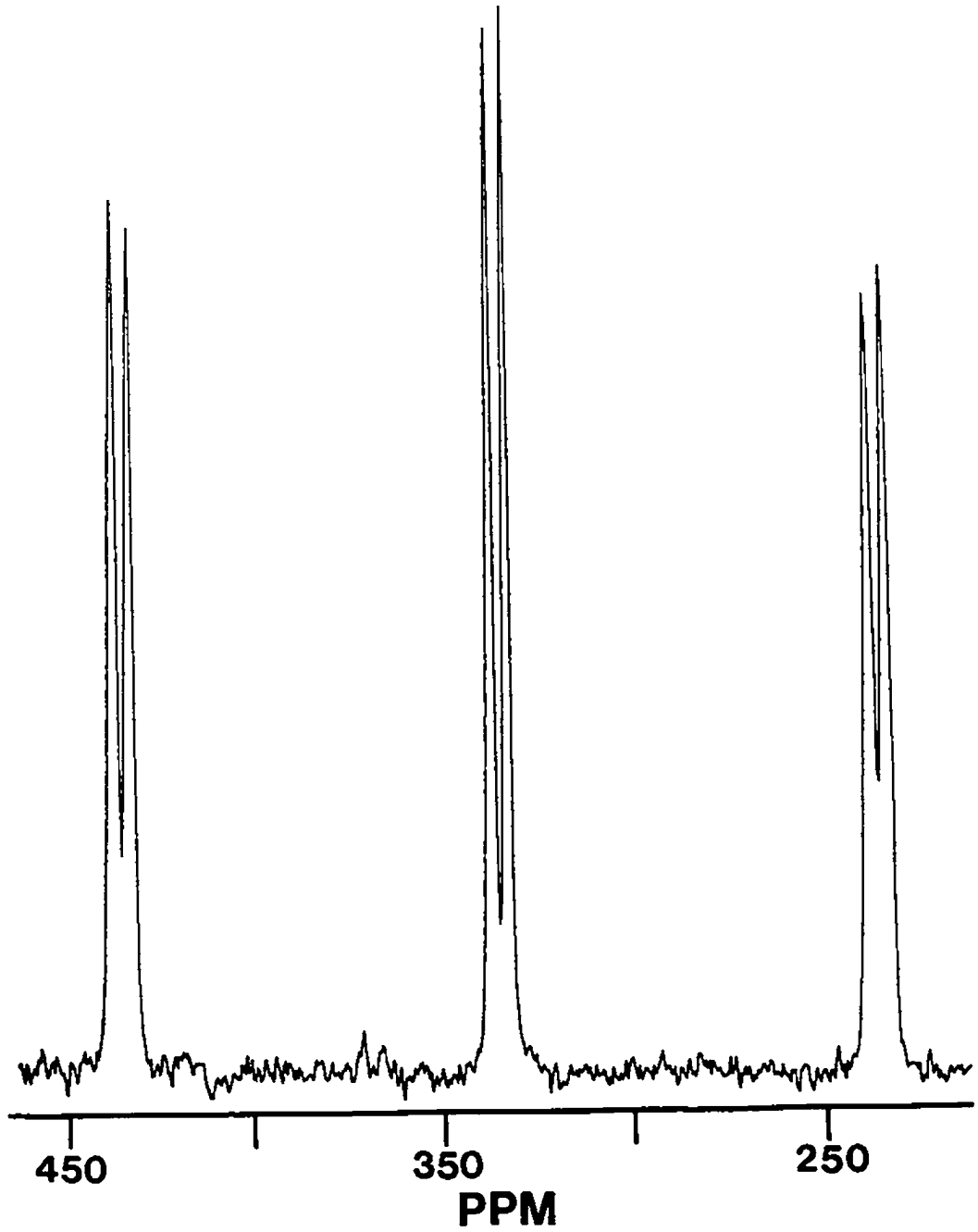

this observation. The space group was determined to be monoclinic $P2_1/n$ with two crystallographically nonequivalent molecules per unit cell. The principal differences between the two independent molecules of the $P2_1/n$ space group (site I and II) are the different imine C,N bond lengths, 1.26 Å and 1.23 Å, and the different torsional angles of the N-aryl rings, 24.6° and 41.4°, respectively. Minkin et al. [164] have demonstrated that the nitrogen lone-pair orbital becomes less energetically stable the closer the N-aryl ring is to being planar. That is, the $\Delta E_{n\rightarrow\pi^*}$ gap decreases the more planar the benzylideneaniline (i.e., smaller torsional angle). In view of the previous arguments, the δ_{11} principal component of the more planar form was anticipated to have the greater ^{15}N chemical shift. Comparison of the two δ_{11} values for 1b in table IV.2 indicates a difference of 46 ppm for the two crystallographically independent sites. On the basis of energy considerations, the ^{15}N chemical shift parameters for site II of 1c were assigned to coincide with the higher frequency δ_{11} as indicated in table IV.2.

A second example of the influence of the solid state structure on the ^{15}N cp nmr spectra of the imines investigated was observed for p-methoxybenzylideneaniline (1b). In this case, two isotropic ^{15}N signals were observed in the cp/mas nmr spectrum which differed by approximately 3 ppm. This sample forms a powder when allowed to solidify from methanol and therefore single crystal investigations could not be pursued.

However, the intensity of the two signals in the ^{15}N cp/mas nmr spectrum of 1b are approximately equal thereby suggesting that the two signals arise due to a crystallographic effect and not polymorphism. More specifically, it would be unlikely for two polymorphs to cystallize from the same solution in a 1:1 ratio. The similarity of the ^{15}N chemical shift parameters derived for 1b and 1c suggest that similar crystallographic effects may be present in the two compounds. On this basis, the ^{15}N chemical shift anisotropy of 1b with the higher frequency δ_{11} principal component (site II) is most likely associated with a more planar form. That is, site II of 1b is expected to have a smaller value for the torsional angle of the N-aryl ring than site I.

The 4-cyanonaphthylideneaniline derivative (2c) provided the most interesting ^{15}N cp/mas nmr spectrum of the imines investigated (figure IV.6). Close inspection of the nmr spectrum indicates at least three different isotropic resonance signals. The two highest frequency resonances are similar in intensity and most likely correspond to a single polymorph which is exhibiting crystallographic nonequivalence similar to compound 1c. The lowest frequency resonance signal, δ_{iso}=338.3 ppm, has a higher ^{15}N signal intensity than the other two isotropic resonances and most likely corresponds to a different crystallographic form. The static ^{15}N nmr spectrum for a powdered sample of 2c contained three overlapping powder patterns which were difficult to assign.

Figure IV.6

A ^{15}N cp/mas nmr spectrum of 4-cyanonaphthylideneaniline spinning at a speed of 2.72 kHz.

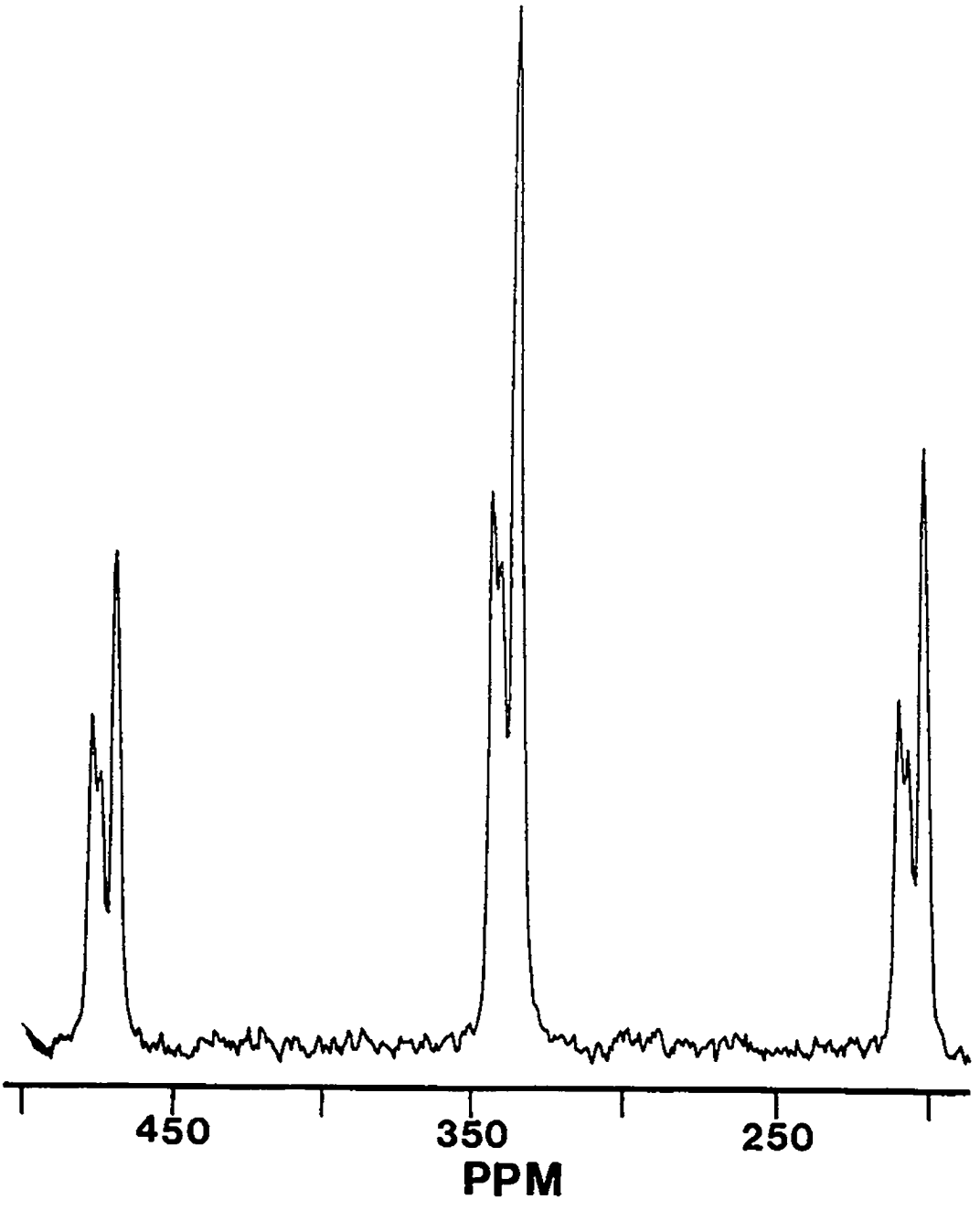

Comparison of the shoulders and discontinuities in the static nmr spectrum with the observed isotropic signals permitted only the assignment of the signals as indicated in table IV.2. The ^{15}N chemical shift parameters of 2c which are associated with the lowest isotropic chemical shift have a significantly different asymmetry parameter from the other two chemical shift anisotropies (e.g., η_σ=0.81 versus $\eta_\sigma \geq 0.90$). This low value of η_σ is also different from the corresponding values for the benzylideneanilines and naphthylideneanilines in table IV.2 and provides further evidence that the lowest frequency isotropic ^{15}N resonance arises from a slightly different polymorphic form of 2c.

A.4 Summary

Using the technique of dipolar-chemical shift nmr spectroscopy, both the magnitudes and orientations of the principal components of the imine carbon and nitrogen chemical shift tensors in benzylideneaniline have been determined. The relative orientations of the three principal components of both shift tensors are consistent with those determined for related molecules. Comparison of the magnitudes of the three principal components of both tensors with ab initio MO calculations on methyleneimine indicate reasonable agreement between experiment and theory for the imine ^{13}C shift tensors but less satifactory results for nitrogen. Since the high-field approximation is not strictly valid for the imine ^{13}C, ^{14}N

spin-pair at 4.7 T, it was necessary to use expressions which describe the orientational dependence of the three allowed ^{13}C nmr transitions in terms of the ^{14}N electric field gradient.

The presence of the nitrogen lone pair has been shown to have a significant effect on the least shielded principal component, δ_{11}, of the imine nitrogen shift tensor. More specifically, it was demonstrated that substituents, hydrogen bonding and the conformational orientation of the N-aryl ring all influence the least shielded element of the nitrogen shift tensor. This is attributed to variations of the $n\rightarrow\pi^*$ transition energy and the otomic orbital coefficients associated with these energy levels. Finally, the experiments described here have demonstrated the sensitivity of ^{15}N cp/mas nmr for investigating polymorphism and crystallographic effects of several solid imines.

B. Characterization of the Nitrogen-15 and Phosphorus-31 Chemical Shift Tensors for a Novel System Containing a Nitrogen-Phosphorus Triple Bond

B.1 Introduction

Recently, Niecke, Nieger and Riechart [165] reported the synthesis of the first stable compound with a nitrogen-phosphorus triple bond. The iminophosphenium cation, 4, was characterized by ^{31}P, ^{13}C and ^{1}H nmr in toluene/benzene-d_6 and benzene-d_6 solutions as well as by x-ray crystallography

[165]. The x-ray diffraction results indicate that this system crystallizes from toluene with one molecule of toluene

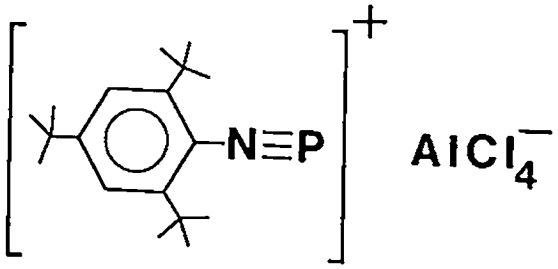

4

as solvate. The orthorhombic unit cell (P_{bca}) contains eight crystallographically equivalent molecules. The CNP bond angle is approximately 177° with a N,P bond length of 1.475 Å [165]. This combination of near linear geometry and short N,P internuclear separation was observed to be consistent with the bond length calculated for $P{\equiv}NH^+$ (r_{NP}=1.476 Å) [166]; thus, Niecke et al. [165] argue that the N,P bond of 4 has a high degree of triple bond character.

Although ^{13}C chemical shift tensors have been reported for numerous systems in which carbon nuclei are involved in multiple bonding [12,55b,115-126] analogous results for nitrogen chemical shift tensors [55a,115,116,119,122,127-130] and phosphorus chemical shift tensors [115,124,128,167] have been lacking. In addition, it has become apparent that while theoretical calculations of ^{13}C chemical shift parameters have become reasonably accurate [115,120,148,168-170], it is often

difficult to obtain accurate theoretical values for the three principal components of ^{15}N and ^{31}P chemical shift tensors, particularly when these nuclei are involved in multiple bonds [115,144-147,151,168-172].

In order to characterize the nitrogen and phosphorus chemical shift tensors in a system containing a N,P triple bond, the iminophosphenium cation 4 has been prepared with and without ^{15}N isotopic enrichment for study by solid state ^{15}N and ^{31}P dipolar-chemical shift nmr spectroscopy. This represents the first example where a molecule containing a multiple N,P bond has been studied by solid state nmr spectroscopy. The derived nitrogen and phosphorus chemical shift parameters for 4 will be compared to experimental and theoretical results for several compounds containing nitrogen and/or phosphorus involved in a triple bond.

B.1 Experimental

The samples of 4 were prepared by Dr. Mel Schriver in a glove box under an inert atmosphere according to the published results of Niecke et al. [165]. The 1,3,5-tri-t-butylbenzene and 2,4,6-tri-t-butylaniline were procured commercially (Aldrich Chemical Company). Nitrogen-15 enriched (95 %) HNO_3 was purchased from the Sigma Chemical Company and was reacted with 1,3,5-tri-t-butylbenzene to form 2,4,6-tri-t-butyl-^{15}N-nitrobenzene [173]. This sample was then reduced as outlined in ref. 173 to give the corresponding ^{15}N enriched amine for

preparation of 4. It was determined by ^{31}P cp/mas nmr (*vide infra*) that samples of 4 produced according to the procedure in ref. 165 were a mixture of solvated and non-solvated material. Pure samples of the toluene solvate of 4 were prepared by recrystallization of the crude product from toluene. Prolonged evacuation of the samples was shown to cause partial solvate dissociation.

Nitrogen-15 and ^{31}P solid state nmr spectra were recorded at 20.30 MHz and 81.03 MHz, respectively, on a Bruker MSL-200 nmr spectrometer (B_o=4.7 T). Samples were ground into a fine powder (~300 mg) and packed into zirconium oxide rotors (7 mm o.d.) in the glove box. Rotors were topped with solid caps that had been coated with a medium tipped felt marker around the inner edge to form an air tight seal. Samples packed in this manner were found to be stable on the lab bench for periods in excess of one month. All nmr spectra were acquired with high-power hydrogen decoupling and ^{1}H, ^{15}N and ^{31}P $\pi/2$ pulse widths of 2.5-5.5 μs. For the ^{15}N nmr experiments, the conditions of the Hartmann-Hahn match [65] were optimized using a sample of doubly ^{15}N enriched NH_4NO_3. Nitrogen-15 chemical shifts are referenced with respect to $NH_3(\ell)$ at 0 ppm by setting the observed chemical shift of the $^{15}NH_4^+$ ion of NH_4NO_3 at 23.8 ppm (293 K). A sample of $NH_4H_2PO_4$ was used for optimizing the conditions for the ^{31}P cp nmr experiments. Phosphorus-31 chemical shifts were referenced with respect to

H_3PO_4 (85%) at 0 ppm by setting the observed chemical shift of $NH_4H_2PO_4$ at 0.81 ppm (293 K). Contact times of 8-10 ms were used for all ^{15}N and ^{31}P cp nmr experiments. The cp/mas nmr spectra were acquired with mas speeds of 1-4.5 kHz with acquisition times of approximately 50-400 ms. The static cp ^{31}P nmr spectra were acquired with the Hahn-echo cross polarization sequence depicted in figure III.2 [99-101]. This was necessary in order to alleviate spectral distortions associated with the recovery time of the nmr spectrometer. For samples of 4 typical delays between the end of the contact pulse and the π pulse were 30 μs. The filter width was opened to its maximum value of 2 MHz to reduce the dead time associated with filter ringing. Acquisition times for the ^{15}N and ^{31}P static nmr spectra were approximately 30 ms. Sensitivity enhancements corresponding to line broadenings of 5 Hz and 70 Hz were applied to the mas and static FIDs, respectively, prior to Fourier transformation. Calculation of theoretical powder nmr spectra were performed as outlined in section IV.A.2 on the basis of equation II.32.

B.3 Results and Discussion

Nitrogen-15 NMR Spectra

A ^{15}N cp/mas nmr spectrum of the ^{15}N enriched sample of 4 is shown in figure IV.7. The isotropic chemical shift for 4, δ_{iso}=248.1 ± 0.5 ppm, consists of a well resolved doublet from

Figure IV.7

The ^{15}N cp/mas nmr spectrum for an ^{15}N enriched sample of 4. The isotropic chemical shift of a small amount of impurity is labelled with an asterisk (*).

Figure IV.7

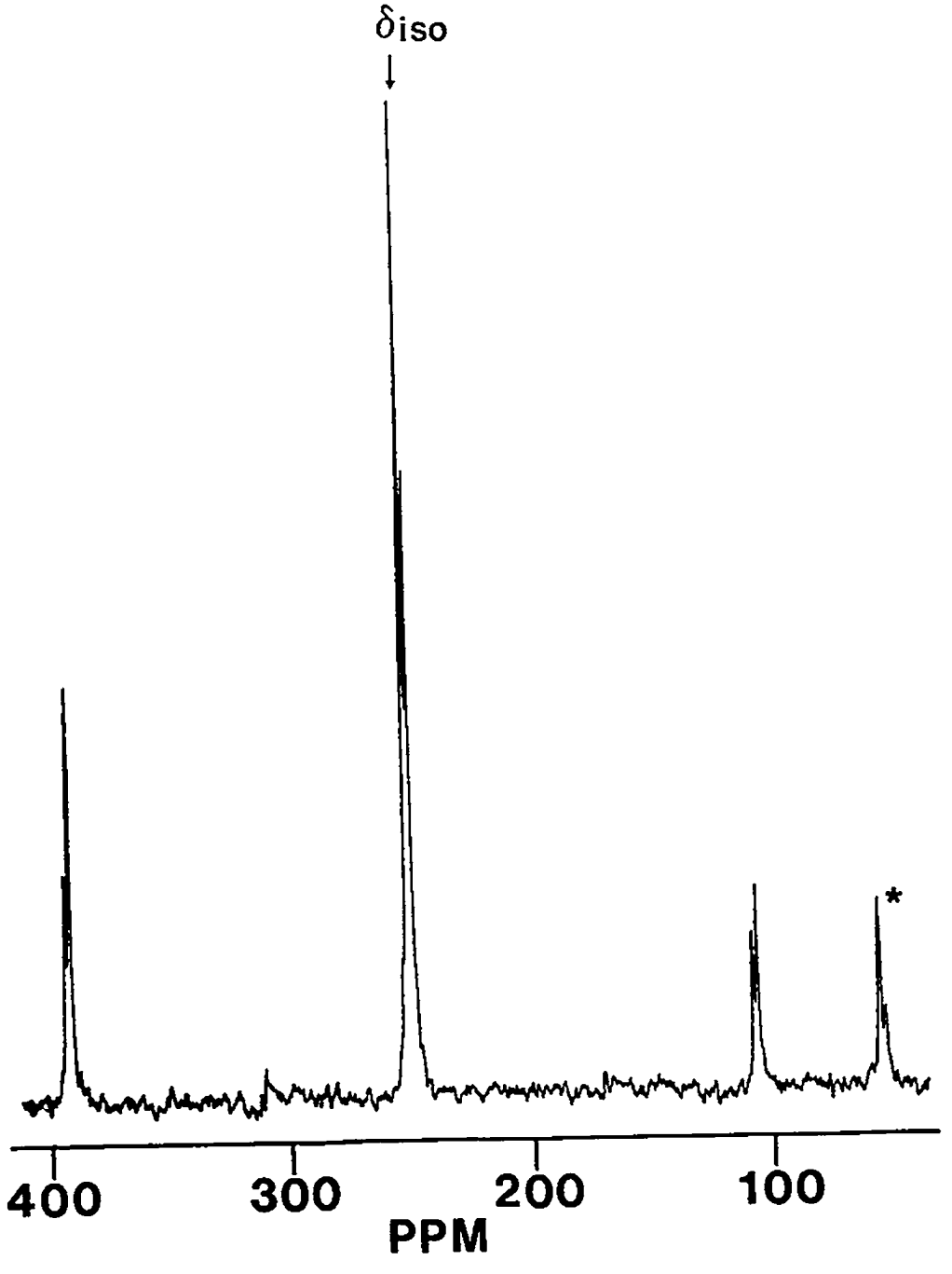

which a spin-spin coupling of $^{1}J(^{15}N,^{31}P)_{iso}=36 \pm 2$ Hz was determined. The observation of a simple doublet is consistent with the x-ray diffraction results which indicate that this system crystallizes with eight crystallographically equivalent molecules per unit cell [165]. This is advantageous since crystallographic nonequivalence can cause difficulties when analyzing nmr spectra of static powdered samples [55a]. The ^{15}N cp/mas nmr spectrum also indicated that a small amount of impurity was present in this sample (i.e., small asymmetric doublet at 52.4 ppm). Based on the intensities of the respective ^{15}N nmr signals, the relative amount of this impurity is small and therefore it should not lead to significant distortions in the static ^{15}N nmr spectrum of this sample.

The static ^{15}N nmr spectrum for the isotopically enriched sample of 4 is shown in figure IV.8a. Inspection of this nmr spectrum indicates six well defined discontinuities characteristic of a non-axially symmetric chemical shift tensor powder pattern split by dipolar coupling with a spin 1/2 nucleus. Based on the N,P bond length determined from single crystal x-ray diffraction experiments [165], 1.475 Å, the direct dipolar coupling constant, R, for the $^{15}N,^{31}P$ spin pair was calculated to be -1538 Hz (see equation II.25). If the dipolar coupling constant is constrained to -1538 Hz and one assumes a negligible anisotropy in J, then computer simulations of the line shape based on equation II.32 indicate

Figure IV.8

The (a) experimental and (b) simulated ^{15}N nmr spectra of a solid powder sample of ^{15}N enriched 4.

Figure IV.8

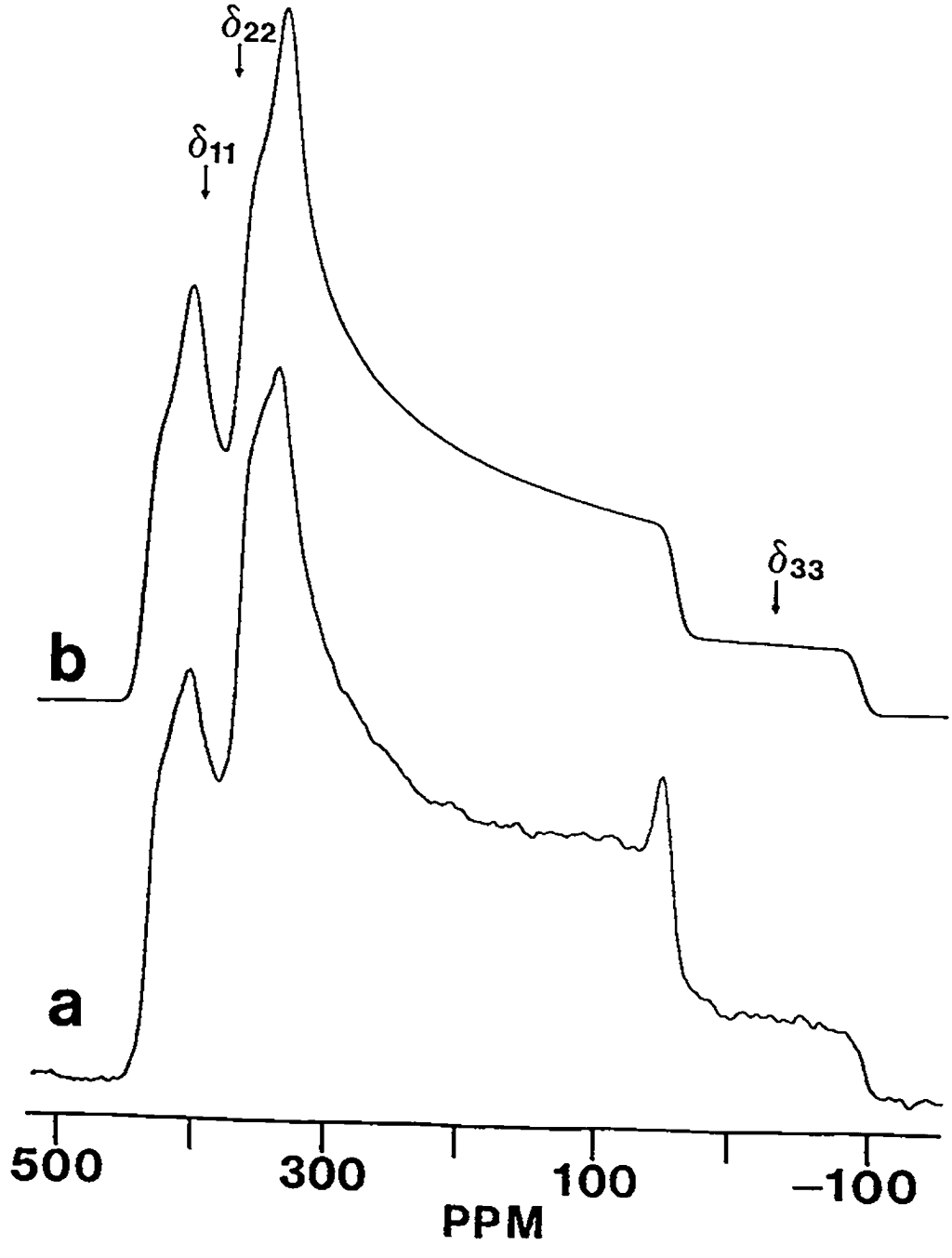

that α=45.0 $\pm$ 2.0° and β=16.4 $\pm$ 2.0°, respectively. This value of β places the most shielded principal component of the ^{15}N chemical shift tensor 16.4° off the N,P bond axis. However, on the basis of local symmetry and results reported for related molecules [115,116,119,122,127-130], one might anticipate a β value equal to 0°. The ^{15}N nmr data can accommodate this possibility if it is assumed that the effective dipolar coupling constant, R', is different than the value calculated on the basis of x-ray diffraction data. Two mechanisms by which the apparent dipolar splitting would be reduced are : (1) contributions from anisotropy in J and (2) averaging due to molecular motions (i.e., librations and vibrations). To account for these effects one can write an effective dipolar coupling constant, R', in terms of an order parameter, S, an anisotropic spin-spin coupling, ΔJ, and a static value for the dipolar coupling constant, R.

$$R' = S\{R-\Delta J/3\} \qquad [IV.1]$$

Simulations of the static ^{15}N nmr spectrum shown in figure IV.8a with β=0 indicates that R' is $\pm$ 1353 $\pm$ 35 Hz. In determining this value of the effective dipolar coupling constant it was found that computer simulations of the observed splittings in the ^{15}N static nmr spectrum could be improved slightly by assuming that $^{1}J(^{15}N,^{31}P)_{iso}$ is positive. However, given the inherent line width of the ^{15}N static nmr spectrum and the small magnitude of $^{1}J(^{15}N,^{31}P)_{iso}$, 36 $\pm$ 2 Hz, any definitive conclusion about the sign is tenuous.

If one assumes β=0 and no motional averaging such that S=1, then ΔJ can be calculated from equation IV.1. Since the value of R based on x-ray crystallographic results is -1538 Hz and R' can be positive or negative, ΔJ can be calculated to be -555 Hz or -8763 Hz. These two values for the J anisotropy are very different and since the nmr experiment is only sensitive to the absolute value of the effective dipolar coupling tensor (equation IV.1), a definitive assignment can not be made. However, considering the fact that $|^1J(^{15}N,^{31}P)|$ is only 36 Hz and that the indirect coupling involves a first row element, it is difficult to envisage a J tensor where $J_\parallel$ and $J_\perp$ are different by over 8000 Hz. Other authors have encountered the same dilemma [39,167,174]; this author makes a tentative conclusion that the effective dipolar coupling constant for the $^{15}N,^{31}P$ spin pair is negative and this assumption imposes an upper limit on ΔJ of -555 Hz.

An alternative explanation for the observed reduction of the dipolar coupling constant, R, for the $^{15}N,^{31}P$ spin pair of 4 is the presence of vibrational and librational motions (i.e., S≠1) [175-178]. Henry and Szabo [177] have demonstrated that vibrations which affect the AX internuclear separation and librations which influence the orientation of the dipolar vector can significantly decrease the magnitude of the dipolar coupling constant, R. They concluded that librational averaging of the dipolar interaction is more important than vibrational averaging particularly as the size

and torsional flexibility of the molecule increase. If it is assumed that β=0 and ΔJ is negligible, then the 12% reduction in R from that calculated on the basis of the x-ray bond length must be attributed to motional averaging. Detailed x-ray diffraction data for the toluene-solvate of 4 have not been published so that librational information is currently unavailable. However, x-ray diffraction results for the structurally related p-benzenediazonium sulphonate indicate that the largest amplitude librations occur about the N-N-C1-C4-S direction with a mean angle of 8 ± 1° [179]. If it is assumed that the symmetry axis of 4 traces the surface of a cone, then the half angle of the cone, ψ, may be estimated from equation IV.2.

$$\cos^2\psi = \frac{2S + 1}{3} \qquad [IV.2]$$

Application of equation IV.2 with the values of R and R' previously discussed indicates a value for ψ of 16.4°. It should be noted that this represents the maximum value of the angle ψ for a single mode of libration in the absence of anisotropy in J. The effective dipolar coupling constant for the $^{15}N,^{31}P$ spin pair is presented together with the ^{15}N chemical shift parameters and isotropic J in table IV.3. The calculated ^{15}N static nmr spectrum using these values is shown in figure IV.8b. The estimated errors in the three principal components of the ^{15}N chemical shift tensor are ± 3 ppm. Note, however, that these values are reported as determined from the

Table IV.3

Nitrogen-15 and phosphorus-31 chemical shift parameters for the iminophosphenium cation, 4.

Nucleus	δ_{11}	δ_{22}	δ_{33}	δ_{iso}	$\Delta\delta$	R'	J_{iso}	β	η_δ
$^{15}\underline{N}$ - ^{31}P	400	366	-21	248.3 (248.1)	421	-1353	+36	0	0.13
$^{31}\underline{P}$ - ^{15}N	308	196	-273	77.0 (78.5)	581	-1353	+36	0	0.32
$^{31}\underline{P}$ - ^{14}N	308	196	-273	77.0 (78.5)	581	960	-24	0	0.32

nmr spectrum in figure 3a and are not corrected for librational averaging.

The three principal components of the ^{15}N chemical shift tensor of compound 4 were converted to an absolute shielding scale [180] and are tabulated in table IV.4. The nitrogen shielding parameters for several other compounds containing nitrogen involved in a triple bond are included in table IV.4 for comparison. With the exception methyl isocyanide, all of these compounds contain a nitrogen which is bonded to one atom only. To this author's knowledge, nitrogen chemical shift parameters for compounds similar to 4 are presently unavailable.

Table IV.4

Absolute nitrogen chemical shielding parameters for several compounds containing nitrogen involved in a triple bond.[a]

Compound	σ_{11}	σ_{22}	σ_{33}	σ_{iso}	$\Delta\sigma$
4	-156	-122	266	-3.3	421
HCN obs.[181]	-215	-215	348	-27	563
CH_3CN obs.[116]	-142	-142	346	21	488
CH_3NC[a]	10	10	370	130	360
N≡N obs.[129]	-	-	-	-	603
obs.[182]	-319	-319	335	-101	654
P≡N obs.[115,128]	-698	-698	350	-349	1047
calc.[171]	-849	-849	341	-452	1190
C_6H_5CN calc.[151]	-216	-181	247	-50	463
p-t-butyl-C_6H_5CN obs.[122]	-149	-130	243	-12	392

a. Chemical shift principal components may be obtained from the expression : $\delta_{ii} = 244.6 - \sigma_{ii}$

b. Experimental results from liquid crystal studies. Reported error in $\Delta\sigma$ is ± 70 ppm.

As demonstrated in section IV.A and by several sources in the literature [20,122,144,151], the orientation dependence of nitrogen shieldings are primarily associated with variations in the paramagnetic term. For linear molecules for example, σ^p is zero when the C_∞ axis is oriented parallel to B_o. Variations in the nitrogen shielding along this symmetry axis will arise solely from the σ^d term. Thus, the most shielded principal component of the nitrogen shielding tensor of linear or pseudolinear molecules should be relatively constant. If the molecule is not perfectly linear, the paramagnetic term may contribute to σ_{33}. From the data in table IV.4, it is clear that σ_{33} is relatively constant for the nitrogen nucleus in simple diatomics, acetonitrile and methylisocyanide. In fact, σ_{33} for these molecules is close to the nitrogen free atom value determined by Malli and Froese, 325.5 ppm [26]. When the molecular symmetry decreases as in 4, the most shielded principal component of the ^{15}N chemical shielding tensor, σ_{33}=265 ppm, is significantly smaller than the corresponding values for the simpler molecules in table IV.4. The implication of this result is that the paramagnetic contribution to σ_{33} of 4 is probably greater than -50 ppm.

Although the presence of a methyl group in acetonitrile and methylisocyanide does not significantly influence the magnitude of σ_{33} compared to the corresponding values in HCN, N_2 and PN, the perpendicular components of the shielding

tensor for CH_3CN and CH_3NC change substantially. For example, $\sigma_\perp$ (σ_{11} and σ_{22}) of the ^{15}N chemical shielding tensor of acetonitrile is more shielded than the corresponding value for HCN by over 75 ppm. Further reduction of the molecular symmetry, as for 4, leads to the observation of nonequivalent values for the σ_{11} and σ_{22} components of the ^{15}N chemical shielding tensor, -156 ppm and -122 ppm, respectively. In addition, these values are substantially larger (i.e., smaller σ^p) than the perpendicular principal components of the nitrogen shielding tensors of N≡N and N≡P, -319 ppm and -698 ppm, respectively. Since the magnitude of these principal components are related to $\sigma \rightarrow \pi^*$ transition energies [171], this observation suggests that $\Delta E_{\sigma \rightarrow \pi^*}$ increases from N≡P to N≡N to 4.

Finally, it is interesting to point out the similarity of the three principal components of the nitrogen shielding tensor of 4 to the corresponding results reported for p-t-butylbenzonitrile [122]. For example, the most shielded principal components (σ_{33}) differ by only 22 ppm in these systems whereas the differences for σ_{11} and σ_{22} are only 7 ppm and 8 ppm, respectively. Note however, that the comparison of the σ_{11} and σ_{22} nitrogen tensor elements of 4 to those of the benzonitrile derivative may be fortuitous since the orientations of the perpendicular components in these systems are not known.

Phosphorus-31 NMR Spectra

The phosphorus-31 cp/mas nmr spectrum for the ^{15}N enriched sample of 4 is shown in figure IV.9. The isotropic spin-spin coupling constant, $^{1}J(^{15}N,^{31}P)_{iso}$, could be determined directly from figure IV.9 and was found to be 35 ± 2 Hz in close analogy to the value observed in the ^{15}N cp/mas nmr spectrum. The large breadth of spinning sidebands suggests that the ^{31}P chemical shift anisotropy is quite large. Indeed, the width of the static ^{31}P nmr spectrum in figure IV.10a exceeds 600 ppm. In acquiring the static ^{31}P nmr spectrum it was found that a Hahn-echo [99-101] was essential in order to alleviate severe distortions in the line shape. This can be attributed to the fact that the ^{31}P nucleus of the N,P bond has three strong contacts (316 pm) [165] with the chlorine nuclei of the tetrachloroaluminate counterions. Chlorine has two magnetically active isotopes with spin 3/2 and the direct dipolar coupling constants, R_{PCl}, can be calculated (see equation II.25) to be 151 Hz and 126 Hz for coupling with ^{35}Cl and ^{37}Cl, respectively. This leads to a very fast decay of the time domain ^{31}P FID (i.e., the signal completely decayed in less then 400 μs), and hence to substantial line broadening in the Fourier transformed nmr spectrum.

In analogy to the interpretation of the ^{15}N static nmr spectrum, a value for the effective $^{15}N,^{31}P$ dipolar coupling constant of -1353 Hz (assuming $^{1}J(^{15}N,^{31}P)_{iso}$ is +36 Hz) was anticipated. Indeed, the observed dipolar splittings in

Figure IV.9

The ^{31}P cp/mas nmr spectrum for a ^{15}N enriched sample of 4. The isotropic chemical shift of a small amount of impurity is labelled with an asterisk (*).

Figure IV.9

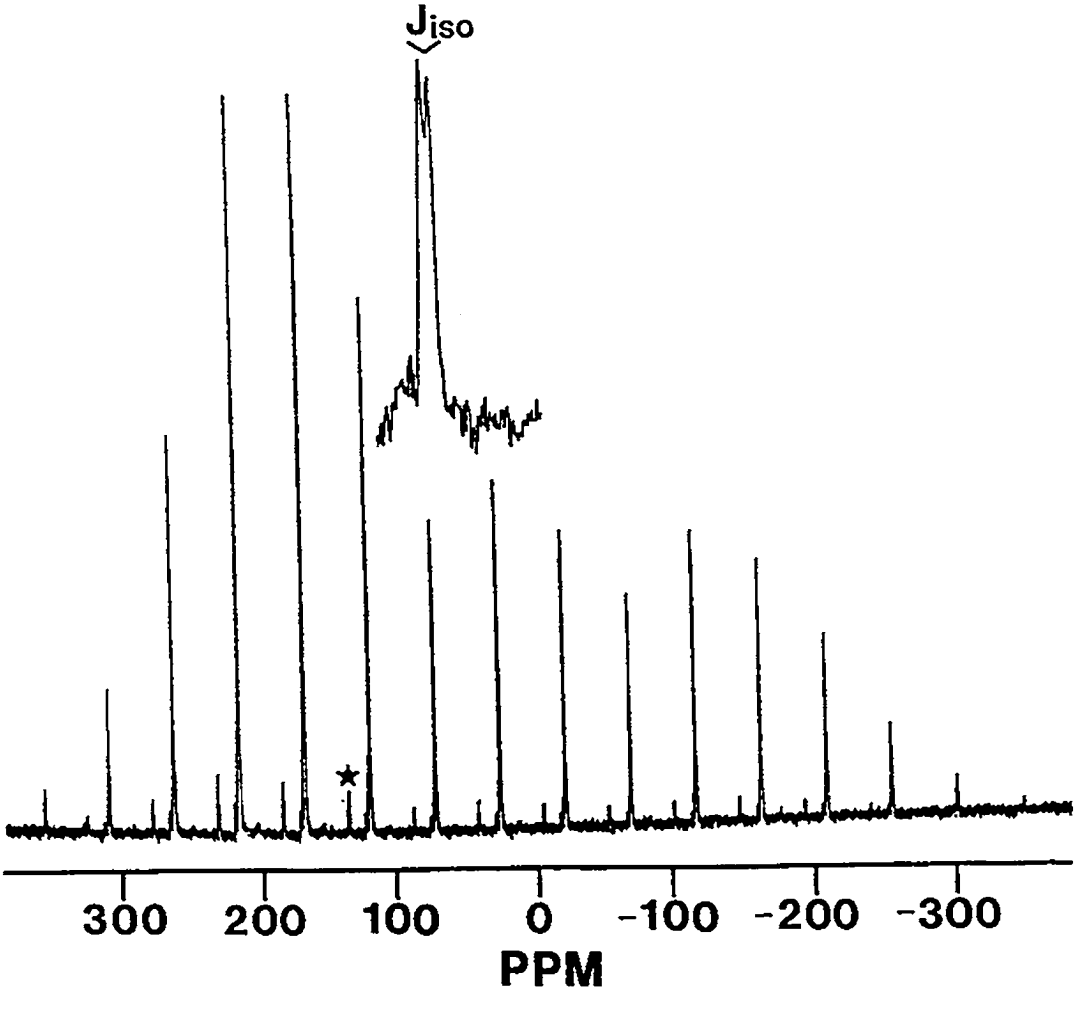

Figure IV.10

The (a) experimental and (b) simulated ^{31}P static nmr spectra of a solid powder sample of ^{15}N enriched 4.

Figure IV.10

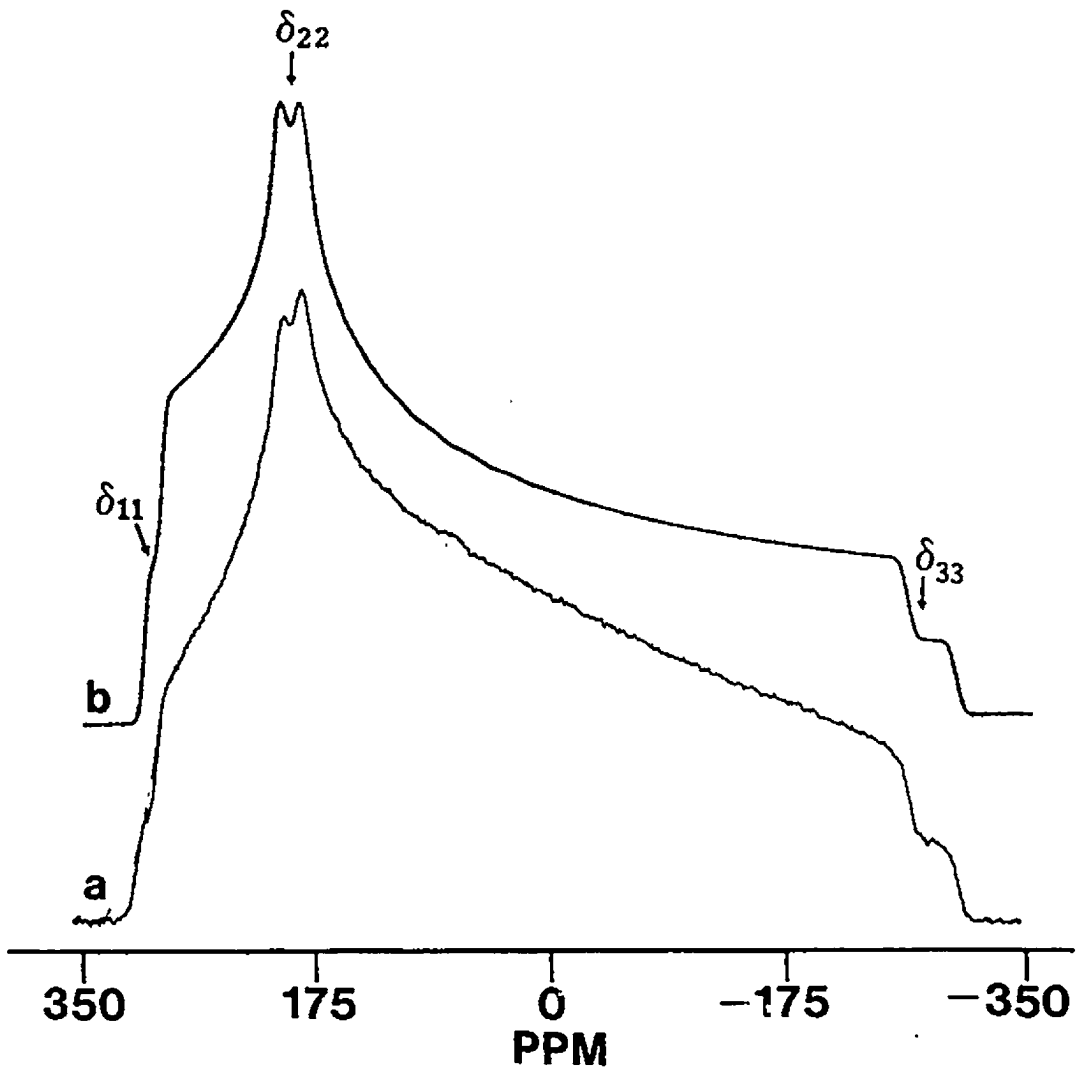

figure IV.10a are consistent with this value. The three principal components of the ^{31}P chemical shift tensor obtained from these simulations are tabulated in table IV.3; the simulated static ^{31}P nmr spectrum is shown in figure IV.10b. The value for β is zero degrees in analogy to the ^{15}N nmr results. This places the most shielded element of the ^{31}P chemical shift tensor along the N,P bonding axis and is consistent with intuitive arguments based on symmetry. Line broadening of 800 Hz was applied to the simulated ^{31}P static nmr spectrum in order to accurately portray the experimental ^{31}P static nmr spectrum. For the corresponding ^{15}N static nmr spectrum (figure IV.8b), line broadening of only 200 Hz was sufficient for accurate spectral simulation. In view of the previous discussion, this observation can be attributed to the influence of intermolecular dipolar interactions involving the chlorine nuclei of the tetrachloroaluminate counterions and the nitrogen and phosphorus nuclei in neighbouring molecules.

A sample of unenriched 4 (i.e., containing an "isolated" $^{14}N,^{31}P$ spin-pair) was the initial sample to be prepared in this laboratory for study by solid state nmr. When a ^{31}P cp/mas nmr spectrum of this sample was obtained, it was surprising to observe two independent sets of spinning sidebands with isotropic chemical shifts of 78.5 ppm and 64.8 ppm (figure IV.11). Upon recrystallization of this sample from toluene, only a single isotropic resonance was observed

Figure IV.11

Phosphorus-31 cp/mas nmr spectrum of a solid sample containing a mixture of the toluene-solvated and non-solvated 4.

Figure IV.11

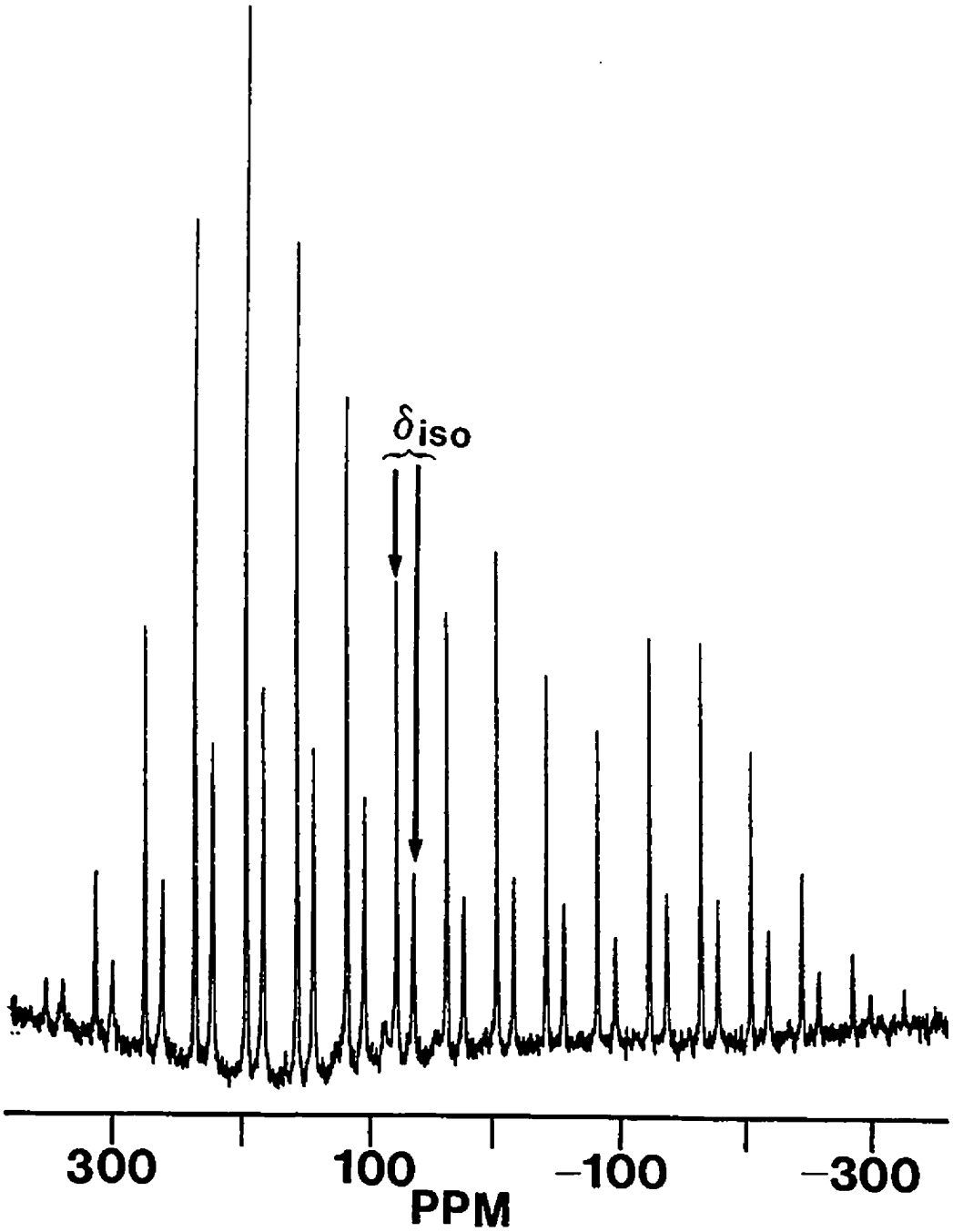

at 78.5 ppm. This is similar to the ^{31}P chemical shift reported by Niecke et al. for 4 dissolved in a solution of toluene/benzene-d_6, δ_{iso}=79.3 ppm [165]. Interestingly, prolonged evacuation of the sample vesicle containing the recrystallized compound 4 resulted in an increase in the intensity of the lower frequency ^{31}P nmr resonance signal, δ_{iso}=64.8 ppm. Thus, it was concluded that the higher frequency ^{31}P nmr resonance (δ_{iso}=78.5 ppm) is associated with the toluene-solvated iminophosphenium cation 4 studied by x-ray diffraction [165] whereas the lower frequency ^{31}P nmr resonance arises from non-solvated 4. Further attempts to isolate the non-solvated material in pure form have been unsuccessful although the solvated species can be prepared readily with reasonably high purity (figures IV.7 and IV.9).

Acquisition of a static ^{31}P nmr spectrum for a recrystallized $^{14}N,^{31}P$ sample of the toluene-solvate of 4 was performed in similar fashion to that for the $^{15}N,^{31}P$ sample. Using a value of β=0 and the δ_{11} values in table IV.3, the effective dipolar coupling constant for the $^{14}N,^{31}P$ spin-pair was determined to be 960 Hz. In determining this value of R', a value for $^{1}J(^{14}N,^{31}P)_{iso}$ of -24 Hz which was calculated from the corresponding value observed for the ^{15}N enriched sample of 4 was assumed. The ratio observed for the effective dipolar coupling constants, $R'(^{15}N,^{31}P)$ versus $R'(^{14}N,^{31}P)$ is 1.409 which compares very well to the value determined from the ratio of $\gamma(^{15}N)/\gamma(^{14}N)$, 1.403. Therefore, it was concluded

that the ^{31}P chemical shift tensor parameters in table IV.3 are reliable and that the high-field approximation [33-35] is valid for the ^{14}N nuclei involved in the N,P bond of 4. That is, the magnitude of $\chi(^{14}N)$ is expected to be small (<2 MHz) and therefore the ^{31}P nmr results for the $^{14}N,^{31}P$ spin-pair could be accurately interpreted based on equation II.32. This conclusion is also consistent with previous results for methylisocyanide [127,183,184] which indicate that $\chi(^{14}N)$ in these systems is less than 1 MHz. Finally, based on the arguments presented for the ^{15}N nmr results, it was anticipated that librational motions would be more important in reducing the dipolar coupling constant, R, than is ΔJ. However, if no motional averaging (i.e., S = 1) and a value for R=1097 Hz (r_{PN} = 1.475 Å) are assumed, then ΔJ for the $^{14}N,^{31}P$ spin pair can be calculated to be 411 Hz or 6171 Hz if the value of R' is taken to be positive and negative, respectively. On the basis of earlier discussions, this author concludes that an upper limit on the J anisotropy for the $^{14}N,^{31}P$ spin-pair is approximately 411 Hz.

There are very few cases in the literature where ^{31}P chemical shift tensors for compounds containing P(III) centres involved in multiple bonds have been reported [115,128,167]. To this authors knowledge, the only experimental values for the ^{31}P chemical shift parameters of the phosphorus centre of a N,P triple bond are those determined for the diatomic molecule, N≡P, from gas phase microwave data [115,128]. The

absolute ^{31}P chemical shielding parameters for this compound (experimental [115,128] and theoretical [171]) as well as the experimental ^{31}P nmr results for 4 and theoretical [171] results for P≡P are tabulated in table IV.5.

Table IV.5

Absolute phosphorus chemical shielding parameters for 4 and two diatomic molecules, N≡P and P≡P.[a]

Compound	σ_{11}	σ_{22}	σ_{33}	σ_{iso}	$\Delta\sigma$
4	21	132	601	251	580
P≡N obs.[115,128]	-406	-406	970	53	1376
calc.[171]	-497	-497	966	-10	1463
P≡P calc.[171]	-934	-934	969	-299	1903

a. Absolute shielding constant of H_3PO_4 (85 %), 328.35 ppm determined relative to σ_{abs} of PH_3, 594.45 ppm [185]. Relative chemical shifts can be obtained from the expression : $\delta_{ii} = 328.35-\sigma_{ii}$

The most shielded principal component of the ^{31}P chemical shielding tensor, σ_{33}, for the linear molecules N≡P and P≡P is approximately 970 ppm. This is very close to the value for the free P atom, 961.1 ppm [26], and is consistent with previous discussion of ^{15}N shieldings. As the symmetry of the

molecular environment decreases, such as for compound 4, shielding of the σ_{33} principal component decreases to 601 ppm. The implication of this result is that $\sigma_p \neq 0$ for the σ_{33} principal component of the ^{31}P chemical shielding tensor of 4 and in fact, the paramagnetic contribution to σ_{33} is probably greater than -350 ppm. The σ_{11} and σ_{22} principal components of the ^{31}P chemical shielding tensor of 4 are considerably different (over 100 ppm) and this is reflected in the value of the asymmetry parameter, η_σ=0.32 ± 0.02. The ^{31}P chemical shielding anisotropy for 4, 581 ± 4 ppm, is significantly smaller than values of 1376 ppm and 1903 ppm previously reported for the diatomic molecules N≡P and P≡P, respectively. The results in table IV.5 indicate that this difference is primarily associated with changes in the perpendicular components (i.e., σ_{11} and σ_{22}). As previously discussed, the perpendicular components are dominated by paramagnetic contributions from low lying $\sigma \rightarrow \pi^*$ transition energies [171]. Thus, in analogy to the ^{15}N nmr results, the ^{31}P shielding parameters suggest that the $\Delta E_{\sigma \rightarrow \pi^*}$ transition energy for compound 4 is larger than the corresponding values for N≡P and P≡P. It is interesting to point out that the magnitude of the ^{31}P chemical shielding anisotropy reported here, 581 ± 4 ppm, is intermediate to values reported for P(III) centres involved in single and double bonds [167]. Accordingly, the observed isotropic ^{31}P chemical shift, δ_{iso}=78.5 ppm, follows the same empirical trend (i.e., $\delta_{iso}(P-X) < \delta_{iso}(P\equiv X) < \delta_{iso}(P=X)$) and

Niecke et al. used this to help interpret their solution ^{31}P nmr data of 4 and its precursor [165].

B.4 Summary

Dipolar-chemical shift solid state nmr spectroscopy has been used to characterize the ^{15}N and ^{31}P chemical shift tensors for a novel system (4) containing a N,P triple bond. The presence of librational motion has been postulated to account for the decrease in the observed value of the dipolar coupling constant, R, with perhaps a small but indeterminate contribution from ΔJ. Analysis of the nmr spectra indicates that the most shielded principal component of both the ^{15}N and ^{31}P chemical shift tensors, δ_{33}, is oriented parallel to the N,P bond axis. The ^{15}N and ^{31}P chemical shift anisotropies for 4 are 421 $\pm$ 4 ppm and 581 $\pm$ 4 ppm, respectively. Comparison of the results obtained here with chemical shift tensors reported for the nitrogen and phosphorus centres in related compounds suggests that the electronic environment around the N,P moiety of 4 is similar to other systems containing nitrogen or phosphorus involved in a triple bond. Interestingly, the asymmetry of the molecular environment in 4, has a substantial affect on the three principal components of both the ^{15}N and ^{31}P chemical shift tensors. The most striking example of this is the implication that the most shielded component of the ^{31}P chemical shift tensor for 4 has a paramagnetic contribution in excess of -350 ppm. It is

hoped that the information provided here will stimulate the interest of theoreticians to investigate nitrogen and phosphorus shielding parameters in more complex organo-phosphorus and organo-nitrogen compounds.

C. High Resolution Carbon-13 and Nitrogen-15 Solid State NMR Studies of the Tetracycline Antibiotics

C.1 INTRODUCTION

The discovery of the tetracycline family of antibiotics in the late 1940's marked the beginning of a new era in the treatment of bacterial infections [186-188]. Since that time, scientists have been concerned with characterizing their detailed structural and conformational properties in both the solid [189-202] and solution states [203-216]. The underlying objective has been to understand how the antibiotics work at the molecular level and what structural features may enhance their in vivo antibacterial activity. The detailed structures of several solid tetracyclines which are relevant to this thesis are indicated in table IV.6.

X-ray diffraction experiments have revealed definitive evidence of the existence of several stable forms of the tetracyclines in the solid state. Crystal structures have been reported for tetracycline hexahydrate (TC±) [189,190a], tetracycline urea tetrahydrate (TCUREA) [191], oxytetracycline dihydrate (OTC±) [190a], anhydrous oxytetracycline (OTC^{o})

Table IV.6

The structures of several solid tetracycline antibiotics.

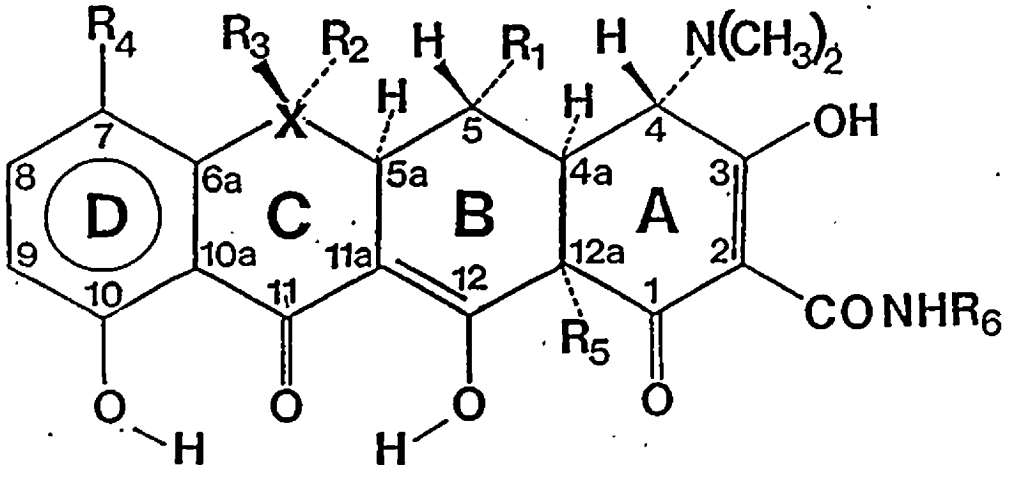

Generic Name	X	R_1	R_2	R_3	R_4	R_5	R_6	Abbreviation
Tetracycline	C	H	CH_3	OH	H	OH	H	TC
Oxytetracycline	C	OH	CH_3	OH	H	OH	H	OTC
Chlortetracycline	C	H	CH_3	OH	Cl	OH	H	CTC
Demeclocycline	C	H	H	OH	Cl	OH	H	DEMTC
Doxycycline	C	OH	CH_3	H	H	OH	H	DOXYTC
Minocycline	C	H	H	H	$N(CH_3)_2$	OH	H	MINTC
Rolitetracycline	C	H	CH_3	OH	H	OH	$CH_2NC_4H_8$	ROLITC
Thiatetracycline	S	H	-	-	H	OH	H	6-STC
Diacetyloxy-tetracycline	C	$OCOCH_3$	CH_3	OH	H	$OCOCH_3$	H	DIAOTC

[190], anhydrous thiatetracycline (6-STC) [192], 5-12a-diacetyloxytetracycline (DIAOTC) [193], and the hydrochloride salts of tetracycline (TCHCl) [194], oxytetracycline (OTCHCl) [195], chlortetracycline (CTCHCl) [196], doxycycline (DOXYTC) [197], and demeclocycline (DEMTC) [198]. The hydrobromide salt of oxytetracycline (OTCHBr) has also been investigated by x-ray crystallography [199]. Although several other members of the tetracycline family have been investigated by x-ray diffraction, the hydrochloride salts of rolitetracycline (ROLITC) [200], minocycline (MINTC) [201] and thiatetracycline (6-STC) [192b] have not been studied by diffraction techniques.

The x-ray diffraction results have indicated that the A ring of anhydrous oxytetracycline exists in a neutral "enol" form (5a) whereas the dihydrate of oxytetracycline exists exclusively in an ionized "keto" form (5b) [190]. The

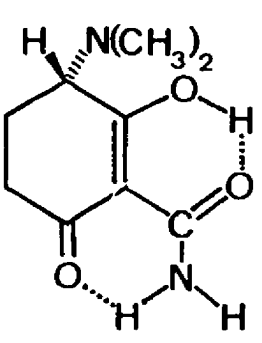

OTC°

5a

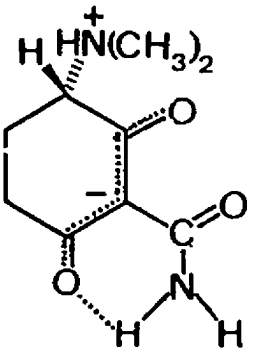

OTC±

5b

principal differences between these two tautomers are the site of protonation of the A ring, the conformation about the

C_{4a}-C_{12a} bond axis and the relative amounts of intermolecular and intramolecular hydrogen bonding. OTC° has been shown to exist with the N,N-dimethylamino nitrogen not protonated as in 5a whereas OTC± is present in the solid state with a hydrogen bonded to the N,N-dimethylamino group as in 5b. Conformational differences between OTC° and OTC± are primarily associated with the orientation of the A ring relative to the approximately planar B, C and D rings. For OTC°, the A ring is flipped up and oriented at approximately 110° with respect to B, C and D rings. In this conformation, the $N(CH_3)_2$ group is directed above the B, C, D plane and the dihedral angle, H-C_4-C_{4a}-H, is approximately 170° [190]. OTC± on the other hand, adopts a conformation where the A ring is oriented closer to the approximate plane of the B, C and D rings. In this case, the $^{+}N(CH_3)_2H$ group is directed below this plane and the dihedral angle, H-C_4-C_{4a}-H, is approximately 74° [190].

The difference in the conformations of OTC° and OTC± can, in part, be attributed to significant differences in the hydrogen bonding exhibited by these two tautomers. More specifically, Stezowski et al. [190] have demonstrated that OTC° displays a substantial amount of intramolecular hydrogen bonding and is much less polar in nature than OTC± which exhibits a significant amount of intermolecular hydrogen bonding. For example, the $N(CH_3)_2$ group of OTC° is not involved in hydrogen bonding whereas the $^{+}N(CH_3)_2H$ group of OTC± exhibits intermolecular hydrogen bonds with the solvated

water molecules [190]. Other members of the tetracycline family of antibiotics such as 6-STC [192a] and DIAOTC [193] have been shown to exist in the neutral enol form in the solid state whereas the hexahydrate of the parent compound, TC±, has been shown to be present exclusively in the ionized keto form [189,190]. In all reported cases, the x-ray data of a number of tetracyclines has indicated that the stuctural form represented by 5a, is associated with the conformation having a large $H-C_4-C_{4a}-H$ dihedral angle of approximately 170°. An analogous structure-conformation relationship has been reported for the solid state structures of the various hydrated tetracycline free bases [190,192,216].

The N,N-dimethylamino nitrogen of the hydrochloride salts of TC, OTC, CTC, DEMTC, DOXYTC, and the hydrobromide salt of OTC have been shown [194-199] to be protonated in the solid state. These salts display an overall conformation which is similar to that described for TC± and OTC± [189,190a]. The main difference between the various hydrohalide salts is the conformation of the A ring amide substituent as depicted in 5c and 5d. The hydrochloride salt of DOXYTC crystallizes from aqueous ethanol with two crystallographically unique molecules per unit cell [197]. One of the two nonequivalent sites in DOXYTCHCL exists in conformation 5c while the other is in conformation 5d [197]. The only other known example of this phenomenon for the tetracycline family was the observation of two different amide conformations for single crystals of

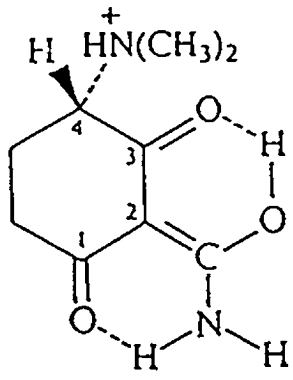

5c

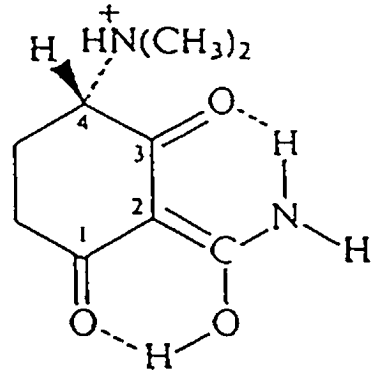

5d

OTCHBr [199]. From the available x-ray data [194,198], TCHCl and DEMTCHCl have been shown to exist with opposite conformations of the amide substituent; the hydrochloride salt of TC being in conformation 5c and DEMTCHCl being in conformation 5d. The conformation of the amide substituent of the remaining tetracyclines in table IV.6 will be discussed later.

In contrast to the x-ray diffraction results, there has been no definitive evidence for the existence of the enol (5a) and keto (5b) structural forms of the tetracyclines in solution. However, on the basis of vicinal spin-spin couplings, $^3J(H_4,H_{4a})$, observed in high-resolution ^1H nmr experiments, several authors have demonstrated that the conformational integrity of the tetracyclines are maintained in $(CD_3)_2SO$ and pyridine-d_5 solutions [209,211c,192c]. For example, Gulbis and Everett observed significantly larger $^3J(H_4,H_{4a})$ values for the anhydrous forms of TC, OTC and CTC

dissolved in $(CD_3)_2SO$ as compared to the corresponding values observed for their respective hydrochloride salts in $(CD_3)_2SO$ [211c]. Based on the forementioned H-C_4-C_{4a}-H dihedral angles deduced from x-ray diffraction results for these compounds [189,190,194-196], Gulbis and Everett concluded that the conformations in $(CD_3)_2SO$ are similar to those reported in their respective crystal structure analyses.

A previous investigation of several solid tetracyclines in this laboratory demonstrated the utility of high-resolution solid state ^{13}C cp/mas nmr for distinguishing the enol and keto forms of the tetracycline free bases [202]. The basis of this method relied on the ^{13}C cp/mas line shapes observed for those carbon atoms which are bonded to a nitrogen [58,83-90]. This provided a method for monitoring the state of ionization of the A ring although it does not study the site of protonation directly. The work of Mooibroek and Wasylishen [202] has been extended in this thesis to include several other structurally important members of the tetracycline antibiotics not previously investigated.

To date there has been no ^{15}N nmr data presented for the tetracycline antibiotics in either the solid or solution state. Given the inherent sensitivity of ^{15}N chemical shifts to subtle changes in the local electronic environment [217], it was anticipated that this method would provide a sensitive probe of the site of protonation of the A ring of the tetracyclines. To this end, the solid tetracycline

antibiotics indicated in table IV.6 were examined by natural abundance ^{15}N cp/mas solid state nmr. To determine if the structural integrity of the tetracyclines are maintained when dissolved in solution, ^{15}N nmr spectra of several derivatives were investigated in $(CD_3)_2SO$ and pyridine-d_5 solutions for comparison to the results from the solid state ^{15}N cp/mas experiments.

C.2 Experimental

The hydrochloride salts of OTC, CTC, DEMTC, DOXYTC and MINTC and the free base hydrates of TC and OTC were purchased from the Sigma Chemical Company. The hydrochloride salt of TC was purchased from the Aldrich Chemical Company. ROLITCHCL was supplied by C. Marcotte of the Pharmaceutical Division of Hoescht Company in Montreal. The anhydrous form of oxytetracycline, OTC°, was prepared by azeotropic distillation of a toluene solution of the dihydrate, OTC± [190]. DIAOTC was prepared by the addition of acetic anhydride to a solution of OTC° in anhydrous dioxane [218]. The 1:1 tetracycline urea adduct was precipitated from a saturated aqueous solution of urea by the addition of tetracycline hexahydrate [219]. A sample of 6-STCHCL was supplied by R. Kirchlechner of Merck Company in Darmstadt, West Germany. For completeness, additional solid samples of the hydrates of TC and OTC and the hydrochloride salt of DEMTC were all crystallized according to the methods outlined in their respective x-ray studies

[189,190a,198]. Purity of the prepared samples (i.e., OTC° and DIAOTC) was checked by the appearance of their respective solid state ^{13}C cp/mas nmr spectra.

Carbon-13 and ^{15}N nmr spectra of solid samples were recorded on a Bruker MSL-200 spectrometer operating at 50.32 MHz and 20.30 MHz, respectively. The tetracycline samples (≈500 mg) were ground into fine powder and packed into cylindrical rotors (7 mm o.d.) made from aluminum or zirconium oxide. Hydrogen cross polarization to the ^{13}C and ^{15}N nuclei was performed under the conditions of the Hartmann-Hahn match with ^{13}C, ^{15}N and ^{1}H $\pi/2$ pulse widths of 3.5-5 μs and contact times of 3 to 5 ms. All nmr spectra were acquired with high-power hydrogen decoupling and mas rates of 3-5 kHz. For the ^{13}C nmr experiments, approximately 500-1000 transients were acquired with recycle times of 4-6 s. For the ^{15}N cp/mas nmr experiments, approximately 5000 transients were required to obtain a S:N ratio of about 10:1. This was readily obtainable over night with recycle times of 4 to 6 s. Prior to Fourier transformation, sensitivity enhancements corresponding to 5 Hz and 20 Hz of line broadening were applied to the ^{13}C and ^{15}N FIDs respectively. For the dipolar dephasing nmr experiments, decoupler windows of 40 to 100 μs were used for all samples. The solid state ^{13}C cp/mas nmr spectra are referenced with respect TMS at 0 ppm by setting the observed ^{13}C chemical shift of the methylene carbon ($\underline{C}H_2$) of adamantane at 38.57 ppm [133]. Nitrogen-15 cp/mas nmr spectra are referenced with

respect to $NH_3(\ell)$(293 K) at 0 ppm by setting the ammonium ion signal of doubly isotopically enriched $^{15}NH_4{}^{15}NO_3$ at 23.80 ppm.

Samples for ^{15}N solution state nmr were prepared as saturated solutions in $(CD_3)_2SO$ (c.a. 1 M) or pyridine-d_5 just prior to obtaining the nmr spectra. Solution nmr spectra were recorded on a Nicolet-360 nmr spectrometer with ^1H and ^{15}N operating frequencies of 361.05 MHz and 36.61 MHz, respectively. With the exception of OTC°, all ^{15}N spectra were acquired using the INEPT pulse sequence [220,221] with a delay time between ^1H $\pi/2$ and π pulses of 2.78 ms and a delay time for refocussing the ^{15}N signals of 2.25 ms. The ^{15}N nmr spectrum of OTC° in $(CD_3)_2SO$ was acquired using bilevel broadband decoupling and a delay of 30 s between acquisition of transients. The ^{15}N nmr spectrum of OTC° in pyridine-d_5 was acquired using a single pulse experiment without hydrogen decoupling and a recycle time of 30 s. The ^{15}N $\pi/2$ pulse length was typically 60 to 65 μs. Signal averaging on the order of 5000 to 10000 transients was employed for all samples. Line broadening of 15 Hz was applied to all FIDs prior to Fourier transformation. ^{15}N nmr spectra were referenced with respect to liquid NH_3 (293 K) by setting the observed ^{15}N chemical shift of external formamide at 112.3 ppm [222].

C.3 RESULTS AND DISCUSSION

Carbon-13 CP/MAS NMR Spectra

The carbon-13 chemical shifts for several tetracycline antibiotics not previously discussed in ref. 202 are given in table IV.7. The ^{13}C chemical shifts determined for a sample of OTC° are included in the table for discussion.

Typical high-resolution ^{13}C cp/mas nmr spectra are shown for 6-STCHCL and TCUREA in figure IV.12. The ^{13}C cp/mas nmr spectra were assigned using dipolar dephasing nmr experiments and by comparison to reported solid [202] and solution [210,213,214a,215] ^{13}C nmr results. In some cases, carbons directly bonded to nitrogen could be assigned on the basis of their asymmetric line shapes. The only significant differences between the ^{13}C assignments reported here and those previously reported by Mooibroek and Wasylishen [202] are with respect to C_1, C_{11}, C_7 and C_9. Recent solution ^{13}C nmr experiments performed on a ^{13}C enriched sample of tetracycline [215] indicated that the previous assignments of C_7 and C_9 should be interchanged as should those of C_1 and C_{11}. The assignments in table IV.7 have included this consideration. With the exception of OTCHBr, the ^{13}C line widths observed for most carbons were approximately 10 to 15 Hz. The line broadening observed for the hydrobromide salt of OTC was sufficient that the high frequency resonances could not be adequately resolved for assignment. This line broadening can be attributed to the influence of intermolecular dipolar

Table IV.7

Carbon-13 chemical shifts of several solid tetracycline antibiotics.

	Carbon											
Compound	CH_3	C_5	C_{4a}	C_{5a}	$N(CH_3)_2$	C_6	C_4	C_{12a}	C_2	C_{11a}	C_7	C_{10a}
6-STCHCL	-	32.6	34.0	37.2	37.8 44.2	-	68.2	73.9	95.4	108.3	116.3	116.3
TCUREA	21.5	29.3	34.0	43.8	38.5 43.1	71.4	70.1	76.4	103.9	109.7	114.6	116.5
DIAOTC	22.3	71.8	43.1	47.9	37.2 46.3	69.2	63.9 66.4	81.4	102.2	105.1	120.3	115.3
OTC[o]	26.6	68.5	48.0	50.3	35.1 45.9	69.7	61.3 63.6	74.9	102.4	104.9	119.4	113.1
OTCHBr	24.3 25.2	65.2	41.5	49.3	38.6 46.4	70.4	65.2	74.0 72.9	96.1	106.0 105.5	120.8 120.1	115.4
ROLITCHCL	21.6	22.1 22.9	36.8 37.9	42.3 43.2	43.8	69.8 70.9	74.3 74.6	76.2 77.9	100.9 101.3	104.1 106.5	118.8 120.0	114.8 116.4

Table IV.7 Continued

Compound	Carbon									
	C_9	C_8	C_{6a}	C_{10}	CONH2	C_{12}	C_3	C_{11}	C_1	Others
6-STCHCL	122.2	139.9	140.7	162.7	171.7 173.8	177.4	185.3	193.8	197.0	
TCUREA	118.1	139.3	146.8	159.8	170.9 173.0	178.8	184.1	192.8	192.8	163.4 (urea)
DIAOTC	120.3	136.0	147.5	163.0	173.1	173.1	184.8	193.9	193.9	24.3 ($\underline{C}OCH_3$) 197.8 ($\underline{C}OCH_3$)
OTC°	119.4	141.4	147.1	164.5	171.6	171.2	192.4	193.4	194.3	
OTCHBr	115.4	140.2 139.5	149.9 148.7	162.9 162.3	173.3 172.3	173.3 172.3	190 - 195 (see text)			
ROLITCHCL	116.4 118.4	135.9 139.0	147.7	162.6 163.0	171.5	181.4 182.9	188.8	193.4 193.8	194.5 194.3	24.3, 25.2 54.0, 52.5 57.8, 59.6

Figure IV.12

Carbon-13 cp/mas nmr spectra for (a), (b) 6-STCHCL and (c), (d) TCUREA·$4H_2O$. The nmr spectra (b) and (d) were acquired using the dipolar dephasing pulse sequence with a delay of 50 μs.

Figure IV.12a and b

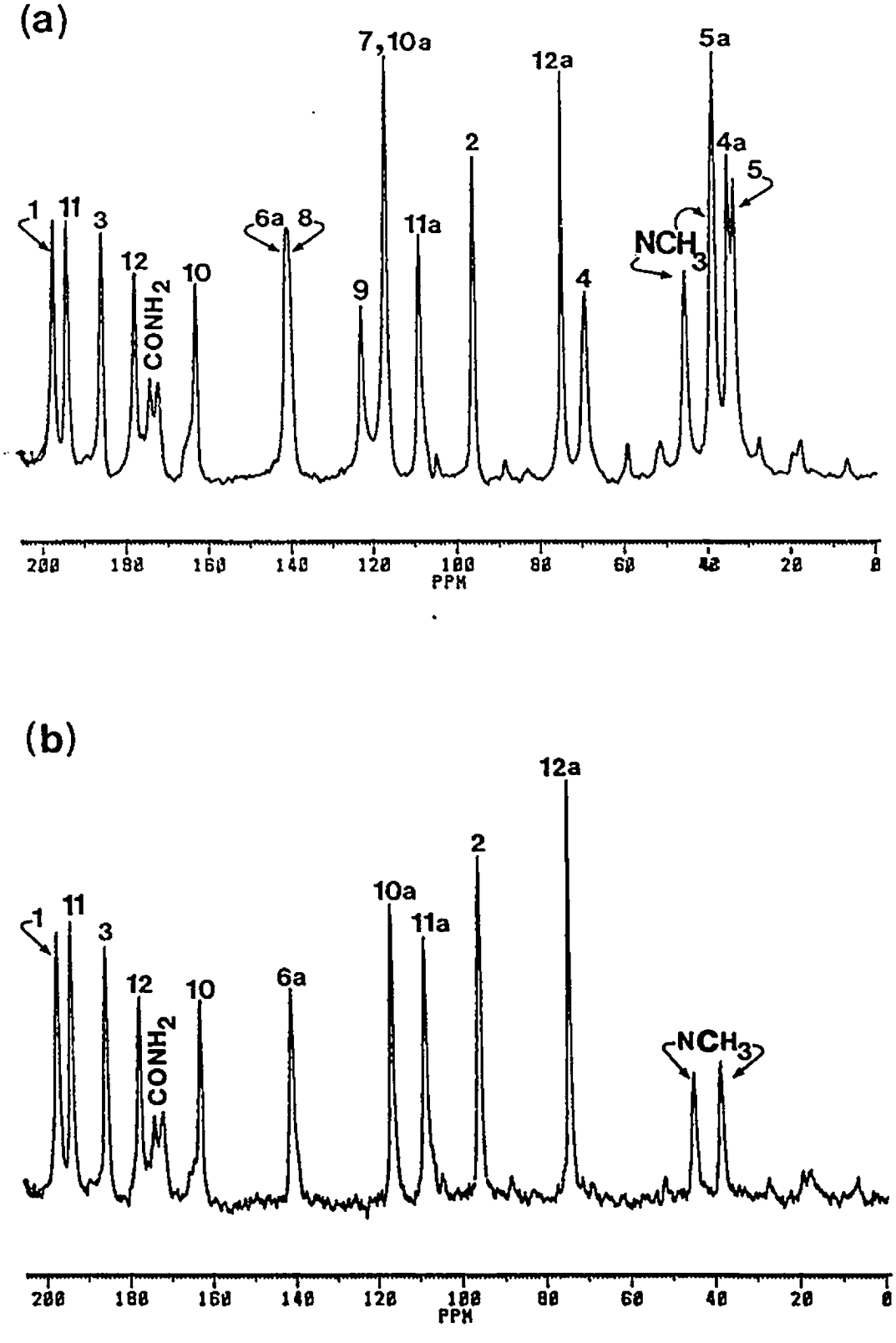

Figure IV.12c and d

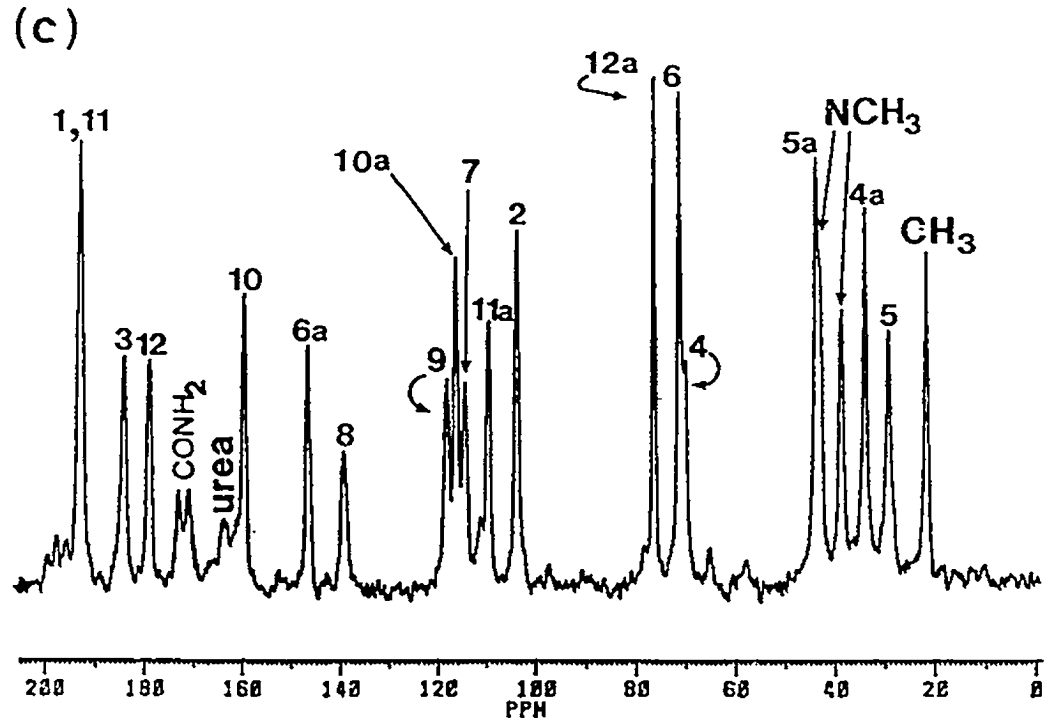

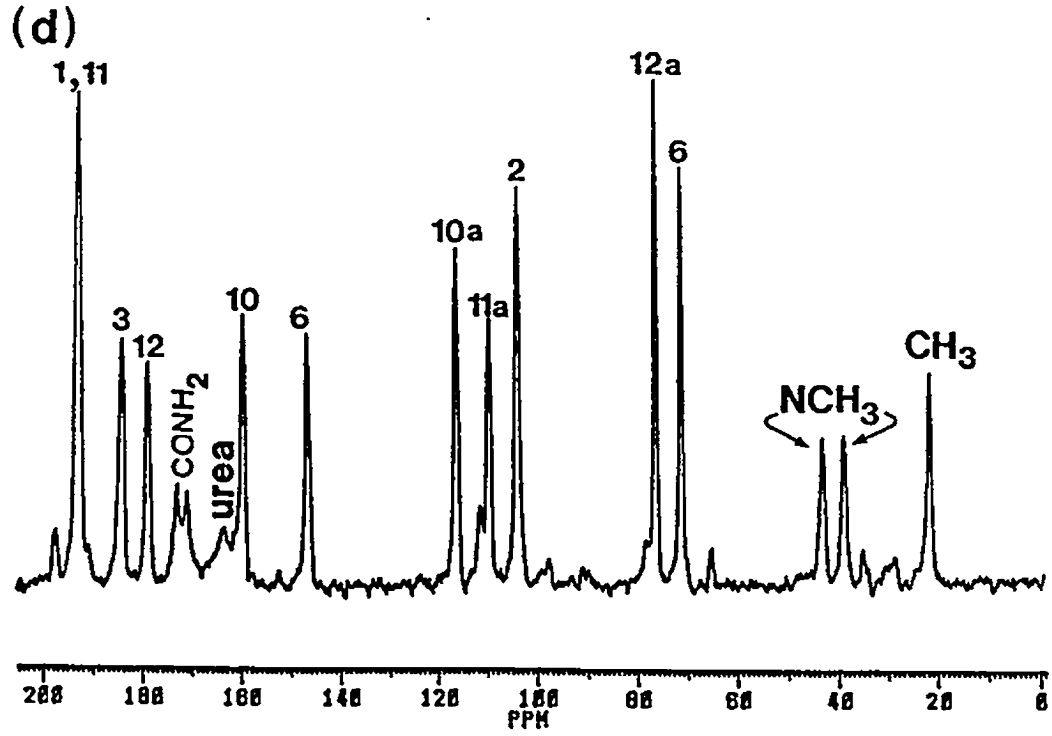

interactions of the ^{13}C nuclei with the bromide counterions. The analogy of this observation to the results reported for the iminophosphenium cation, 4, in section IV.B is noted.

As already mentioned and demonstrated in figures II.13 the ^{13}C cp/mas nmr line shape for a carbon nucleus bonded to a quadrupolar ^{14}N nucleus is sensitive to both the orientation and magnitude of the efg tensor. For an approximately tetrahedral ^{14}N nucleus such as the $^{+}N(CH_3)_2H$ nitrogen, 5b, the magnitude of the principal component of the efg tensor (V_{33}) is usually less than 1 MHz [223]. Under these circumstances, deviations from the high-field approximation are small at B_o=4.7 T and the line shapes observed for the carbon nuclei bonded to this nitrogen should be reasonably sharp. This is clearly demonstrated for the C_4 and $^{+}N(\underline{C}H_3)_2H$ resonances in figure IV.13b where line widths of less than 40 Hz are observed for these carbons. For the enol tautomer, 5a, the N,N-dimethylamino nitrogen is not protonated in the solid state and V_{33} of the nitrogen efg is anticipated to be quite large (i.e., >3.5 MHz) [224]. Thus, the ^{13}C resonance signals for C_4 and $N(\underline{C}H_3)_2$ in this case should be substantially broadened or split into asymmetric doublets. This was observed in the ^{13}C cp/mas nmr spectra for DIAOTC (figure IV.13d) which is known from single crystal x-ray diffraction experiments [193] to be present exclusively in the enol form. The magnitude of the splitting of the C_4 resonance in figure IV.13d is approximately 126 Hz. This compares very well with

Figure IV.13

Selected regions of the ^{13}C cp/mas nmr spectra of (a), (b) 6-STCHCL and (c), (d) DIAOTC showing the residual dipolar splittings of the $\underline{C}ONH_2$, C_4 and $N(CH_3)_2$ carbon signals.

Figure IV.13

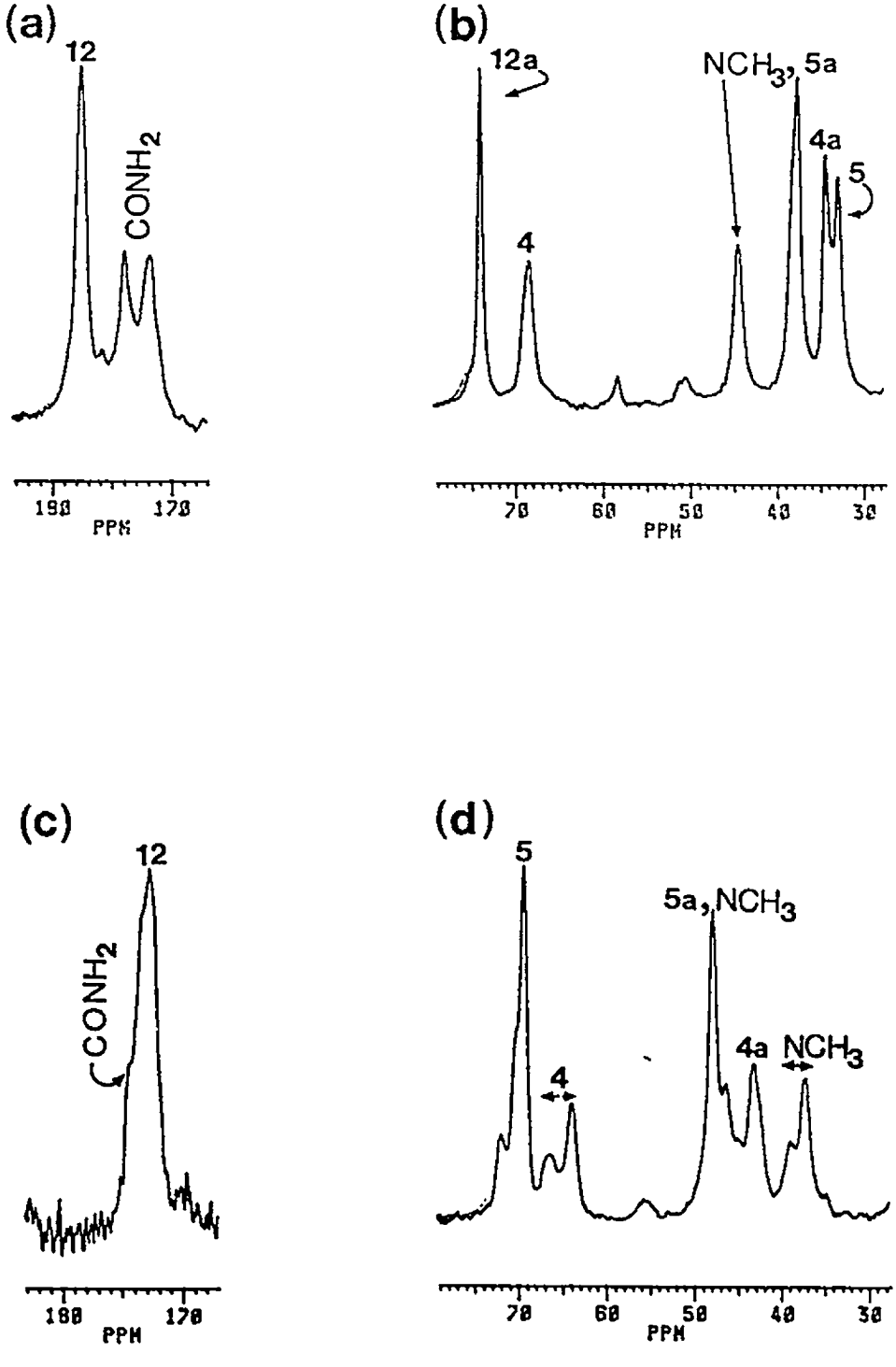
(a)
12
CONH2
190
170
PPM
(b)
12a
NCH3, 5a
4a
5
4
70
60
50
40
30
PPM
(c)
12
CONH2
180
170
PPM
(d)
5
5a, NCH3
4a
NCH3
4
70
60
50
40
30
PPM

the reported splitting of 116 Hz for the C_4 resonance signal of OTC° [202]. Obviously then, ^{13}C cp/mas solid state nmr provides a reasonable method for distinguishing the O-protonated (5a) and N-protonated (5b) tautomeric forms of the tetracycline free bases.

Nitrogen-15 NMR Spectra

The ^{15}N chemical shifts of several tetracycline antibiotics are given in table IV.8. Since only two ^{15}N resonance signals were present in most of these compounds, assignment of the resonances was straightforward. Without exception, the high frequency resonance was assigned to the amide nitrogen.

The ^{15}N cp/mas nmr spectra provided two distinct methods of distinguishing between the neutral ("enol") (5a) and ionized ("keto") (5b) forms of the tetracycline free bases in the solid state. First, the ^{15}N chemical shift of the N,N-dimethylamino nitrogen is expected to be sensitive to the state of ionization of the nitrogen. For example, in solution nmr studies of a series of 15 tertiary amines, the average ^{15}N chemical shift of the ionized amine was 12.8 ppm to high frequency of the free base [225,226]. Comparison of the ^{15}N nmr results for ionized OTC± and the free base OTC° in table IV.8 indicate that the chemical shift of OTC± is 13.9 ppm to high frequency of the corresponding value for OTC°. The corresponding ^{15}N cp/mas nmr spectra are shown in figure IV.14a

Table IV.8

Nitrogen-15 chemical shifts of several tetracycline antibiotics. The values in parentheses indicate solution state measurements in $(CD_3)_2SO$.

Compound		Nitrogen		
		$^{15}N(CH_3)_2$	$CO^{15}NHR$	Other
TCHCl		44.9 (46.1)	113.0 (111.6)	
TC±		41.8	107.5	
TCUREA		43.4	107.2	81.9
OTCHCl		43.5 (44.3)	113.3 (111.5)	
OTCHBr	I	41.4	a	
	II	45.7	111.6	
OTC±		41.6 (b)	105.6 (108.9)	
OTC°		27.7 (25.3)	109.5 (109.3)	
		(22.3 (c))	(108.5 (c))	
CTCHCl		45.3	113.1	
DEMTCHCl		45.7	111.6	
DOXYTCHCl	I	41.4	105.5	
	II	45.3	111.6	
MINTCHCl		41.9	99.8	49.8
ROLITCHCl		34.9	113.6	79.9 74.8
6-STCHCl		41.7	111.7	
DIAOTC		20.6	104.6	

a. Not resolved due to line broadening.

b. Not observed in the solution nmr spectrum.

c. Single pulse experiment in pyridine-d_5.

Figure IV.14

Nitrogen-15 cp/mas nmr spectra of (a) OTC± (b) and (c) OTC^{o}. The nmr spectrum in (c) was acquired with the dipolar dephasing pulse sequence with τ_{DD}=65 μs.

Figure IV.14

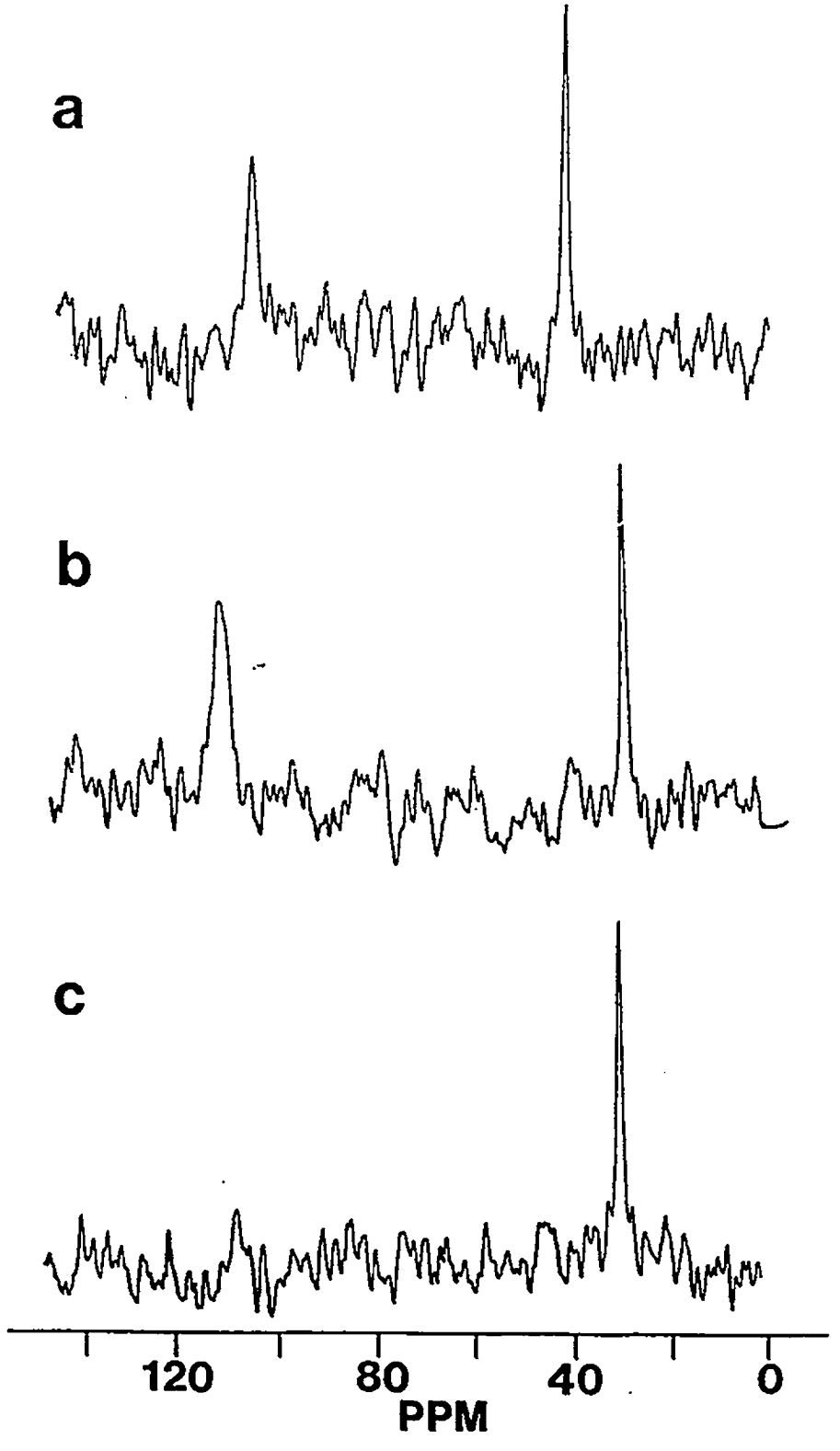

and IV.14b for OTC± and OTC°, respectively. It should also be pointed out that the ^{15}N chemical shift of OTC° is similar to that observed for the N,N-dimethylamino nitrogen of DIAOTC (δ_{iso}=20.6 ppm). This is an important observation since as already mentioned, x-ray diffraction experiments [193] have concluded that DIAOTC exists exclusively in the enol form.

Applying the dipolar dephasing nmr experiment to the nitrogen nuclei of several of the compounds in table IV.6 provided an alternative method for studying the state of ionization of the A ring. The ^{15}N nmr spectrum obtained for OTC° using this pulse sequence is shown in figure IV.14c. Comparison with figures IV.14a and IV.14b indicate that there is no ^{15}N resonance signal observed for the amide nitrogen in the nmr spectrum of OTC° acquired with the dipolar dephasing pulse sequence [106,107]. This was not surprising since this nitrogen is strongly dipolar coupled to two hydrogens and therefore the corresponding signal dephases rapidly during the time τ_{DD}. Of greater significance, the resonance signal corresponding to the N,N-dimethylamino nitrogen of OTC° was still present in this nmr spectrum (figure IV.14c). Analogous results were obtained when a dipolar dephasing ^{15}N nmr experiment was performed on a sample of DIAOTC confirming that both OTC° and DIAOTC exist exclusively in the enol tautomeric form in the solid state.

The ^{15}N chemical shifts for TCHCl, OTCHCl, OTC± and OTC° in $(CD_3)_2SO$ and pyridine-d_5 solutions are given in parentheses

in table IV.8. Preliminary ^{15}N nmr experiments were performed with the INEPT pulse sequence <u>without</u> hydrogen decoupling [221] on samples of OTCHCL dissolved in $(CD_3)_2SO$. This solvent was chosen since relatively concentrated solutions of OTCHCl could be prepared (c.a. 1 M) and because previous ^1H nmr experiments indicated that its conformational integrity is maintained when dissolved in this solvent [211c]. It is important to point out that the INEPT experiment is a polarization transfer technique which depends on the presence of a spin-spin coupling (J) between the nuclei involved. In this study, polarization transfer was from the directly bonded hydrogens to the nitrogen and therefore a $^1J(^{15}N,^1H)$ coupling is essential for the INEPT nmr experiment to be applied successfully. Since no previous ^{15}N nmr investigations of the tetracyclines have been reported, a value for $^1J(^{15}N,^1H)$ for the amide and protonated N,N-dimethylamino nitrogens was assumed to be similar to that reported for formamide (i.e., approximately 90 Hz) [130]. This value for $^1J(^{15}N,^1H)$ was then used to calculate the spin dephasing delay time $(1/4 \cdot J)$ required for performing the INEPT nmr experiment [220,221]. Subsequent acquisition of a ^{15}N nmr spectrum of OTCHCl in $(CD_3)_2SO$, provided a hydrogen coupled ^{15}N nmr spectrum. In this nmr spectrum, the amide resonance signal was a 1:0:-1 triplet with a $^1J(^{15}N,^1H)$ of 95 Hz whereas the low frequency signal for the N,N-dimethylamino resonance was observed as a 1:-1 doublet with a $^1J(^{15}N,^1H)$ of 62 Hz. The average of these

two values was then used to calculate the spin dephasing delay for further ^{15}N nmr experiments performed with the INEPT sequence and hydrogen decoupling.

Inspection of table IV.8 indicates that the observed ^{15}N chemical shifts of the tetracyclines in solution are similar to the corresponding chemical shifts observed in the solid state. In addition, both TCHCl and OTCHCl exhibited a signal due to the N,N-dimethylamino nitrogen in their respective solution ^{15}N nmr spectrum. Since a resolvable spin-spin coupling between hydrogen and nitrogen is essential for the INEPT experiment to work [220,221], it can be concluded that TCHCl and OTCHCl exist exclusively with the N,N-dimethylamino nitrogen protonated in $(CD_3)_2SO$. More importantly, the low frequency resonance signal was not observed when a ^{15}N solution nmr spectrum of OTC± was acquired under identical experimental conditions as those for the hydrochloride salts. Based on this observation, it can be concluded that the N,N-dimethylamino nitrogen of OTC± in $(CD_3)_2SO$ does not have a resolvable $^1J(^{15}N,^1H)$ spin-spin coupling. This situation could result if either the nitrogen is not protonated or if it is involved in rapid hydrogen exchange. The ^{15}N nmr spectra of OTC° dissolved in $(CD_3)_2SO$ and pyridine-d_5 solutions were acquired with and without hydrogen decoupling, respectively. For both of these samples, the ^{15}N nmr signal observed for the N,N-dimethylamino nitrogen was a single line with a $\nu_{1/2}$ of less than 5 Hz. The observed ^{15}N chemical shifts for the N,N-dimethylamino nitrogen

in $(CD_3)_2SO$ and pyridine-d_5, 25.3 ppm and 22.3 ppm, respectively, compare reasonably well with the corresponding value determined for OTC[c] from solid state cp/mas nmr, 27.7 ppm. Thus, based on the similarity of ^{15}N chemical shifts in the solid and solution states and on the results from the INEPT experiments, it can be concluded that the structural integrity of the two tautomeric forms represented by 5a and 5b is maintained in $(CD_3)_2SO$ and pyridine-d_5 solutions. Also, a similar conclusion is valid for the hydrochloride salts of OTC and TC.

The ^{15}N cp/mas nmr spectrum for DOXYTCHCl is shown in figure IV.15. Two independent sets of isotropic resonances are apparent for the amide and protonated N,N-dimethylamino nitrogens of this sample. The observation of two sets of isotropic ^{15}N resonances is consistent with the reported x-ray diffraction results for this compound [197]. The chemical shift difference observed for the dimethylamino nitrogen resonances was approximately 4 ppm whereas for the amide nitrogens, the chemical shift difference was approximately 6 ppm. For OTCHBr, which also displays two crystallographic nonequivalent forms [199], the ^{15}N chemical shifts of the N,N-dimethylamino nitrogens were also different by approximately 4 ppm. For this sample, the amide resonance signals were significantly broadened such that both ^{15}N chemical shifts could not be resolved. Several hydrochloride salts of the tetracycline family of antibiotics have been

Figure IV.15

A nitrogen-15 cp/mas nmr spectrum of DOXYTCHCl.

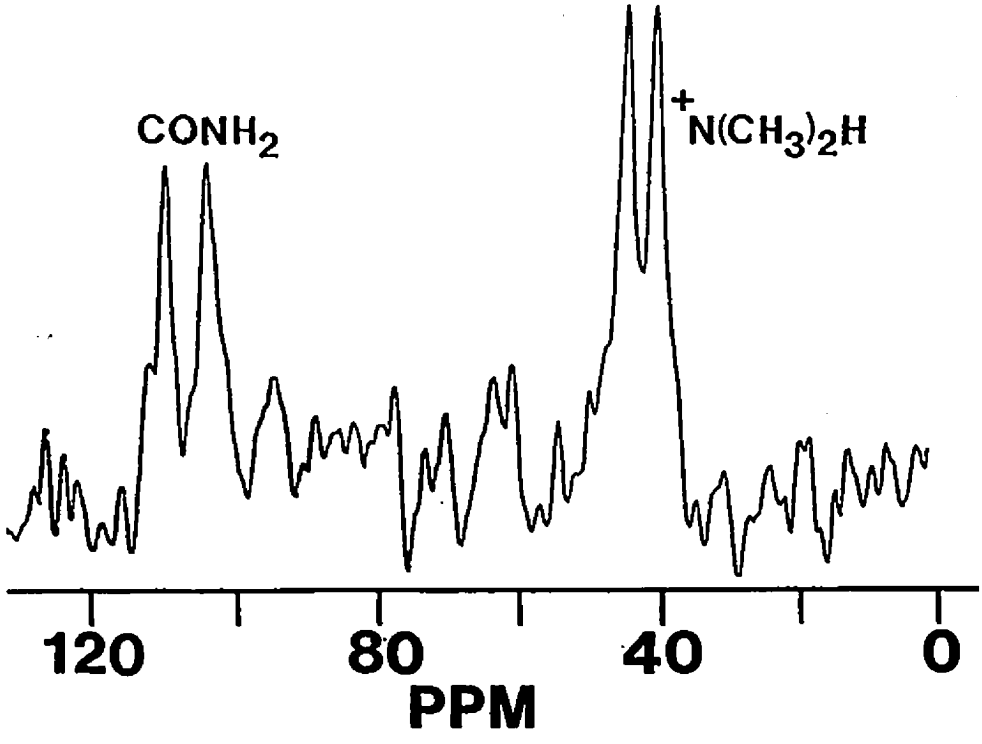

shown to exist in the solid state with only a single conformation of the amide substituent. For example, TCHCl and OTCHCl have been shown to exist in the solid state with the amide nitrogen oriented cis to the oxygen at C-1 (5c) [194,195]. On the other hand, DEMTCHCl has been shown to exist with the opposite conformation of the amide substituent (i.e., amide nitrogen trans to O-1 as in 5d) [198]. Although the ^{15}N chemical shifts of solid TCHCl and OTCHCl are approximately 1.4 ppm and 1.7 ppm to high frequency of the corresponding value for DEMTCHCl (table IV.8), the small range of ^{15}N chemical shifts for the amide nitrogen prevents any definitive assignment of the amide conformations in these systems. In addition, it is not possible with the data in table IV.8 to distinguish unequivocally between the two amide conformers of DOXYTCHCl.

Several other points regarding the ^{15}N cp/mas nmr spectra should be discussed. The ^{15}N signal observed at 81.9 ppm for the 1:1 tetracycline urea adduct provided definitive evidence for the formation of an adduct in the crystalline solid. This value compares well to the ^{15}N chemical shift determined for a saturated solution of urea in H_2O/ethanol, 76 ppm [227]. For MINTCHCl, an additional nitrogen signal was observed at 48.9 ppm. This was assigned to the N,N-dimethylamino nitrogen attached at the C-7 position of the aromatic D ring. When a dipolar dephasing cp/mas nmr spectrum of this compound was obtained, neither N,N-dimethylamino nitrogen exhibited a ^{15}N

nmr signal. This provides definitive evidence that both of these nitrogens are protonated in the solid state. Finally, the ^{15}N cp/mas nmr spectrum of ROLITCHCl consisted of single resonance lines for the N,N-dimethylamino and amide nitrogens, however, a doublet of peaks (separated by ~5 ppm) was observed for the nitrogen of the pyrrolidine ring. One possible explanation is the presence of two conformations of the A ring amide substituent in this sample.

C.4 Summary

High-resolution ^{13}C cp/mas nmr spectra of the tetracycline antibiotics demonstrate the capabilities of modern solid state spectrometers for obtaining well resolved ^{13}C nmr spectra of powdered solids. In particular, the resolution was sufficient to resolve and assign most of the 21 carbon resonance signals for the tetracyclines. The only modification of the earlier reported ^{13}C assignments involved interchanging the C_7 and C_8 resonance signals and interchanging the C_1 and C_{11} signals. The line shapes observed in the ^{13}C cp/mas nmr spectra for those carbon nuclei with directly bonded nitrogens provided an indirect method for monitoring the structural form of the tetracyclines in solid samples.

Natural abundance ^{15}N cp/mas nmr has proven to be a viable method for studying the structural forms of the tetracycline free bases in the solid state. The inherent sensitivity of the ^{15}N chemical shifts to N-protonation effects and the

conclusive evidence obtained with the dipolar dephasing experiments provide an even more sensitive probe of the structure of the A ring than ^{13}C cp/mas nmr experiments. In addition, comparison of solid state ^{15}N chemical shifts with corresponding values in $(CD_3)_2SO$ and pyridine-d_5 solutions provided the first definitive evidence that the structural integrity of the tetracyclines are maintained in solution.

V. Conclusions

This thesis has been concerned with several applications of solid state nmr to the study of spin I=1/2 nuclei in solids of chemical interest. The underlying theme has been the study of the anisotropic nature of spin interactions in solids and how one can tailor an experiment such that the information in the nmr spectrum will reflect specific internal Hamiltonians. Of primary importance to this thesis is the nuclear shielding properties of several spin 1/2 nuclei - ^{13}C, ^{15}N and ^{31}P. Since chemical shielding is closely associated with the electron density distribution around the nucleus, characterization of shielding tensors serves as a fundamental source of information regarding the nature of the local electronic environment.

Dipolar-chemical shift nmr of "isolated" spin-pairs has proven to be a useful technique for determining chemical shift parameters of nuclei from nmr spectra of static powder solids. The investigation of the carbon chemical shielding properties in benzylideneaniline demonstrated the need for the nmr experimentalist to consider possible influences of all internal Hamiltonians on the nmr spectrum. More specifically, when a quadrupolar nucleus such as ^{14}N is a member of the "isolated" spin-pair under investigation, then the simple description of nmr interactions as first order perturbations of the Zeeman energy levels may not be strictly valid. The benefit of recognizing this fact allows one to obtain accurate

information from a thorough theoretical interpretation of the dipolar-chemical shift nmr spectrum. Thus, for the imine carbon of benzylideneaniline, the interpretation of the shielding parameters when the magnitude of the ^{14}N electric field gradient was taken into account allowed the complete specification of the orientation of the carbon chemical shielding tensor. Obviously, it would be of interest to investigate the $^{13}C,^{14}N$ spin-pair of benzylidene-aniline at higher magnetic fields since this would help reduce spectral distortions due to a break-down of the high-field approximation.

The nitrogen chemical shift parameters determined for several imines have provided further evidence that the chemical shielding of a nucleus is often characteristic of the type of molecular fragment being investigated. Excluding the salicylideneanilines, the most shielded principal component of the imine nitrogen shift tensors, δ_{33}, was observed to vary from 2 ppm to 74 ppm; similarly, the intermediate component, δ_{22}, varies from 309 ppm to 343 ppm and the least shielded principal component, δ_{11}, varies from 594 ppm to 674 ppm. It was demonstrated that the minor variations in each δ_{11} can be interpreted in terms of variations of their respective paramagnetic term. The influence of only a modest number of substituents was sufficient to establish some basic qualitative trends between the imine nitrogen shielding and the atomic orbital coefficients, $C_{j\beta}$. Clearly, a more detailed

approach with a larger number of substituents and/or molecular orbital calculations could be pursued. In addition, this type of investigation does not need to be restricted to the ^{15}N nucleus of the imine system since other nuclei in a variety of molecular environments should be equally susceptible to the influence of substituents.

The solid state nmr results for the iminophosphenium cation demonstrated that other factors can play a significant role in the dipolar-chemical shift nmr experiment. For example, it was shown that both librational motions of the moiety of interest and contributions from an anisotropic J tensor can, in principle, modify the effective dipolar coupling between nuclei. For second row elements, the anisotropy in J has been assumed to be negligible but for indirect couplings involving heavier elements such as phosphorus, this assumption may not be valid. Since the dipolar-chemical shift nmr spectrum is only sensitive to the absolute value of the total dipolar interaction, it is difficult to obtain accurate values for internuclear separations from observed dipolar splittings. It would be informative to measure the dipolar coupling constant for the N,P spin-pairs of the iminophosphenium cation as a function of temperature. This may provide useful information on the relative contributions of librations and ΔJ to the effective dipolar coupling constants.

Contrary to popular belief, natural abundance ^{15}N nmr can

be used to examine the structural properties of larger biomolecules. The ^{15}N nmr results for the tetracycline antibiotics exemplify this fact and demonstrate the utility of solid state nmr for bridging the gap between the x-ray crystal structure and the molecular structure in solution. That is, the observed ^{15}N chemical shifts have been used to demonstrate that the structural integrity of the solid tetracyclines is maintained when dissolved in $(CD_3)_2SO$ solutions. Although the structure and conformation of these antibiotics have now been completely specified, no definitive evidence for the existence of an equilibrium between the two forms in solution has been described. This problem could be addressed by examining high-resolution ^1H nmr spectra of the tetracyclines dissolved in mixed solvent systems such as pyridine-d_5/D_2O.

In closing, I would like to stress a final point to those desiring to perform experimental solid state nmr. The importance of optimizing the initial set-up procedure on the nmr instrument is often the <u>key</u> to unlocking the internal Hamiltonians which can then manifest themselves in the nmr spectrum. A judicious choice of experimental parameters which are consistent with the limitations of the nmr instrument and are suitable for the sample under consideration can "make or break" the success of the nmr experiment. In other words, it is up to the nmr experimentalist to recognize and manipulate the internal Hamiltonians lurking within solid samples.

References

[1] G.E. Pake, *J. Chem. Phys.* **16**, 327 (1948).

[2] (a) N.L. Alpert, *Phys. Rev.* **72**, 637 (1947).
(b) N.L. Alpert, *Phys. Rev.* **75**, 398 (1949).

[3] H.S. Gutowsky and G.E. Pake, *J. Chem. Phys.* **18**, 162 (1950).

[4] (a) E.R. Andrew, A. Bradbury and R.G. Eades, *Nature* **182**, 1659 (1958).
(b) E.R. Andrew, A. Bradbury and R.G. Eades, *Nature* **183**, 1802 (1959).

[5] I.J. Lowe, *Phys. Rev. Lett.* **2**, 285 (1959).

[6] E.R. Andrew, *Phil. Trans. Roy. Soc. Lond. A* **299**, 505 (1981).

[7] T.C. Farrar and E.D. Becker, *Pulse and Fourier Transform NMR*, Academic Press : New York, 1971.

[8] R.R. Ernst and W.A. Anderson, *Rev. Sci. Instrum.* **37**, 93 (1966).

[9] (a) A. Pines, M.G. Gibby and J.S. Waugh, *Chem. Phys. Lett.* **15**, 373 (1972).
(b) A. Pines, M.G. Gibby and J.S. Waugh, *J. Chem. Phys.* **59**, 569 (1973).

[10] J. Schaefer and E.O. Stejskal, *J. Am. Chem. Soc.* **98**, 1031 (1976).

[11] (a) D.J. O'Donnell, V.J. Bartuska, A.R. Palmer and D.W. Sindorf, *Amer. Lab.* **10**, 96 (1986).
(b) V.J. Bartuska, S.J. Freeland, D.W. Sindorf and D.G. Dalbow, *Amer. Lab.* **2**, 139 (1987).

[12] M. Mehring, *High Resolution NMR in Solids*, 2nd ed., Springer-Verlag : Berlin, 1983.

[13] E.R. Andrew, *Nuclear Magnetic Resonance*, Cambridge University Press : Cambridge, 1955.

[14] A. Abragam, *Principles of Nuclear Magnetism*, Oxford University Press : Oxford, 1963.

[15] J.D. Macomber, *The Dynamics of Spectroscopic Transitions*, John Wiley and Sons Ltd. : New York, 1976.

[16] C.P. Slichter, *Principles of Magnetic Resonance*, 2nd ed., Springer-Verlag : Berlin, 1978.

[17] B.C. Gerstein and C.R. Dybowski, *Transient Techniques in NMR of Solids*, Academic Press : Orlando, Fla., 1985.

[18] R.R. Ernst, G. Bodenhausen and A. Wokaun, *Principles of Nuclear Magnetic Resonance in One and Two Dimensions*, Oxford University Press : Oxford, 1987.

[19] M. Munowitz, *Coherence in NMR*, Wiley-Interscience : New York, 1988.

[20] C.J. Jameson and J. Mason, In *Multinuclear NMR*, J. Mason, ed., Plenum Press : New York, 1987.

[21] R.F. Schneider, *J. Chem. Phys.* **48**, 4905 (1968).

[22] R.G. Griffin, J.D. Ellet, M. Mehring, J.G. Bulitt and J.S. Waugh, *J. Chem. Phys.* **57**, 2147 (1972).

[23] U. Haeberlen, *Adv. Magn. Reson., Suppl. 1*, Academic Press : New York, 1976.
[24] W. Lamb, *Phys. Rev.* **60**, 817 (1941).
[25] (a) N.F. Ramsey, *Phys. Rev.* **77**, 567 (1950).
(b) N.F. Ramsey, *Phys. Rev.* **78**, 699 (1950).
[26] (a) G. Malli and S. Frago, *Theoret. Chim. Acta.* **5**, 275 (1966).
(b) G. Malli and C. Froese, *Int. J. Quant. Chem., Suppl. 1*, 95 (1967).
[27] (a) W.H. Flygare and J. Goodisman, *J. Chem. Phys.* **49**, 3122 (1968).
(b) T.D. Gierke, H.L. Tigelar and W.H. Flygare, *J. Am. Chem. Soc.* **94**, 330 (1972).
(c) T.D. Gierke and W.H. Flygare, *J. Am. Chem. Soc.* **94**, 7277 (1972).
[28] A. Saika and C.P. Slichter, *J. Chem. Phys.* **22**, 26 (1954).
[29] (a) J. Pople, *Proc. Roy. Soc. A* **239**, 541 (1956).
(b) J.A. Pople, W.G. Schneider and H.J. Bernstein, *High Resolution Nuclear Magnetic Resonance*, McGraw-Hill : New York, 1959.
(c) J. Pople, *J. Chem. Phys.* **37**, 5360 (1962).
(d) M. Karplus and J.A. Pople, *J. Chem. Phys.* **38**, 2803 (1963).
[30] W.T. Raynes, In *Nuclear Magnetic Resonance : Specialist Periodic Report*, The Chemical Society : London, 1978, Vol. 7.
[31] A.D. Buckingham and S.M. Malm, *Mol. Phys.* **22**, 1127 (1971).
[32] J. Kempf, H.W. Spiess, U. Haeberlen and H. Zimmermann, *Chem. Phys.* **4**, 269 (1974).
[33] D.L. VanderHart, H.S. Gutowsky and T.C. Farrar, *J. Am. Chem. Soc.* **89**, 5056 (1967).
[34] M.E. Stoll, R.W. Vaughan, R.B. Saillant and T.J. Cole, *J. Chem. Phys.* **61**, 2896, (1974).
[35] R.M. Dickson, M.S. McKinnon, J.F. Britten, and R.E. Wasylishen, *Can. J. Chem.* **65**, 941 (1987).
[36] P. Pyykkö and L. Wiesenfeld, *Mol. Phys.* **43**, 557 (1981).
[37] J. Kowalewski, In *Ann. Rep. NMR Spectrosc.*, G.A. Webb, ed., Academic Press Inc. : London, 1982, Vol. 12.
[38] J.B. Robert and L. Wiesenfeld, *Phys. Rep.* **86**, 388 (1982).
[39] (a) P.N. Tutunjian and J.S. Waugh, *J. Magn. Reson.* **49**, 155 (1982).
(b) P.N. Tutunjian and J.S. Waugh, *J. Chem. Phys.* **76**, 1223 (1982).
[40] J. Lounila and J. Jokisaari, *Prog. Nucl. Magn. Reson. Spectrosc.* **15**, 249 (1982).
[41] P. Lazzeretti, E. Rossi, F. Taddei and R. Zanasi, *J. Chem. Phys.* **77**, 408 (1982).

[42] J. C. Facelli and M.J. Barfield, *J. Magn. Reson.* **59**, 452 (1984).
[43] J. Jokisaari, Y.Hiltunen and J. Lounila, *J. Chem. Phys.* **85**, 3198 (1986).
[44] G.H. Penner, W.P. Power and R.E. Wasylishen, *Can. J. Chem.* **66**, 1821 (1988).
[45] M.-R. Van Calsteren, G.I. Birnbaum and I.C.P. Smith, *J. Chem. Phys.* **86**, 5404 (1987).
[46] A. Naito, D.L. Sastry and C.A. McDowell, *Chem. Phys. Lett.* **115**, 19 (1985).
[47] H. Hauser, C. Radloff, R.R. Ernst, S. Sundells and I. Pascher, *J. Am. Chem. Soc.* **110**, 1054 (1988).
[48] W.S. Veeman, *Prog. Nucl. Magn. Reson. Spectrosc.* **16**, 193 (1984).
[49] (a) M.A. Kennedy and P.D. Ellis, *Concepts in Magnetic Resonance* **1**, 35 (1989).
(b) M.A. Kennedy and P.D. Ellis, *Concepts in Magnetic Resonance* **1**, 109 (1989).
[50] D.L. VanderHart and H.S. Gutowsky, *J. Chem. Phys.* **49**, 261 (1968).
[51] M. Linder, A. Höhener and R.R. Ernst, *J. Chem. Phys.* **73**, 4959 (1980).
[52] K.G. Valentine, A.L. Rockwell, L.M. Gierasch and S.J. Opella, *J. Magn. Reson.* **73**, 519 (1987).
[53] J.E. Roberts, G.S. Harbison, M.G. Munowitz, J. Herzfeld and R.G. Griffin, *J. Am. Chem. Soc.* **109**, 4163 (1987).
[54] W.P. Power, R.E. Wasylishen and R.D. Curtis, *Can. J. Chem.* **67**, 454 (1989).
[55] (a) R.E. Wasylishen, W.P. Power, G.H. Penner and R.D. Curtis, *Can. J. Chem.* **67**, 1219 (1989).
(b) R.E. Wasylishen, G.H. Penner, W.P. Power and R.D. Curtis, *J. Am. Chem. Soc.* **111**, 6082 (1989).
[56] R.D. Curtis, G.H. Penner, W.P. Power and R.E. Wasylishen, *J. Phys. Chem.* **94**, 4000 (1990).
[57] G. Arfken, *Mathematical Methods for Physicists*, 3rd ed., Academic Press : New York, 1985.
[58] (a) A.C. Olivieri, L.F. Frydman and L.E. Diaz, *J. Magn. Reson.* **75**, 50 (1987).
(b) A. Olivieri, L. Frydman, M. Grasselli and L. Diaz, *Magn. Reson. Chem.* **26**, 615 (1988).
[59] J.S. Waugh, L.M. Huber and U. Haeberlen, *Phys. Rev.* **20**, 180 (1968).
[60] P. Mansfield, *J. Phys. C* **4**, 1444 (1971).
[61] (a) W.-K. Rhim, D.D. Elleman and R.W. Vaughan, *J. Chem. Phys.* **58**, 1772 (1973).
(b) W.-K. Rhim, D.D. Elleman and R.W. Vaughan, *J. Chem. Phys.* **59**, 3740 (1973).
(c) W.-K. Rhim, D.D. Elleman, L.B. Schreiber and R.W. Vaughan, *J. Chem. Phys.* **60**, 4595 (1974).
[62] G. Sinning, M. Mehring and A. Pines, *Chem. Phys. Lett.* **43**, 382 (1976).

[63] M. Mehring amd G. Sinning, *Phys. Rev. B* **15**, 2519 (1977).
[64] U. Haeberlen, *Magn. Reson. Rev.* **10**, 81 (1985).
[65] (a) S.R. Hartmann and E.L. Hahn, *Bull. Amer. Phys. Soc.* **5**, 498 (1960).
(b) S.R. Hartmann and E.L. Hahn, *Phys. Rev.* **128**, 2042 (1962).
[66] F.M. Lurie and C.P. Slichter, *Phys. Rev. A* **133**, 1108 (1964).
[67] H.E. Bleich and A.G. Redfield, *J. Chem. Phys.* **67**, 5040 (1977).
[68] (a) L.B. Alemany, D.M. Grant, R.J. Pugmire, T.D. Alger and K.W. Zilm, *J. Am. Chem Soc.* **105**, 2133 (1983).
(b) L.B. Alemany, D.M. Grant, R.J. Pugmire, T.D. Alger and K.W. Zilm, *J. Am. Chem. Soc.* **105**, 2142 (1983).
(c) L.B. Alemany, D.M. Grant, R.J. Pugmire and T.D. Alger, *J. Am. Chem. Soc.* **105**, 6697 (1983).
[69] M. Sardashti and G.E. Maciel, *J. Magn. Reson.* **72**, 467 (1987).
[70] S. Zhang and X. Wu, *Chem. Phys. Lett.* **156**, 333 (1989).
[71] L.W. Jelinski and M.T. Melchoir, In *NMR Spectroscopy Techniques*, C. Dybowski and R.L. Lichter, eds., Marcel Dekker Inc. : New York, 1987, Chapter 6.
[72] D.E. Axelson, *Solid State Nuclear Magnetic Resonance of Fossil Fuels*, Multiscience Publications Ltd. : Canada, 1985.
[73] H. Saitô, *Magn. Reson. Chem.* **24**, 835 (1986).
[74] C.A. Fyfe, *Solid State NMR for Chemists*, C.F.C. Press : Guelph, Canada, 1983.
[75] D.L. VanderHart, W.L. Earl and A.N. Garroway, *J. Magn. Reson.* **44**, 361 (1981).
[76] M.A. Heminga, P.A. DeJager, J. Krüse and R.M.J.N. Lamerichs, *J. Magn. Reson.* **71**, 446 (1987).
[77] (a) M. Alla and E. Lippmaa, *Chem. Phys. Lett.* **87**, 30 (1982).
(b) S. Pausak, J. Tegenfeldt and J.S. Waugh, *J. Chem. Phys.* **61**, 1338 (1974).
[78] J.S. Frye and G.E. Maciel, *J. Magn. Reson.* **48**, 143 (1982).
[79] G. Bodenhausen, P. Caravetti, J. Deli and R.R. Ernst, *J. Magn. Reson.* **48**, 143 (1982).
[80] J. Herzfeld and A.E. Berger, *J. Chem. Phys.* **73**, 6021 (1980).
[81] M.M. Maricq and J.S. Waugh, *J. Chem. Phys.* **79**, 3300 (1979).
[82] N.J. Clayden, C.M. Dobson, L.-Y. Lian and D.J. Smith, *J. Magn. Reson.* **69**, 476 (1986).
[83] C.J. Groombridge, R.K. Harris, K.J. Packer, B.J. Say and S.F. Tanner, *J. Chem. Soc. Chem. Commun.*, 174 (1980).

[84] G.E. Balimann, C.J. Groombridge, R.K. Harris, K.J. Packer, B.J. Say and S.F. Tanner, *Phil. Trans. Roy. Soc. A* **299**, 643 (1981).
[85] A. Naito, S. Ganapathy, K. Akasaka and C.A. McDowell, *J. Chem. Phys.* **74**, 3190 (1981).
[86] M.H. Frey and S.J. Opella, *J. Chem. Soc. Chem. Commun.*, 474 (1980).
[87] S.J. Opella, J.G. Hexem, M.H. Frey and T.A. Cross, *Phil. Trans. Roy. Soc. A* **299**, 665 (1981).
[88] (a) J.G. Hexem, M.H. Frey and S.J. Opella, *J. Am. Chem. Soc.* **103**, 224 (1981).
(b) J.G. Hexem, M.H. Frey and S.J. Opella, *J. Chem. Phys.* **77**, 3847 (1982).
(c) J.G. Hexem, Ph.D. Thesis, University of Pennsylvania, 1982.
[89] N. Zumbulyadis, P.M. Henrichs and R.H. Young, *J. Chem. Phys.* **75**, 1603 (1981).
[90] E.M. Menger and W.S. Veeman, *J. Magn. Reson.* **46**, 257 (1982).
[91] R.K. Harris, *J. Magn. Reson.* **78**, 389 (1988).
[92] R.E. Wasylishen and C.A. Fyfe, In *Ann. Rep. NMR Spectrosc.*, G.A. Webb, ed., 1982, Vol. 12.
[93] R. Richards and K.J. Packer, *Phil. Trans. Roy. Soc. A*, **299**, 477 (1981).
[94] E. Fukishima and S.B.W. Roeder, *Experimental Pulse NMR - A Nuts and Bolts Approach*, Addison - Wesley Publishing Company : Reading, MA, 1981.
[95] D.I. Hoult and R.E. Richards, *J. Magn. Reson.* **24**, 71 (1976).
[96] L.W. Jelinski, *Chem. Eng. News* **11**, 26 (1984).
[97] Y.J. Jiang, R.J. Pugmire and D.M. Grant, *J. Magn. Reson.* **71**, 485 (1987).
[98] D.D. Traficante, *Concepts in Magnetic Resonance* **1**, 73 (1989).
[99] M.E. Stoll, A.J. Vega and R.W. Vaughan, *J. Chem. Phys.* **65**, 4093 (1976).
[100] E.L. Hahn, *Phys. Rev.* **80**, 580 (1950).
[101] M. Rance and R.A. Byrd, *J. Magn. Reson.* **52**, 221 (1983).
[102] R.K. Harris, *Nuclear Magnetic Resonance Spectroscopy : A Physiochemical View*, Pitman Publishing Inc. : Marshfield, MA, 1983, Chapter 6.
[103] D.P. Barron, *Simfit : An Optimization Routine for Bruker MSL NMR Spectrometers*, Brisbane NMR Centre, Griffith University, Nathan, Australia, 1986.
[104] W.H. Press, B.P. Flannery, S.A. Teukolsky and W.T. Vetterling, *Numerical Recipes : The Art of Scientific Computing*, Cambridge University Press : Cambridge, 1986, pp. 289-294.
[105] J. Tegenfeldt and U. Haeberlen, *J. Magn. Reson.* **36**, 453 (1979),

[106] M. Alla and E. Lippmaa, *Chem. Phys. Lett.* **37**, 260 (1976).
[107] (a) S.J. Opella and M.H. Frey, *J. Am. Chem, Soc.* **101**, 5854 (1979).
(b) S.J. Opella, M.H. Frey and T.A. Cross, *J. Am. Chem. Soc.* **101**, 5856 (1979).
[108] J.A. Ripmeester, J.S. Tse and D.W. Davidson, *Chem. Phys. Lett.* **86**, 428 (1982).
[109] D.J. O'Donnell, J.J.H. Ackerman and G.E. Maciel, *J. Agric. Food Chem.* **29**, 514 (1981).
[110] B.C. Gerstein, P.D. Murphy and L.M. Ryan, In *Coal Structure*, R.A. Meyers, ed., Academic Press : New York, 1982, pp. 87-129.
[111] F.P. Miknis, M. Sullivan, V.J. Bartuska and G.E. Maciel, *Org. Geochem.* **3**, 19 (1981).
[112] E.W. Hagaman and M.C. Woody, *Proc. Int. Coal Sci.*, Dusseldorf, W. Germany, 807, 1981.
[113] J. Schaefer, M.D. Sefcik, E.O. Stejskal and R.A. McKay, *Macromolecules* **14**, 188 (1981).
[114] N. Zumbulyadis and H.J. Gysling, *J. Am. Chem. Soc.* **104**, 3246 (1982).
[115] B.R. Appleman and B.P. Dailey, *Adv. Magn. Reson.* **7**, 231 (1974).
[116] S. Kaplan, A. Pines, R.G. Griffin and J.S. Waugh, *Chem. Phys. Lett.* **25**, 78 (1974).
[117] H.W. Spiess. In *NMR Basic Principles and Progress*, P. Diehl, E. Fluck, R. Kosfeld, eds., Springer-Verlag : New York, 1978, Vol. 15, pp. 55-214.
[118] B.M. Fung, *J. Am Chem. Soc.* **105**, 5713 (1983).
[119] M.A. Doverspike, M.-C. Wu and M.S. Conradi, *Phys. Rev. Lett.* **56**, 2284 (1986).
[120] (a) J.C. Facelli, D.M. Grant and J. Michl, *Acc. Chem. Res.* **20**, 152 (1987).
(b) J.C. Facelli and D.M. Grant, In *Topics in Stereochemistry*, E.L. Eliel and S.H. Wilen, eds., John Wiley and Sons : New York, 1989, Vol. 19, pp. 1-61.
[121] T.M. Duncan, *J. Phys. Chem. Ref. Data* **16**, 125 (1987).
[122] M. Sardashti and G.E. Maciel, *J. Phys. Chem.* **92**, 4620 (1988).
[123] C.M. Carter, J.C. Facelli, D.W. Alderman, D.M. Grant, N.K. Dalley and B.E. Wilson, *J. Chem. Soc. Farad. Trans.* **84**, 3673 (1988).
[124] C.J. Jameson, In *Specialist Periodic Report-NMR Spectroscopy*, G.A. Webb, ed., The Chemical Society : London, 1989, Vol. 18 and previous volumes of this annual review.
[125] A.M. Orendt, J.C. Facelli, A.J. Beeler, K. Reuter, W.J. Horton, P. Cutts, D.M. Grant amd J. Michl, *J. Am. Chem. Soc.* **110**, 3386 (1988).
[126] K.R. Morgan and R.H. Newman, *J. Am. Chem. Soc.* **112**, 4 (1990).

[127] C.S. Yannoni, *J. Chem. Phys.* **52**, 2005 (1970).
[128] J. Raymonda and W.J. Klemperer, *J. Chem. Phys.* **55**, 232 (1971).
[129] L.M. Ishol and T.A. Scott, *J. Magn. Reson.* **27**, 23 (1977).
[130] M. Witanowski, L. Stefaniak and G.A. Webb, In *Ann. Rep. NMR Spectrosc.*, G.A. Webb, ed., Academic Press Inc. : London, 1986, Vol. 18.
[131] (a) H.B. Burgi, J.D. Dunitz and C.Zust, *Acta Cryst. B* **24**, 463 (1968).
(b) H.B. Burgi and J.D. Dunitz, *J. Chem. Soc., Chem. Commun.*, 472 (1969).
(c) H.B. Burgi and J.D. Dunitz, *Helv. Chem. Acta.* **52**, 1747 (1970).
[132] G.S. Harbison, J. Herzfeld and R. G. Griffin, *Biochemistry*, **22**, 1 (1983).
[133] W.L. Earl and D.L. VanderHart, *J. Magn. Reson.* **48**, 35 (1982).
[134] D.W. Alderman, M.S. Solum and D.M. Grant, *J. Chem. Phys.* **84**, 3717 (1986).
[135] G.W. Buchanan and B.A. Dawson, *Can. J. Chem.* **55**, 1437 (1977).
[136] Z.-H. Gan, J.C. Facelli and D.M. Grant, *J. Chem. Phys.* **89**, 5542 (1988).
[137] E. Hadjaudis and F. Milia, *Chem. Phys.* **47**, 105 (1980).
[138] (a) D.R. Johnson and F.J. Lovas, *Chem. Phys. Lett.* **15**, 65 (1972).
(b) R. Pearson, Jr. and F.J. Lovas, *J. Chem. Phys.* **66**, 4149 (1977).
[139] S. Gerber and H. Huber, *Z. Naturforsch* **429**, 753 (1987).
[140] W. Gordy and R.L. Cook, *Microwave Molecular Spectra*, 3rd ed., Wiley : New York, 1984, Chapter 9.
[141] C.R. Brett and D.T. Edmonds, *J. Magn. Reson.* **49**, 304 (1982).
[142] (a) S.J. Opella, *Ann. Rev. Phys. Chem.* **33**, 533 (1982).
(b) S.J. Opella, P.L. Stewart and K.G. Valentine, *Biophys.* **10**, 7 (1987).
(c) S.O. Smith and R.G. Griffin, *Ann. Rev. Phys. Chem.* **39**, 511 (1988).
[143] K.A. Ebraheem and G.A. Webb, *Prog. Nucl. Magn. Reson. Spectrosc.* **11**, 149 (1977).
[144] (a) U. Fleischer, M. Schindler and W. Kutzelnigg, *Chemical Shifts of H_mX-YH_n Compounds : A Theoretical Study*, Poster presented at PSIBLOCS, 1988.
(b) M. Schindler, personal communication, 1989.
[145] R. Höller and H. Lischka, *Mol. Phys.* **41**, 1017 (1980).
[146] F. Ribas Prado and C. Giessner-Prettre, *J. Magn. Reson.* **47**, 103 (1982).

[147] M. Schindler and W. Kutzelnigg, *J. Chem. Phys.* **76**, 1919 (1982).
[148] A.E. Hansen and T.D. Bouman, *J. Chem. Phys.* **82**, 5035 (1985).
[149] J. van Dongen Torman, W.S. Veeman and E. deBoer, *J. Magn. Reson.* **32**, 49 (1978).
[150] M.A. El-Bayoumi, M. El-Aasser and F. Abdel-Halim, *J. Am. Chem. Soc.* **93**, 586 (1971).
[151] M. Schindler, *J. Am. Chem. Soc.* **109**, 5950 (1987).
[152] (a) J. Mason, D.M. Mingas, J. Schaefer, D. Sherman and E.O. Stejskal, *J. Chem. Soc., Chem. Commun.*, 444 (1985).
(b) P.A. Duffin, L.F. Larkworthy, J. Mason, A.N. Stephens and R.M. Thompson, *Inorg. Chem.* **26**, 2034 (1987).
[153] G.W. Buchanan and B.A. Dawson, *Org. Magn. Reson.* **13**, 293 (1980).
[154] G.A. Gartman and V.D. Pak, *Zhurnal Strukturnoi Khimii* **25**, 39 (1984). English translation.
[155] A. Echevarria, J. Miller and M. Graça Nasçimento, *Magn. Reson. Chem.* **23**, 809 (1985).
[156] L.E. Khoo, *Spectrosc. Lett.* **21**, 55 (1988).
[157] G.A. Olah and D.J. Donovan, *J. Org. Chem.* **43**, 860 (1978).
[158] M.E.L. Saraiva, F.F.G. Geraldes and V.M.S. Gil, *Tetrahedron* **44**, 163 (1988).
[159] F. Milia, E. Hadjaudis and J. Seliger, *J. Mol. Struct.* **177**, 191 (1988).
[160] M. Allen and J.D. Roberts, *J. Org. Chem.* **45**, 130 (1980).
[161] (a) J. Bregman, L. Leiserowitz and G.M.J. Schmidt, *J. Chem. Soc.* 2068 (1964).
(b) J. Bregman, L. Leiserowitz and K. Osaki, *J. Chem. Soc.* 2086 (1964).
[162] (a) J. Bernstein and A.T. Hagler, *J. Am. Chem. Soc.* **100**, 673 (1978).
(b) J. Bernstein, T.E. Anderson and C.J. Echhardt, *J. Am. Chem. Soc.* **101**, 541 (1978).
(c) J. Bernstein, *Acta Cryst. B* **35**, 360 (1979).
(d) J. Bernstein, Y.M. Engel and A.T. Hagler, *J. Chem. Phys.* **75**, 2346 (1981).
(e) I. Bar and J. Berstein, *Acta Cryst. B* **37**, 569 (1981).
[163] H. Nakai, K. Ezumi and M. Shiro, *Acta Cryst. B* **37**,193 (1981).
[164] V.I. Minkin, Y.A. Zhdanov, E.A. Medyantzeva and Y.A. Ostroumov, *Tetrahedron* **23**, 3651 (1967).
[165] E. Niecke, M. Nieger and F. Riechart, *Angew. Chem.Int. Ed. Engl.* **27**, 1715 (1988).
[166] R.J. Buenker, P.J. Bruna and S. Peyerimhoff, *Isr. J. Chem.* **19**, 309 (1980).

[167] K.W. Zilm, G.G. Webb, A.H. Cowley, M. Pakulski and A. Orendt, *J. Am. Chem. Soc.* **110**, 2032 (1988).
[168] D.B. Chesnut and C.G. Phung, *J. Chem. Phys.* **91**, 238 (1989).
[169] A.E. Hansen, *J. Chem. Phys.* **91**, 3552 (1989).
[170] T.D. Bouman and A.E. Hansen, *Int. J. Quant. Chem. : Quant. Chem. Symp.* **23**, 281 (1989).
[171] P. Lazzeretti and J.A. Tossell, *J. Phys. Chem.* **91**, 800 (1987).
[172] D.B. Chesnut. In *Phosphorus-31 NMR Spectroscopy in Stereochemical Analysis-Organic Compounds and Metal Complexes*, J.G. Verkade and L.D. Quin, eds., VCH Publishers : Deerfield Beach, Fla., 1987, pp. 185-204.
[173] J. Burgers, M.A. Hoefnagel, P.E. Verkade, H. Visser and B.M. Webster, *Rec. Trav. Chim.* **77**, 491 (1958).
[174] D.C. Apperley, B. Haiping and R.K. Harris, *Mol. Phys.* **68**, 1277 (1989).
[175] T.P. Das and E.L. Hahn, In *Solid State Physics, Suppl. 1*, F.Seitz and D. Turnbull, eds., Academic Press Inc. : New York, 1958. .
[176] K.W. Zilm and D.M. Grant, *J. Am. Chem. Soc.* **103**, 2913 (1981).
[177] E.R. Henry and A. Szabo, *J. Chem. Phys.* **82**, 4753 (1985).
[178] J.M. Millar, A.M. Thayer, D.B. Zax and A. Pines, *J. Am. Chem. Soc.* **108**, 5113 (1986).
[179] C. Rømming, *Acta Chem. Scand.* **26**, 523 (1976).
[180] C.J. Jameson, A.K. Jameson, D. Oppusunggu, S. Wille, P.M. Burrell and J. Mason, *J. Chem. Phys.* **74**, 81 (1981).
[181] R.M. Garvey and F.C. DeLucia, *J. Mol. Spectrosc.* **50**, 38 (1974).
[182] (a) I. Chan, M.R. Baker and N.F. Ramsey, *Phys. Rev. A* **136**, 1224 (1964).
(b) M.R. Baker, C.H. Anderson and N.F. Ramsey, *Phys. Rev. A* **133**, 1533 (1964).
[183] W.B. Moinz and C.F. Poranski, Jr., *J. Phys. Chem.* **73**, 4145 (1969).
[184] T.M. Barbara, *Mol. Phys.* **54**, 651 (1985).
[185] C. Jameson, private communication, 1989.
[186] B.M. Duggar, *Ann. N.Y. Acad. Science*, **51**, 177 (1948).
[187] R.B. Broschard, A.C. Dornbush, S. Gordon, B.L. Hutchings, A.R. Kohler, G. Krupka, S. Kushner, S.V. LeFemine and C. Pidacks, *Science* **109**, 199 (1949).
[188] W. Dürckheimer, *Angew. Chem. Int. Ed. Engl.* **14**, 721 (1975).
[189] M.R. Caira, L.R. Nassimbeni and J.C. Russell, *Acta Cryst. B.* **33**, 1171 (1977).
[190] (a) J.J. Stezowski, *J. Am. Chem. Soc.* **99**, 6012 (1976).

(b) R. Prewo and J.J. Stezowski, *J. Am. Chem. Soc.* **99**, 1117 (1977).
[191] G.J. Palenik and M. Mathew, *J. Am. Chem. Soc.* **100**, 4464 (1978).
[192] (a) R. Prewo, J.J. Stezowski and R. Kirchlechner, *J. Am. Chem. Soc.* **102**, 7021 (1980).
(b) R. Prewo and J.J. Stezowski, *Tetrahedron Lett.* **21**, 251 (1980).
(c) R. Kirchlechner and W. Rogalski, *Tetrahedron Lett.* **21**, 247 (1980).
[193] R.B. Von Dreele and R.E. Hughes, *J. Am. Chem. Soc.* **93**, 7290 (1971).
[194] K. Kamiya, M. Asai, Y. Wada and M. Nishikawa, *Experientia* **27**, 363 (1971).
[195] (a) Y. Takeuchi and M.J. Buerger. *Proc. Nat. Acad. Sci.* **46**, 1366 (1960).
(b) H. Cid-Dresdner, *Z. Kristallogr. Kristallgeom. Kristallphys. Kristallchem.* **121**, 170 (1965).
[196] J. Donohue, J.D. Dunitz, K.N. Trueblood and M.S. Webster, *J. Am. Chem. Soc.* **85**, 851 (1963).
[197] J.J. Stezowski, *J. Am. Chem. Soc.* **99**, 1122 (1963).
[198] (a) G.J. Palenik and M. Mathew, *Acta Cryst. A.* **28**, S47 (1972).
(b) G.J. Palenik, M. Mathew and R. Restino, *J. Am. Chem. Soc.* **100**, 4458 (1978).
[199] K.H. Jogun and J. J. Stezowski, *Cryst. Struct. Commun.* **5**, 381 (1976).
[200] W.J. Bottstein, W.F. Minor and L.C. Cheney, *J. Am. Chem. Soc.* **81**, 1198 (1959).
[201] M.J. Martell and J.H. Boothe, *J. Med. Chem.* **10**, 44 (1967).
[202] S. Mooibroek and R.E. Wasylishen, *Can. J. Chem.* **65**, 357 (1987).
[203] R.M. Evans, *Quart. Rev.* **13**, 61 (1959).
[204] J. Harley-Mason and E.H. Pavri, *J. Chem. Soc.* , 2565 (1963).
[205] E.F. Pratt and S.P. Suskind, *J. Org. Chem.* **28**, 638 (1963).
[206] R.B. Kelly, *J. Org. Chem.* **28**, 453 (1963).
[207] R.B. Kelly, G.R. Umbreit and W.F. Liggert, *J. Org. Chem.* **29**, 1273 (1964).
[208] O.H. Wheeler and D. Gonzalez, *Tetrahedron*, **20**, 189 (1964).
[209] (a) M. Schach Von Wittenau, R.K. Blackwood, L.H. Conover, R.H. Glauert and R.B. Woodward, *J. Am. Chem. Soc.* **87**, 134 (1965).
(b) M. Schach Von Wittenau and R.K. Blackwood, *J. Org. Chem.* **31**, 613 (1966).
[210] (a) G.L. Asleson, Ph.D. Thesis, University of Iowa, 1975.

(b) G.L. Asleson and C.W. Frank, *J. Am. Chem. Soc.* **97**, 6246 (1975).
(c) G.L. Asleson and C.W. Frank, *J. Am. Chem. Soc.* **98**, 4745 (1976).

[211] (a) D.E. Williamson and G.W. Everett, Jr., *J. Am. Chem. Soc.* **97**, 2397 (1975).
(b) J. Gulbis and G.W. Everett, Jr., *J. Am. Chem. Soc.* **97**, 6248 (1975).
(c) J. Gulbis and G.W. Everett, Jr., *Tetrahedron* **32**, 913 (1976).
(d) J.Y. Lee and G.W. Everett, *J. Am. Chem. Soc.* **103**, 5221 (1981).

[212] L.J. Hughes, J.J. Stezowski and R.E. Hughes, *J. Am. Chem. Soc.* **101**, 7655 (1979).

[213] E.P. Mazzola, J.A. Melin and L.G. Wayland, *J. Pharm. Sci.* **69**, 229 (1980).

[214] (a) A.F. Casy and A. Yasin, *J. Pharm. Biomed. Anal.* **1**, 281 (1983).
(b) A.F. Casy and A. Yasin, *J. Pharm. Biomed. Anal.* **2**, 19 (1984).
(c) A.F. Casy and A. Yasin, *Magn. Reson. Chem.* **23**, 767 (1985).

[215] I.-K. Wang and L.C. Vining, *J. Antibiot.* **39**, 1281 (1986).

[216] J.J. Stezowski, *Proc. Symp. Steric Effects in Biomolecules*, Eger, Hungary, 1981, pp. 3-13.

[217] G.W. Buchanan, *Tetrahedron* **45**, 581 (1989).

[218] F.A. Hochstein, C.R. Stephens, L.H. Conover, P.P. Regna, R. Pasternack, P.N. Gordon, F.J. Pilgrim, K.J. Brunnings and R.B. Woodward, *J. Am. Chem. Soc.* **75**, 5455 (1953).

[219] L.L. Smith, S.A. Muller, M. Marx, R. Winterbottom and A.P. Doerschuk, *Org. Chem.* **23**, 721 (1958).

[220] G.A. Morris and R. Freeman, *J. Am. Chem. Soc.* **101**, 760 (1979).

[221] G.A. Morris, *J. Am. Chem. Soc.* **102**, 428 (1980).

[222] P.R. Srinivasan and R.L. Lichter, *J. Magn. Reson.* **28**, 227 (1977).

[223] M.J. Hunt, *J. Magn. Reson.* **15**, 113 (1974).

[224] J.M. Lehn and J.P. Kintzinger, In *Nitrogen NMR*, M. Witanowski and G.A. Webb, eds., Plenum Press : London, 1973.

[225] G.C. Levy and R.L. Lichter, *Nitrogen-15 Nuclear Magnetic Resonance Spectroscopy*, John Wiley and Sons : New York, 1979, Chapter 3.

[226] R.O. Duthaler and J.D. Roberts, *J. Am. Chem. Soc.* **100**, 3889 (1978).

[227] M.L. Martin, M. Filleux-Blanchard, G.J. Martin and G.A. Webb, *Org. Magn. Reson.* **13**, 396 (1980).